Investigating the role of gamma-tubulin in coordinating microtubule plus end behaviour with regulation at the spindle pole

Lara Marie Cuschieri

Doctor of Philosophy

Department of Biology
McGill University
Montreal, Quebec, Canada

June 2008

A thesis submitted to McGill University in partial fulfillment of the requirement of requirements of the degree of Doctor of Philosophy

“ It always seems impossible until it is done.”

(Nelson Mandela)

ACKNOWLEDGEMENTS

I would like to sincerely thank my supervisor Dr. Jackie Vogel for her constant support, guidance, friendship and excellent mentorship she has given me throughout my Ph.D. I thank her for also teaching me the importance of well-planned experiments, believing in myself and never backing down from a challenge.

I am grateful to my supervisory committee, Dr. Laura Nilson and Dr. Craig Mandato for their continued feedback and stimulating discussions about my research. Additionally I thank Dr. Howard Bussey, Dr. Guillaume Lesage and Dr. Elke Kuster-Schöck for their scientific discussions and technical expertise. I would also like to thank past and present members of the Vogel Lab for excellent discussions, technical advice and comic relief during stressful experiments especially, Dr. Mike Logan, James Knockleby, Thao Nguyen, Daici Chen, Hanting Por and Nicolas Szapiel for their constant support and amazing friendships throughout my PhD.

I am forever indebted to my family especially my loving parents Anthony and Helen Cuschieri and my parent in-laws, Willie and Judy O'Donnell, who have given me unending encouragement, love and support. I wish to express my deepest gratitude to my husband Paul O'Donnell who has continued to love, understand, encourage and support me throughout the entire course of my Ph.D. Without his support none of this could have been possible.

Finally, I would like to acknowledge generous financial support from Dr. Jackie Vogel through her grant from the Canadian Institutes for Health Research

TABLE OF CONTENTS

LIST OF TABLES

LIST OF FIGURES

LIST OF ABBREVIATIONS

α-factor	Alpha-factor
AB	Apical-Basal
AP	Anterior-Posterior
APC	Adenomatous Poliposis Coli tumor suppressor
CDK	Cyclin Dependent Kinase
EB1	End Binding Protein 1
γ-tubulin	Gamma-tubulin
γTuRC	γ-tubulin Ring Complex
γTuSC	γ-tubulin Small Complex
GAP	GTPase Activating Protein
GEF	Guanine Nucleotide Exchange Factor
λ–PPase	Lambda Phosphatase
LatB	Latrunculin B
MAP	Microtubule Associating Protein
-end	Minus End
MTOC	Microtubule Organizing Centre
NZ	Nocodazole
+end	Plus End
+TIP	Plus End Interacting Protein
SDS-PAGE	Sodium Dodecyl Sulfate Polyacrylamide Gel Electrophoresis
SPB	Spindle Pole Body
SPB_b	Bud Spindle Pole Body
SPB_m	Mother Spindle Pole Body
YPAD	Yeast Extract, Peptone, Adenine Sulfate, Dextrose

AUTHOR CONTRIBUTION

Some sections of the introduction (chapter 1) are taken from a published review. All the data collection and results obtained during my PhD are presented here as two manuscript-based chapters.

Chapter 1 is derived from a published literature review:

Cuschieri L., Nguyen T. and Vogel J. (2007). Control at the cell center: the role of spindle poles in cytoskeletal organization and cell cycle regulation. *Cell Cycle* **22,** 2788-2794.

I wrote the Abstract and performed the literature search for the major sections of the review. I wrote the Introduction with Thao Nguyen and the sections “MTOCs coordinate cytoskeletal organization and function with cell cycle progression”, “MTOCs and the checkpoint response” and “MTOCs and microtubule organization”. I wrote the Conclusion, the Figure Legends and prepared Figure 3. I also contributed to the editing of all sections of the review.

Thao Nguyen wrote the Introduction and prepared Figures 1 and 2 of the review. She also contributed towards the literature search.

Jackie Vogel edited and revised all sections of the review. She contributed her ideas towards the overall topics of discussion and review layout.

Chapter 2 is a published manuscript:

Cuschieri L., Miller R., and Vogel J. (2006). γ-tubulin is required for proper recruitment and assembly of Kar9-Bim1 complexes in budding yeast. *Mol. Biol. Cell* **10**, 4420-34.

I performed all the experiments, data analyses and literature review described within this chapter. I wrote the Introduction, Materials and Methods, and Figure Legends. I also participated with Jackie Vogel in the writing of the Results section, the Discussion section, the preparation of all the figures and editing of the manuscript.

Rita Miller provided the Bim1 antibody and Kar9 2μ vector used within this study. She also edited various versions of the manuscript prior to its publication.

Jackie Vogel wrote the Abstract and Results section. She edited and revised my contributions in all sections. She provided the original scientific plan of which this research was based upon. She also guided this research and supervised my progress during this project.

Chapter 3 is a manuscript in preparation:

I performed all the experiments, data analyses and literature review described within this chapter. I wrote the Summary, Introduction, Results and Discussion section, Materials and Methods, Conclusion and Figure Legends. I also made all the figures in this chapter. I developed the research plan with Jackie Vogel.

Jackie Vogel provided the original scientific plan of which this research was based upon. She also guided this research and supervised my progress during this section of my project. She also edited all sections included in this chapter.

ABSTRACT

Proper spindle placement during asymmetric division is essential for cell fate determination and chromosome inheritance in polarized cells and is achieved through interactions between astral microtubules and the cortex. In the polarized budding yeast, *Saccharomyces cerevisiae,* the proteins Bim1 and Kar9 facilitate spindle placement by localizing to microtubule plus ends (+ends) and promoting their dynamic interactions with the cortex. Both proteins also localize to spindle pole bodies (SPBs), the fungal equivalent to centrosomes, though the functional significance of this localization has remained unclear.

We demonstrate that the localization of Bim1 and Kar9 to SPBs is required for their function on microtubule +ends, and is dependent on the conserved centrosome/SPB component, γ-tubulin (Tub4 in yeast). Canonically Tub4 is involved in microtubule nucleation however, by characterizing a Tub4 mutant (*tub4-*Δ*dsyl*), we demonstrate a novel function for Tub4 in spindle placement. We show that Tub4 facilitates the assembly of functional Bim1-Kar9 complexes at SPBs, prior to their deployment to microtubule +ends by mediating their phosphorylation via the Cdk1 ortholog Cdc28. In *tub4-*Δ*dsyl* cells, Kar9 and Bim1 fail to localize to SPBs and as a result, their regulation and assembly into functional complexes is compromised and microtubule dynamics and spindle placement are perturbed.

Collectively, this work identifies a novel contribution of γ-tubulin/Tub4 in the control of microtubule +end organization during spindle placement. We propose that γ-tubulin/Tub4 is a putative scaffold at centrosomes/SPBs that promotes the proper regulation and assembly of protein complexes involved in coordinating microtubule organization and dynamics.

ABRÉGÉ

Le positionnement du fuseau mitotique est crucial, pour la ségrégation des chromosomes pendant la division asymétrique des cellules, et est facilité par des interactions entre les microtubules astraux et le cortex cellulaire. Chez la levure *Saccharomyces cerevisiae,* les protéines Bim1 et Kar9 facilitent le placement du fuseau en se localisant aux extrémités positives (+end) des microtubules favorisant ainsi leurs interactions dynamiques avec le cortex. Les deux protéines sont également localisées aux corps polaires du fuseau (spindle pole bodies, SPBs), l'équivalent des centrosomes chez la levure cependant, la fonction de cette localisation demeure nébuleuse.

Nous démontrons que la localisation de Bim1 et Kar9 aux SPBs est essentielle pour leur fonction sur les +ends des microtubules et dépend du composant du centrosome/SPB γ-tubulin/Tub4. Tub4 est impliqué dans la nucléation des microtubules cependant, par la caracterisation d'un mutant de Tub4 (*tub4-*Δ*dsyl*), nous avons identifié une nouvelle fonction pour Tub4 dans le positionnement du fuseau mitotique. Nous démontrons que Tub4 facilite l'assemblage des complexes fonctionnels Bim1-Kar9 aux SPBs, avant leur déploiement aux +ends des microtubules, en favorisant leur phosphorylation par Cdk1/Cdc28. Dans les cellules mutantes *tub4-*Δ*dsyl*, Kar9 et Bim1 sont absentes aux SPBs, leur régulation et recrutement dans des complexes fonctionnels est compromis et par conséquent, le positionnement du fuseau est perturbé.

Ce travail identifie une nouvelle contribution de γ-tubulin/Tub4 dans l'organisation des +ends des microtubules pendant le placement du fuseau. Nous proposons ainsi que Tub4 échafaude les centrosomes/SPBs et favorise la régulation et l'assemblage des complexes de protéines impliqués dans l'organisation coordonnée des microtubule.

Introduction

Proper placement of the mitotic spindle during asymmetric cell division is essential for high fidelity chromosome segregation and for determination of the division plane in many polarized cells. Spindle placement is mediated by interactions between astral microtubules and discrete areas of the cortex. Coordination of these interactions depends on the function of microtubule plus end (+end) interacting proteins (+TIPs), which localize primarily to microtubule +ends and govern their dynamics and cortical attachments at these sites. In the polarized budding yeast, *Saccharomyces cerevisiae*, pre-anaphase spindle placement to the bud neck is dependent upon two +TIPs, the EB1 ortholog Bim1 and the APC functional ortholog, Kar9. These +TIPs promote astral microtubule dynamics and link microtubule +ends to polarized actin cables, in order to place the spindle at the bud neck. While Bim1 and Kar9 function primarily on microtubule +ends, they also exhibit a pronounced localization to spindle pole bodies (SPBs) the fungal equivalent to centrosomes, though the functional significance for this localization has remained unclear for some time.

Previously a mutation within the evolutionarily conserved protein γ-tubulin or Tub4 in yeast (*tub4-Δdsyld*)(Vogel and Snyder, 2000), was found to perturb astral microtubule organization, dynamics and spindle placement. This was a surprising finding as γ-tubulin/Tub4 is a conserved component of centrosomes/SPBs and is canonically involved in microtubule nucleation. This result revealed a novel function for Tub4 in spindle placement and more importantly, identified a previously uncharacterized contribution of SPB components in microtubule +end behaviour.

The first major focus of my research has been to understand how the SPB component Tub4 can influence microtubule +end organization and dynamics. To gain further insight into this question, I characterized defects of the *tub4-Δdsyl* mutant. Since *tub4-Δdsyl* cells have defects in pre-anaphase spindle placement, I suspected that this mutation perturbs Bim1 and/or Kar9 function on microtubule +ends. Moreover, I hypothesized that the ability of Tub4

to influence the function of these proteins during spindle placement was related to their localization at SPBs.

Using live cell imaging, I identified that the *tub4-*Δ*dsyl* mutation perturbs the localization of Bim1 and Kar9 to SPBs. Surprisingly I found that in *tub4-*Δ*dsyl* cells, Kar9 localization to microtubule +ends remains intact however, these microtubules still fail to position the spindle. In addition, by performing microscopic and biochemical analyses, I found that the Kar9 complexes in *tub4-*Δ*dsyl* cells contain reduced levels of Bim1. Microtubule dynamics are suppressed in *tub4-*Δ*dsyl* cells, but are restored when Kar9 is deleted from the cell, or when microtubule attachments to the bud cortex are inhibited. This data reveals that defective Kar9 complexes tether microtubule +ends to the cortex in *tub4-*Δ*dsyl* cells, which results in perturbed spindle placement. Therefore, the data presented in Chapter 2 collectively reveals that SPBs, via Tub4, promote the proper assembly of functional Bim1-Kar9 complexes prior to their deployment to microtubule +ends.

The second major focus of my research has been to understand how Tub4 mechanistically influences these events at SPBs, why the function of Kar9 is perturbed in *tub4-*Δ*dsyl* cells and whether the *tub4-*Δ*dsyl* mutation affects the function of Bim1. In Chapter 3, I demonstrate that the inability of Kar9 to promote proper astral microtubule dynamics and spindle placement in *tub4-*Δ*dsyl* cells is a consequence of disrupted Bim1 function. Additionally, I show that Bim1 is differentially regulated throughout the cell cycle in a manner that is dependent on Tub4, Cdc28 and the early B-type cyclins. My work predicts that Bim1 phosphorylation is important for the assembly of Bim1-Kar9 complexes and for their synergistic function in regulating microtubule +end dynamics.

Finally, the results presented in this thesis elucidate a mechanism in which SPBs, via Tub4, promote the formation of functional Bim1-Kar9 complexes by scaffolding cyclins in order to mediate their proper regulation via Cdc28. These findings may represent an evolutionarily conserved mechanism of coordinating microtubule +end behaviour with regulation at centrosomes/SPBs.

Chapter 1: Literature Review

1.1 Overview

Understanding mechanisms that govern the development of a single cell embryo into a multi-cellular organism remains one of the most intriguing areas of study in cell and developmental biology. Cellular diversity is essential to generate all the necessary cell types that constitute the adult organism and in most cases, this occurs via asymmetric cell division. The general mechanisms that underlie asymmetric cell division are conserved from yeast to mammals and are heavily centered upon one major task, spindle placement. Proper spindle placement is a particularly important step, as its placement dictates the plane of cleavage in many animal divisions and is critical for proper segregation of the DNA in all polarized cell types.

Spindle placement is a challenging process for polarized cells, as they must coordinate positional and temporal information with force generation in order to move the spindle to a distinct sub-cellular location. This process is dictated by microtubule interactions with the cortex and a large repertoire of proteins that properly target microtubules and modulate their dynamics and interactions within sub-cellular domains (Pearson and Bloom, 2004). Due to the complexity of this process the polarized budding yeast, *Saccharomyces cerevisiae* has served as a powerful model system for studying mechanisms underlying asymmetric cell division, in particular, those that govern spindle placement. The reason for this is that budding yeast are easily amenable to genetic manipulation, have an obvious polarity that is coupled to distinct stages of the cell cycle, have a simple cytoskeleton and above all, the mechanisms that govern spindle placement in this organism involve evolutionarily conserved proteins.

Studies performed in budding yeast have identified two genetically distinguishable, yet partially redundant pathways for spindle placement (Adames and Cooper, 2000). Both pathways are comprised of many proteins

that localize primarily to astral microtubule +ends in order to regulate microtubule dynamics or facilitate their attachment to the cortex (Adames and Cooper, 2000). Many of these proteins also localize to microtubule organizing centres (MTOCs) such as SPBs in yeast and centrosomes in higher eukaryotes. The functional significance for their localizations to MTOCs has remained elusive for some time. However, recent studies (including work presented here) have begun to uncover novel roles for MTOC components, in particular γ-tubulin, in coordinating the function of microtubule +end protein complexes that regulate microtubule organization and dynamics during spindle placement.

The following literature review begins with a general summary on the establishment of cortical polarity during asymmetric division in three model systems. It then summarizes the combined roles of astral microtubules, molecular motor proteins and +TIPs in translating microtubule organization into force generation that is needed for spindle placement. Finally, a central focus is given to the mechanisms of spindle placement in budding yeast and on recent studies that have demonstrated non-canonical functions of the MTOC component γ-tubulin, in microtubule organization.

1.2 Asymmetric cell division and polarity establishment

Cell division is a fundamental hallmark of life, in which a single cell divides and generates two daughter cells. The simplest type of division is symmetric cell division, where the mother cell divides through its geometric centre and produces two daughter cells of equal size, biochemical content and cell fate (Figure 1.2 A). Such divisions proliferate cell numbers for the formation and replenishment of many tissues. Conversely, cell division can also be asymmetric and generate unequal daughter cells with distinct fates (Figure 1.2 B). The ability of cells to divide asymmetrically is paramount for the establishment of cellular diversity, spatial organization of the developing embryo and the production of stem cell niches.

Figure 1.2 Examples of cell division

Cell division can be symmetric or asymmetric. **(A)** Symmetric cell division. During symmetric cell division, the mother cell divides in its geometric centre (dashed line) to give to two equal daughter cells (size and biochemical content) of identical cell fate. **(B)** Asymmetric cell division. **(B, left panel)** During asymmetric cell division, the mother cell may asymmetrically position its cleavage plane (dashed line) to produce two structurally distinct daughter cells of unequal size and fate. **(B, right panel)** During asymmetric cell division, the mother cell may asymmetrically position cell fate determinants (depicted as yellow shading) relative to the cleavage plane (dashed line) within the cytosol to give rise to two biochemically distinct daughter cells of unequal fate. Double-sided arrow indicates that during asymmetric cell division, the mother cell can use a combination of these methods to produce distinct daughter cells.

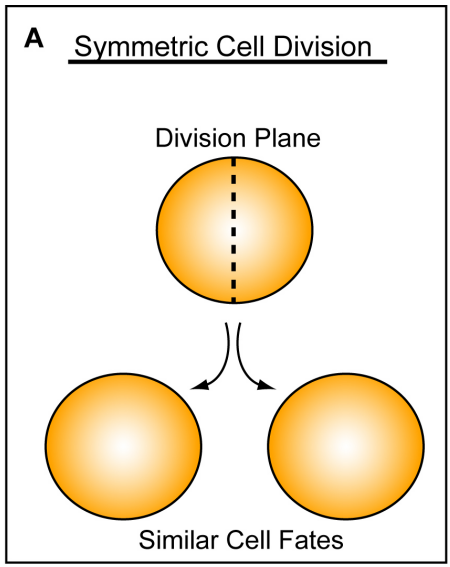
A
Symmetric Cell Division
Division Plane
Similar Cell Fates

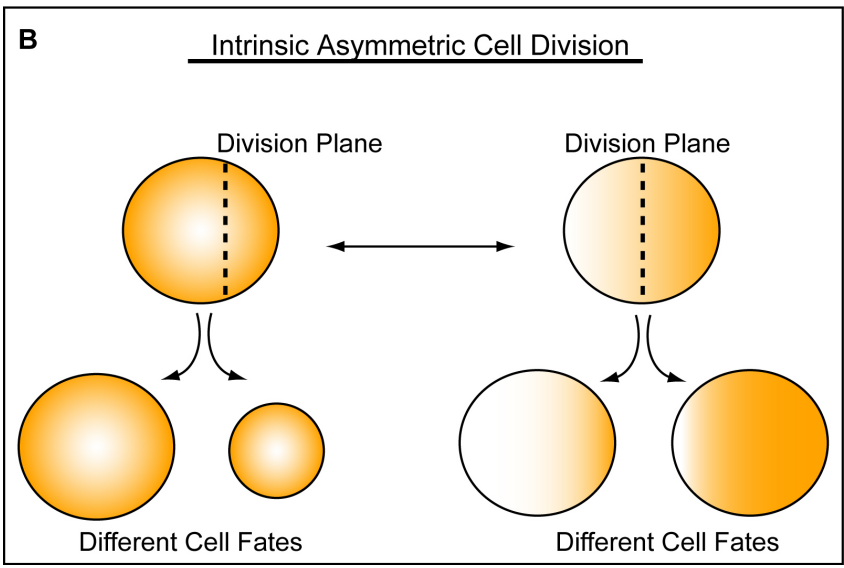
B
Intrinsic Asymmetric Cell Division
Division Plane
Division Plane
Different Cell Fates
Different Cell Fates

Following the completion of an asymmetric cell division, the two resulting cells are created distinct from one another, either biochemically, structurally or a combination of both (Figure 1.2 B) (Horvitz and Herskowitz, 1992). This can result from two mechanisms, i) intrinsic asymmetric cell divisions, where daughter cells are created distinct from one another at the time of division, or ii) the daughter cells are created initially identical but become differentiated as a consequence of later non-autonomous events (Horvitz and Herskowitz, 1992). Tremendous advancements have been made in understanding intrinsic asymmetric cell division through studies conducted in *C.elegans* embryos, *D. melanogaster* neuroblasts and the budding yeast *S. cerevisiae*. In these cell types, cellular diversity arises largely from a program of polarity establishment that is initiated in the mother cell prior to division. Polarity establishment is the first major task for an asymmetrically dividing cell, as this will generate the positional cues required for spindle placement and in many cases, determination of the division axis.

Polarity establishment generally arises in a three-step manner in which an initial polarity cue denotes the cell axis, resulting in polarization of the cortex and finally polarization of the underlying cytoskeleton (Pearson and Bloom, 2004). Polarization of the cytoskeleton, in turn, leads to proper placement of the mitotic spindle. Thus, to understand spindle placement it is first important to understand how intrinsic polarization of the mother is achieved. The following sections review mechanisms of polarity establishment in *C.elegans* unicellular embryos, *D. melanogaster* neuroblasts and *S. cerevisiae* vegetative cells and reveal evolutionarily conserved as well as unique mechanisms that govern this process.

1.2.1 Polarity establishment in the *C.elegans* single celled embryo

The establishment of cortical polarity in the *C. elegans* single celled embryo begins with designation of the anterior-posterior (AP) axis, via the sperm-derived nucleus and the associate centriole pair (Goldstein and Hird,

1996) (Figure 1.2.1 A, i). The site of sperm entry invariably becomes the posterior end of the embryo (Goldstein and Hird, 1996). Interestingly it is the sperm-contributed centrosome, not the nucleus or DNA that is important for the initiation of AP axis formation (Sadler and Shakes, 2000). Centrosomes provide a 'polarity cue' needed for axis determination, though it is unclear whether this depends on their pericentriolar proteins or associated astral microtubules (Cowan and Hyman, 2004; Tsai and Ahringer, 2007). Following the initial polarization cue, the cortex then becomes polarized via the asymmetric localization of the PAR proteins (Kemphues *et al.*, 1988; Kemphues, 2000) and polarized contraction of the cortex (Cowan and Hyman, 2004) (Figure 1.2.1 A).

The PAR proteins (PAR1-6) were identified in a screen designed to identify regulators of cytoplasmic partitioning in *C.elegans* embryos (Kemphues *et al.*, 1988). An additional protein, atypical protein kinase C (aPKC), was also discovered to similarly work in establishing cortical polarity (Izumi *et al.*, 1998; Tabuse *et al.*, 1998). Many PAR proteins and aPKC are enriched at the cell cortex and following axis determination, exhibit an asymmetric distribution to either the anterior or posterior side of the cortex (Kemphues, 2000). PAR asymmetry at the cortex influences the asymmetric localization of downstream cytoplasmic determinants, fate determinants and cytoskeleton organization. (Kemphues, 2000). Several GTPases, including the evolutionarily conserved Rho family GTPase Cdc42, also contribute to these processes by reinforcing the cortical polarity that is initially established by PAR proteins, through the polarized distribution of F-actin (Figure 1.2.1 A, ii) (Joberty *et al.*, 2000; Lin *et al.*, 2000; Aceto *et al.*, 2006; Motegi and Sugimoto, 2006). It is still largely unclear how PAR proteins polarize the cortex downstream of their asymmetric localization. It is likely through a number of mechanisms including, localization of G-protein signaling regulators, linking the cortex with microtubule motors and locally affecting microtubule dynamics (Munro, 2006).

Figure 1.2.1 Cortical polarity establishment during asymmetric division

(A) Polarity establishment in the single celled *C.elegans* embryo. **(A, i)** Cortical polarity begins with fertilization and anterior-posterior (AP) axis formation. The site of sperm entry becomes the posterior side of the embryo. At this time all PAR proteins (blue & red) are symmetric. **(A, ii)** Following axis determination, cortical polarity is achieved via asymmetric distribution of the PAR proteins and cortical ruffling at the anterior side of the cortex. Par-1/2 are posteriorly localized (blue) while Par-3/6 and aPKC (red) become anteriorly localized. Cdc42 also maintains posterior polarity. Cortical flow (black arrows) contributes to spindle placement. The oocyte pronucleus also migrates towards the anterior side. **(B)** Polarity establishment in *Drosophila* neuroblasts. **(B, i)** Cortical polarity begins with delamination of neuroblasts from the neuroectoderm and apical-basal (AB) axis formation. **(B, ii)** Next, cortical polarity is achieved through the asymmetric distribution of Bazooka/Par-3, Par-6, aPKC (red) to that apical side. Cell fate-determinants are recruited to the basal side (blue). PARs and aPKC recruit additional factors such as, Pins, Ins, Gαi (green) that mediate spindle placement. **(C)** Polarity establishment in vegetative *S.cerevisiae* cells. **(C, i)** Cortical polarity establishment begins with accumulation of polarity proteins (polarisome red disk) to presumptive bud site and determination of the long mother-bud (M-B) axis. Bud site selection is dictated by the bud scar (grey circle) from the previous division. **(C, ii)** Following axis determination, polarized growth begins through recruitment of Cdc42 and deposition of cell wall material. Spindle placement occurs through interactions between astral microtubules (green) and the bud neck and tip. Growth machinery is redirected to the bud neck via regulatory events mediated by Cdc28 and Pho85 during cytokinesis.

A) Polarity establishment of the *C.elegans* single cell embryo

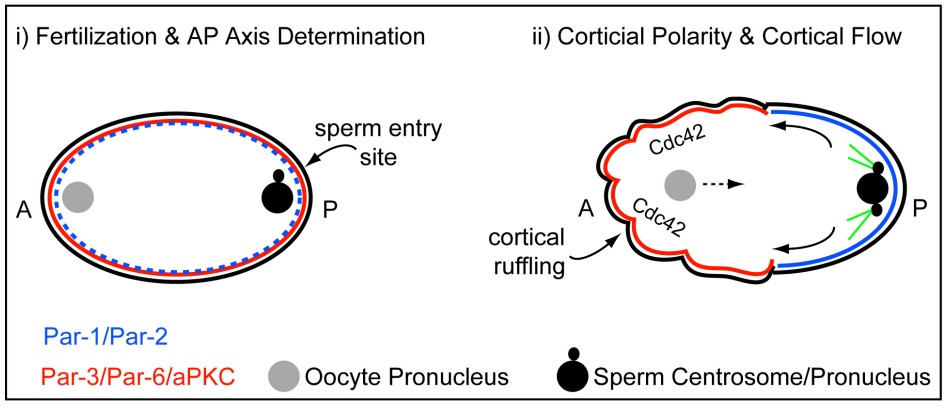

B) Polarity establishment in *Drosophila* neuroblast stem cells

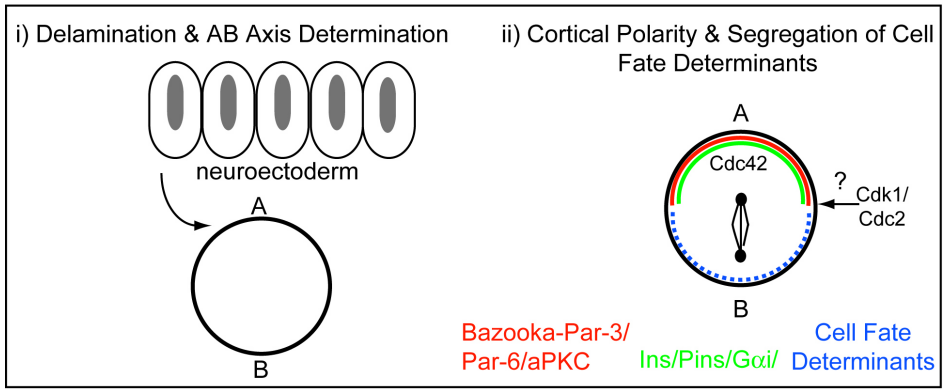

C) Polarity establishment in vegetative *S.cerevisiae* cells

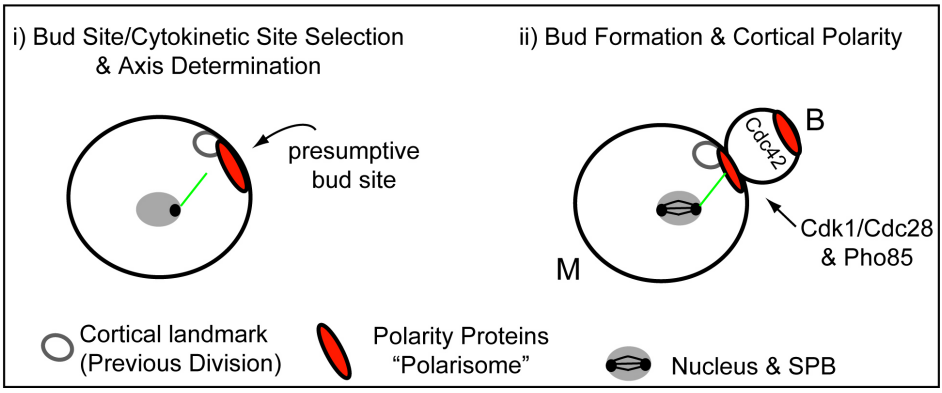

In *C.elegans* embryos, cortical polarization is also achieved via an interesting phenomenon involving polarized contraction of the cortex (Figure 1.2.1 A, ii). This phenomenon results from actin/non-muscle myosin II dependent cortical ruffling of the anterior side of the embryo (Strome, 1986; Cowan and Hyman, 2004). Conversely, the posterior side of the embryo undergoes smoothening of the cortex, resulting in a pseudo-cleavage furrow at the AP (ruffled-smooth) boundary (Hird and White, 1993). The domains of contraction and smoothening correspond to domains defined by the PAR proteins, suggesting that the two processes are coordinated (Cowan and Hyman, 2004). However, neither PAR asymmetry nor cortical ruffling depends on the other to occur, indicating that these are parallel responses to the same polarity cue provided by the sperm centrosome (Cowan and Hyman, 2004).

Cortical polarity establishment in the *C.elegans* zygote via PAR asymmetry and cortical contraction, enables the asymmetric distribution of cytoplasmic determinants during a process termed cortical flow (Hird and White, 1993). Cortical flow enables cytoplasmic material near or adjacent to the cortex to flow in a constant and directed manner from one area of the embryo to the other (Figure 1.2.1 A, ii). Cortical polarity and cortical flow are essential prerequisites for proper asymmetric placement of the spindle (Kemphues *et al.*, 1988), as both processes give rise to an asymmetric distribution of proteins known as 'force generators' within the cortex (Labbe *et al.*, 2003; Labbe *et al.*, 2004). Force generator is a generalized term describing proteins that promote microtubule dynamics and/or facilitate pulling forces on astral microtubules at the cortex to enable spindle placement. A number of structurally and functionally diverse proteins are classified as force generators, some of which are discussed in further detail in later sections. Thus, the *C.elegans* zygote clearly demonstrates that proper spindle placement depends on a number of events that begin on the initial establishment of cortical polarity in the mother cell.

1.2.2 Polarity determination in *Drosophila* neuroblast stem cells

In recent years, the asymmetric divisions of stem cells have emerged as a major focus of investigation. Stem cells asymmetrically divide in order to replicate themselves and remain undifferentiated (totipotent or pluripotent), while producing daughter cells that will follow a specific differentiation path. Unlike embryonic divisions, stem cells are propagated in “niches”, which are distinct cellular locations that protect stem cells from depletion (Scadden, 2006). Stem cells must remain in close proximity to the niche in order to maintain their self-renewing potential. Furthermore, stem cells rely on a combination of both extrinsic and intrinsic mechanisms to properly execute asymmetric division and many of the intrinsic mechanisms just described for *C.elegans* embryos are utilized. These mechanisms have been best characterized during the asymmetric divisions of *Drosophila* nervous system progenitor cells called neuroblasts (Chia *et al.*, 2008).

Neuroblasts are derived from the ventral neuroectoderm of the central nervous system. They delaminate from the overlying epithelial layer and lie beneath this layer to undergo repeated rounds of asymmetric cell division to produce a small basal daughter cell known as the ganglion mother cell (GMC) and a larger apical daughter cell that continues to divide asymmetrically in a stem cell fashion (Betschinger and Knoblich, 2004). Like *C.elegans* embryos, cortical polarity begins with a polarization cue that results in determination of a cell axis. It is thought that in neuroblasts, the polarity cue resulting in the formation of an apical-basal (AB) axis is inherited from the polarity already established in the overlying epithelial layer (Figure 1.2.1 B, i). The reason for this is as neuroblasts delaminate from the epithelial layer a stalk containing PAR proteins is formed, which leads to the PAR proteins becoming localized to the apical cortex of the neuroblast.

Once determination of the AB axis is achieved during neuroblast delamination, cortical polarity is established through the apical localization of several PAR proteins, Bazooka-Par3, Par6 and aPKC (Wodarz *et al.*, 1999)

(Figure 1.2.1 B). The localization of Par6 and aPKC requires the GTPase, Cdc42, suggesting their localization is dependent on polarized cortical F-actin (Atwood *et al.*, 2007). Therefore, a major commonality in both *C.elegans* embryos and *Drosophila* neuroblasts is that an initial polarization cue leads to the establishment of cortical polarity via asymmetric localization of the PAR proteins and Cdc42 dependent actin polarization (Figure 1.2.1 A & B).

In neuroblasts, cell cycle regulators such as the cyclin dependent kinases (CDKs) also appear to be important for establishing cortical asymmetry (Figure 1.2.1 B, ii). It was previously shown that a mutation within the CDK, Cdc2, causes a failure to asymmetrically localize apical and basal components of the neuroblast asymmetric machinery, resulting in the production of symmetric divisions (Tio *et al.*, 2001). While this is a relatively new avenue of study and the mechanism of Cdc2 activity in promoting asymmetry remains elusive, its involvement suggests an interesting coupling between cell cycle progression and the establishment of cortical polarity.

Finally, as is the case for *C.elegans* embryos, cortical polarity establishment is important for proper placement of the spindle in neuroblasts. Apical localization of Bazooka-Par3 and Par-6 promotes the apical localization of cytoplasmic determinants including, Inscuteable (Insc), Partner of Inscuteable (Pins) and heterotrimeric G-protein α-subunit (Gαi) (Figure 1.2.1 B). These proteins positively reinforce Bazooka-Par3/Par-6 asymmetry and also have important roles in spindle placement (Wodarz *et al.*, 1999; Betschinger and Knoblich, 2004). For example, ectopic expression of Insc was shown to reorient the spindles in other epithelial cells (Kraut *et al.*, 1996). In addition, Pins and Gαi bind to the *Drosophila* NuMA-like protein Mud (Mushroom body defect), which is required to orient the spindle by associating directly with microtubules and the microtubule motor (and force generator) dynein/dynactin (Siller *et al.*, 2006).

In sum, the ability of the PAR proteins and the actomyosin cytoskeleton to establish cortical polarity in both *C.elegans* zygotes and *Drosophila* neuroblasts is an essential prerequisite for proper spindle orientation. Studies in

both organisms have been integral to the current understanding of evolutionarily conserved mechanisms of polarity establishment during asymmetric division. One caveat to both systems is that extrinsic factors also contribute to the initiation of asymmetry, such as the entry of sperm in the case of *C.elegans* zygotes. Thus, combining the mechanisms of polarity establishment learnt from these two invertebrate systems with those derived from studies using the unicellular budding yeast has been paramount in strengthening our understanding of intrinsic mechanisms that govern asymmetric cell division.

1.2.3 Polarity establishment in the unicellular budding yeast

In the unicellular budding yeast, *Saccharomyces cerevisiae,* polarization of the cortex begins when the mother cell initiates a program of polarized growth to form a bud, creating a long cell axis (or mother-bud axis) along which the spindle is aligned (Figure 1.2.1 C). Simultaneously, an asymmetric division axis at the mother/bud boundary (known as the bud neck) is also established that will result in the production of a mother and daughter cell of different size and biochemical composition (Figure 1.2.1 C, i) (Mata and Nurse, 1998; Chang and Peter, 2003). This is one major difference between asymmetric divisions of budding yeast versus other systems; the future division plane is established when the cortex becomes polarized, rather than the division plane being dictated by placement of the spindle (Mata and Nurse, 1998).

Bud formation is established via two genetically separable systems that either define the location of the presumptive bud site within the cortex or contribute to the actual formation of the bud (Chant and Herskowitz, 1991). Bud formation involves the polarized accumulation of growth material such as, septins, chitin, actin and secretatory vesicles to a defined region of the cortex (Farkas *et al.*, 1974; Lew and Reed, 1993). To target this growth machinery to the correct localization, numerous polarity proteins (Bud1-5*,* Bud8-10*,* and Rax2) are first recruited to the presumptive bud site (Bender and Pringle, 1989; Chant *et al.*, 1991; Chant and Herskowitz, 1991; Zahner *et al.*, 1996; DeMarini

et al., 1997; Park *et al.*, 1999; Chen *et al.*, 2000; Taheri *et al.*, 2000). Polarity proteins recognize cortical landmarks such as the septin ring and chitin ring from previous divisions (known as the bud scar) and initiate signaling cascades that polarize F-actin at the cortex to form a bud relative to this site (Figure 1.2.1 C, i). F-actin polarization depends on the recruitment and activation of the Cdc42 guanine nucleotide exchange factor (GEF) Cdc24 and GTPase activating protein (GAP) Bem1, though other GAPs and GEFs are involved (Sloat *et al.*, 1981; Adams *et al.*, 1990; Johnson and Pringle, 1990). Cdc42 promotes formation of actin patches and cables at the bud tip during the apical growth. These act as docking sites or highways for the localized secretion of new cell membrane and cell wall material needed for growth (Adams and Pringle, 1984; Kilmartin and Adams, 1984; Chang and Peter, 2003). Thus, Cdc42 has a conserved function in polarizing the cortex during various asymmetric divisions and in the case of budding yeast, for promoting polarized growth.

Interestingly in some budding yeast cells, spindle pole bodies (SPBs), the fungal centrosome equivalent, can play a role in the initial establishment of polarity. During the first zygotic division following mating and cell fusion, bud emergence coincides with the position of the SPB (Maddox *et al.*, 1999). Likewise, it was previously demonstrated that physical disruption of SPB localization in zygotes causes bud formation to occur near the position of the mis-localized SPB (Byers and Goetsch, 1974). Therefore, in certain asymmetric divisions such as *C.elegans* embryos and budding yeast first zygotic divisions, polarity establishment may be dictated by the centrosome/SPB.

Similar to the other asymmetric divisions described, in budding yeast cortical polarization is the major requirement for proper spindle placement. Early spindle placement to the bud neck depends on interactions between astral microtubules and the bud neck and bud tip (sites of polarized actin) (Palmer *et al.*, 1992; Theesfeld *et al.*, 1999; Segal and Bloom, 2001; Kusch *et al.*, 2002). The interactions between astral microtubules and the bud neck/tip are mediated by a number of cortical adaptors and force generators that will be described in later sections. Thus, the studies performed in these three described model

systems reveal that asymmetrically dividing cells exert tremendous efforts to establish cortical polarity so that downstream cytoskeletal elements and force generators are appropriately polarized. In turn, these proteins can then proceed to properly position the spindle to ensure high fidelity chromosome inheritance. As in all divisions, proper inheritance of the DNA during asymmetric cell division must be maintained for the healthy development of the organism or the continued propagation of the species.

1.3 Spindle orientation in asymmetrically dividing cells

In order to promote proper DNA inheritance, the division plane and spindle axis are often perpendicular to one another. This is particularly challenging process for polarized cells, as it must be coordinated with both temporal (proper cell cycle stage) and spatial (cellular polarity) information. Therefore, during asymmetric division cells rely on mechanisms that generate forces needed to move the spindle to a distinct cellular location in a timely manner. Efficient force generation depends largely on interactions between dynamic astral microtubules and cortical domains defined during cortical polarization (Pearson and Bloom, 2004). The proper targeting of microtubules to these sites, as well as the regulation of their dynamics and attachments are governed by a number of force generating proteins that associate with microtubules, the microtubule organizing centre (MTOC) and/or the cortex. Collectively these proteins translate the strength and dynamic properties of microtubules into coordinated and efficient mechanical force that culminates in spindle movement. The following sections provide a general overview on the contributions of astral microtubules, motor proteins and microtubule plus end binding proteins (+TIPs) in generating the force required for accurate spindle placement in polarized cells.

1.3.1 Astral microtubule interactions with the cortex generate forces required to orient the spindle

Microtubules are the main structural components that drive force production for a number of cellular processes. Microtubules are proteinaceous polymers comprised often of 13 protofilaments assembled together into a 25 nm hollow cylindrical structure (reviewed in (Mandelkow and Mandelkow, 1989)). Each protofilament consists of αβ-tubulin heterodimers arranged in a head-to-tail manner, which gives the microtubule an overall polarity (Nogales *et al.*, 1999). Microtubules exhibit a property known as 'dynamic instability' whereby these polymers can switch between phases of growth and shrinkage, a trait that is important for their ability in generating force (Mitchison and Kirschner, 1984a; Desai and Mitchison, 1997). *In vitro* analyses of microtubules revealed that one end (the plus end; +end) is more dynamic than the other end (the minus end; -end) (Mitchison and Kirschner, 1984b). In some eukaryotes, microtubule dynamics are observed at the -end *in vivo* (Mitchison and Salmon, 1992), however in budding yeast, dynamics are largely restricted to the microtubule +end (Maddox *et al.*, 2000). In many cell types, microtubule -ends are associated with a microtubule organizing centre (MTOC) such as the centrosome or SPB, which restricts their dynamic behaviour (Mandelkow and Mandelkow, 1990; Maddox *et al.*, 2000).

An influential study that inhibited centrosome movements provided one of the first clues that spindle orientation occurred via 'connections' between centrosomes and the cell periphery (Hyman, 1989). These connections have since been identified as those between astral (or cytoplasmic in the case of yeast) microtubules and the cortex and understanding how such interactions generate force is a large area of study (Pearson and Bloom, 2004; Tolic-Norrelykke, 2008). It is known that for many cell types, spindle orientation largely results from microtubule-mediated pulling forces at the cortex (Tolic-Norrelykke, 2008). Pulling forces can arise from associations between the lateral surface of the microtubule and the cortex, as well as depolymerization of

microtubule +ends that are dynamically tethered to the cortex (Adames and Cooper, 2000).

To effectively pull the spindle towards a distinct cellular location, astral microtubules must be targeted to specific cortical domains that lie within the vector of desired motion. As already mentioned, these domains are often defined during cortical polarity establishment. For example in *C.elegans* single celled embryos, placement of the spindle towards the posterior side of the embryo depends on targeted interactions between astral microtubules and cortical areas defined by the posterior PAR proteins (Colombo *et al.*, 2003; Labbe *et al.*, 2003). Similarly in *Drosophila* neuroblasts, spindle orientation along the AB axis depends on targeted interactions between microtubules and the apically localized protein Mud, whose localization is dictated downstream of apical Par-3 (Bowman *et al.*, 2006; Izumi *et al.*, 2006; Siller *et al.*, 2006; Nipper *et al.*, 2007). Additionally in yeast, early spindle placement to the bud neck requires astral microtubule targeting to the polarized bud neck and bud tip regions, which are defined during cortical polarity establishment (Byers and Goetsch, 1975; Carminati and Stearns, 1997; Segal *et al.*, 2000; Kusch *et al.*, 2002; Segal *et al.*, 2002; Huisman *et al.*, 2004; Haarer *et al.*, 2007).

Astral microtubule targeting to these cortical domains, as well as their ability to subsequently produce force, depends on their association with force generating proteins. Together these proteins function by linking the microtubules to cortical substructures and/or by locally regulating the dynamical properties of microtubules in order to generate pulling forces that facilitate spindle movement. In *C.elegans* embryos, spindle positioning occurs via an asymmetric distribution of force generators within the posterior cortex that promote astral microtubule dynamics and generate pulling forces on the spindle in this direction (Grill *et al.*, 2001; Grill *et al.*, 2003; Labbe *et al.*, 2003). An analogous situation occurs in budding yeast. To achieve spindle placement at the bud neck, astral microtubules from the SPB proximal to the neck ($SPB_{\mathbf{b}}$) are more dynamic relative to those that emanate from the opposite pole. This is due to the asymmetric recruitment of force generating proteins to their +ends that target

these microtubules to the bud neck and tip and promote dynamics and pulling forces on the spindle at these sites (Miller and Rose, 1998; Segal *et al.*, 2000; Kusch *et al.*, 2002; Liakopoulos *et al.*, 2003). Thus, locally accumulating force generators targets microtubules and promotes pulling forces and spindle movement in a directed manner.

To ensure that spindle placement occurs at the appropriate time of the cell cycle, microtubule dynamics and pulling forces are temporally regulated. In *C.elegans,* asymmetric pulling forces on the spindle from the posterior side of the cortex occur during early prophase, yet prior to this time these forces are balanced by opposing pulling forces on the anterior side (Labbe *et al.*, 2004). Temporal coordination of these forces is governed by a G-protein repression system that inhibits the function of force generators until mitotic onset (Kimura and Onami, 2007). Likewise in yeast, spindle positioning depends on two temporally distinguishable pathways involving the force generators, Kar9 and the microtubule motor dynein (Li *et al.*, 1993; Miller and Rose, 1998; Adames and Cooper, 2000). The transition between these two pathways appears to be temporally regulated by different Cdc28/cyclin complexes (Loog and Morgan, 2005). Kar9 localization and function is temporally coordinated by the efforts of Cdc28 in combination with the early B-type cyclins, Clb4 and Clb5 (Liakopoulos *et al.*, 2003; Moore *et al.*, 2005; Moore and Miller, 2007). Conversely, the localization and function of dynein is coordinated by the efforts of Cdc28 and the late B-type cyclins, Clb1 and Clb2 (Grava *et al.*, 2006).

In sum, astral microtubule interactions with pre-defined cortical sites are essential for the production of forces necessary to position the spindle. This depends on force generating proteins that regulate microtubule dynamics and couple them to precise areas of the cortex. Spatial and temporal restriction of pulling forces enables the cell to confer directionality of spindle movement with appropriate cell cycle progression. A number of studies in various organisms have focused on identifying and characterizing the function of force generators in order to better understand the intricacies involved during spindle placement. The following sections describe two major classes of force generators namely,

motor proteins and +TIPs, that have significant roles in spindle placement. A specific emphasis is placed on force generating proteins that function during spindle placement in budding yeast.

1.3.2 Motor proteins act as force generators during asymmetric spindle placement

Interactions between astral microtubules and the cortex are essential for the generation of pulling forces that facilitate proper spindle placement during asymmetric division. Force generators mediate this process through a number of ways including, locally regulating microtubule dynamics and/or actively pulling on microtubules. Some of the best-studied force generators are cytoskeletal motor proteins, which travel along microtubules or actin filaments. Three cytoskeletal motor protein families exist namely, myosin, kinesin and dynein. Myosin and kinesin motor families share many similarities in terms of their mechanisms of movements since they evolved from a common origin (Vale and Milligan, 2000), whereas dynein is the most divergent motor family and is most similar to the AAA family of ATPases (Neuwald *et al.*, 1999).

Motor proteins are a specialized group of proteins that travel along their cytoskeletal tracks by converting chemical energy from ATP hydrolysis into mechanical movement (reviewed in (Wu *et al.*, 2006)). This process is known as the mechanochemical cycle and involves a series of events that lead to biochemical and conformational alterations of their motor domains; the domain that binds ATP and the track to confer movement (Skowronek *et al.*, 2007). Many motor proteins travel processively, meaning that they can couple multiple rounds of ATP hydrolysis with movement and travel large distances without diffusing away from their tracks (Skowronek *et al.*, 2007). Furthermore, many processive motors have multiple motor domains and travel along their track in a ‘hand-over-hand’ manner (or some variation of this), since having multiple motor domains enables one domain to always remain attached to the track (Yildiz *et*

al., 2003; Yildiz *et al.*, 2004; Reck-Peterson *et al.*, 2006; Toba *et al.*, 2006; Gennerich *et al.*, 2007).

The ability of motors to couple movement along its cytoskeletal track is a result of their ability to bind multiple cargoes, via distinct domains. Depending on the motor in question, cargoes can include other cytoskeletal elements, plasma membrane, membrane vesicles, cortical proteins and/or other force generating proteins that directly regulate microtubule dynamics. Therefore, motors can generate movement directly by linking microtubules to the cortex or other cytoskeletal elements to generate tension, or indirectly generate force by influencing microtubule dynamics via the proteins they transport. Notably, both of these mechanisms are utilized in budding yeast.

One of the best-studied motor proteins involved in force generation during spindle placement is the budding yeast actin-based motor protein, Myo2. Myo2 is a member of the processive class V actin-based motors and travels towards the barbed ends (growing ends) of actin cables (Johnston *et al.*, 1991; Cheney *et al.*, 1993; Mehta *et al.*, 1999; Reck-Peterson *et al.*, 2001). Though Myo2 travels on actin cables, it generates a directed pulling force on the spindle by associating with astral microtubules and targeting them towards the bud neck and tip during early spindle orientation (Beach *et al.*, 2000; Yin *et al.*, 2000; Hwang *et al.*, 2003; Liakopoulos *et al.*, 2003). This is made possible as the cargo-binding domain of Myo2 can bind the protein Kar9, which is localized to astral microtubule +ends (discussed in further detail in section 1.4.2). Interestingly, it was recently discovered that reversible phosphorylation within the cargo binding domain of Myosin V in metazoans dictates its cargo binding specificity, though whether this is relevant for Myo2 and spindle placement in budding yeast remains unknown (Legesse-Miller *et al.*, 2006).

Another motor protein that has a well-characterized role during spindle placement in budding yeast is the microtubule-based motor Kip2, which is a kinesin family motor that travels towards the microtubule +end (Cottingham and Hoyt, 1997; Miller *et al.*, 1998; Carvalho *et al.*, 2004). Kip2 promotes spindle placement and force generation largely in an indirect manner, based on the

cargoes it transports as it travels. For instance, Kip2 has been shown to transport the microtubule binding protein Bik1 to microtubule +ends in budding and fission yeast, which is a force generating protein important for coordinating microtubule dynamics during both G1 and mitosis (Browning *et al.*, 2003; Sheeman *et al.*, 2003; Busch *et al.*, 2004; Carvalho *et al.*, 2004; Wolyniak *et al.*, 2006). Moreover, the association between Kip2 and Bik1 promotes the +end accumulation of cytoplasmic dynein, which generates pulling forces on the spindle during anaphase (Carvalho *et al.*, 2004). Thus, Kip2 indirectly generates force production during spindle placement largely by transporting factors that promote microtubule pulling and or dynamics to the microtubule +end and cortex.

The budding yeast kinesin, Kip3, is also involved in spindle placement yet in contrast to Kip2, this kinesin motor has a more direct role in force generation. Kip3 is both a +end directed motor and +end specific depolymerase (Cottingham and Hoyt, 1997; DeZwaan *et al.*, 1997; Miller *et al.*, 1998; Gupta *et al.*, 2006; Varga *et al.*, 2006). Kip3 helps regulate the length of microtubules that have been properly targeted into the bud by Kar9-Myo2 complexes and also anchor them to the cortex (Gupta *et al.*, 2006). As microtubules make contact with the cortex, the depolymerizing activity of Kip3 is enhanced and shortens the microtubule, which ultimately exerts a pulling force on the spindle towards the bud neck (Gupta *et al.*, 2006; Varga *et al.*, 2006). In divergent cells, loss of Kip3 related Kinesin-8 motors has dramatic effects on microtubule lengths, suggesting that Kinesin-8 in other eukaryotes may have a similar role in force generation and regulation of microtubule length (Howard and Hyman, 2007).

Finally, one of the most evolutionarily conserved force generators involved in spindle placement is the microtubule motor cytoplasmic dynein. Dynein is a –end directed microtubule motor that mediates force generation by anchoring to both microtubules and the cortex. As it moves towards the microtubule –end, it causes microtubules to slide along the cortex which generates force. Dynein is implicated in spindle placement in a number of organisms. In *C.elegans*, Gα and Gα-interacting proteins (GPR-1/2 and Lin-5)

recruit dynein to the cortex in order to promote asymmetric spindle placement (Nguyen-Ngoc *et al.*, 2007). In *Drosophila*, the cortically bound Mud protein (ortholog of mammalian NuMA and *C.elegans* Lin-5) facilitates spindle placement partially through dynein recruitment (Bowman *et al.*, 2006; Izumi *et al.*, 2006; Siller *et al.*, 2006; Nipper *et al.*, 2007). Similarly in budding yeast, cortically attached dynein mediates spindle movement into the bud neck during anaphase (discussed in section 1.4.1) (Eshel *et al.*, 1993; Li *et al.*, 1993; Yeh *et al.*, 1995; Adames and Cooper, 2000; Heil-Chapdelaine *et al.*, 2000b; Sheeman *et al.*, 2003; Lee *et al.*, 2005).

In summary, molecular motors play an important role in force generation during spindle placement in various organisms. Intriguingly, much is still unknown regarding how these motors coordinate their activities with other force generators and whether their function is regulated. Future work directed towards understanding their cargo specificity and regulation will enhance our understanding of how motor-derived force generation is properly coupled with cell cycle progression and coordinated with other force generators.

1.3.3 +TIPs coordinate microtubule organization and dynamics to generate pulling forces involved in spindle placement

Analysis of microtubules *in vivo* has revealed complicated dimensions to microtubule dynamics than what was originally observed *in vitro*. This discrepancy is due to a number of proteins that exist in cellular environments and influence microtubule dynamics. This includes molecular motors as just described, but also a number of other proteins than have dramatic effects on microtubule dynamics and force generation. Many of these proteins localize primarily to microtubule +ends and consequently have been termed plus end interacting proteins (+TIPs) (Schuyler and Pellman, 2001). +TIPs fall under the general category of microtubule associating proteins (MAPs), with the distinction that +TIPs primarily localize and exert their function on microtubule +ends.

Three main +TIP families exist in higher eukaryotes and yeast namely, XMAP215/Stu2, EB1/Bim1 and CLIP-170/Bik1 protein families (Pierre *et al.*, 1992; Perez *et al.*, 1999; Mimori-Kiyosue *et al.*, 2000b; van Breugel *et al.*, 2003). These +TIP families are often referred to as the 'core' +TIP families, due to high structural and functional conservation amongst eukaryotes. However, the list of +TIP proteins is large and includes the CLASP (CLIP-associating proteins) family of proteins, dynactin complex members and motor proteins (including those just described) that primarily localize to the +end. An additional important and conserved +TIP is the adenomatous poliposis coli (APC) protein, which is a product of the tumor suppressor gene mutated in many colorectal cancers (Groden *et al.*, 1991; Mimori-Kiyosue *et al.*, 2000a). APC has an evolutionarily conserved role in microtubule organization and its functional ortholog in budding yeast, Kar9, has an important role during spindle placement.

+TIPs bind to microtubules directly via their own microtubule binding domains or by forming associations with other +TIPs or molecular motors (Su *et al.*, 1995; Goodson *et al.*, 2003; Wolyniak *et al.*, 2006; Slep and Vale, 2007). While different +TIPs share a common localization pattern to the microtubule +end, their microtubule binding domains are structurally distinct across families (Slep and Vale, 2007). The structure and size of these domains differ greatly from one another and interact with tubulin at varying strengths. For some +TIPs, dimerization and/or multiple domains are required for microtubule +end localization (Slep and Vale, 2007). Furthermore, in higher eukaryotes many +TIPs such as CLIP-170 and EB1 (Perez *et al.*, 1999) preferentially localize to the +ends of exclusively growing microtubules, though the budding yeast orthologs associate to the +ends of both growing and shrinking microtubules (Carvalho *et al.*, 2004; Wolyniak *et al.*, 2006).

How +TIPs primarily localize to microtubule +ends is still unclear. In budding and fission yeast, the respective CLIP-170 orthologs, Bik1 and Tip1 are transported to the +end via microtubule motor proteins (Busch and Brunner, 2004; Carvalho *et al.*, 2004). Other +TIPs bind tubulin monomers and co-assemble on the polymerizing +end in solution (Folker *et al.*, 2005). A recent

study proposed that +TIPs oligomerize tubulin prior to loading onto the +end and deliver these larger tubulin oligomers to the ends of microtubules (Slep and Vale, 2007). This suggests that +TIPs act as tubulin chaperones and promote microtubule polymerization when tubulin monomer concentrations are low (Slep and Vale, 2007).

The function of +TIPs with respect to force production is quite complex, given that may of these proteins have multiple roles which are often cell cycle dependent (Wolyniak *et al.*, 2006). Furthermore, many +TIPs function on the +ends of both spindle and cytoplasmic microtubules. Major functions of +TIPs include promoting microtubule dynamics and anchoring microtubules to the cortex. In yeast, cytoplasmic microtubules are much less dynamic in cells lacking Stu2, Bim1 and Bik1 and consequently spindle placement is inefficient (Wolyniak *et al.*, 2006). Similarly in *Drosophila*, EB1 was shown to promote dynamic interactions between microtubules and the cortex to facilitate spindle placement (Rogers *et al.*, 2002). Maintaining microtubule dynamics is important for force generation, as dynamic microtubules are needed to initially probe the intracellular landscape in order to become captured at cortical sites by motor proteins, +TIPs or adaptors within the cortex.

Interestingly, many +TIPs interact and can have synergistic or opposing functions. For example, Bim1 and Stu2 function cooperatively in regulating microtubule dynamics, while Bik1 appears to work alone (Wolyniak *et al.*, 2006). Interactions between EB1 and APC, as well as Bim1 and Kar9 are necessary for proper regulation of microtubule dynamics and associations with the cortex (Berrueta *et al.*, 1999; Beach *et al.*, 2000; Korinek *et al.*, 2000; Miller *et al.*, 2000; Nakamura *et al.*, 2001; Green *et al.*, 2005; Cuschieri *et al.*, 2006). A recent study assessed +TIP interaction networks during various cell cycle stages using a visual immunoprecipitation assay (Niethammer *et al.*, 2007). This study revealed that microtubule dynamics and lengths alter during different stages of the cell cycle due to varying ‘cytoplasmic states’ dictated by different +TIP combinations (Niethammer *et al.*, 2007). In interphase, microtubules were stabilized due to inhibition of the microtubule destabilizing +TIP XKCM1

(Niederstrasser *et al.*, 2002) by associations with XMAP215, APC, EB1 and CLIP-170. Conversely in mitosis, microtubules are dynamic because these interactions are lost and XKCM1 is uninhibited (Niethammer *et al.*, 2007). Thus, varying combinations of +TIPs can have dramatic consequences on microtubule dynamics and associations with the cortex.

Understanding the precise function of various +TIPs has also been made complicated by the finding that some +TIPs have functionally relevant post-translational modifications. For instance, phosphorylation of Kar9 by Cdc28/B-type cyclins is integral for the correct localization and function of Kar9 during spindle orientation (Liakopoulos *et al.*, 2003). Likewise, phosphorylation of APC in higher eukaryotes by Cdc2 causes a 4-fold reduction in its binding to EB1 and therefore reduces APC-EB1 interactions and inhibits their function (Trzepacz *et al.*, 1997; Green *et al.*, 2005; Honnappa *et al.*, 2005). CLIP-170 and $p150^{glued}$ of the dynactin complex are phosphorylated, which appears to alter the binding of these +TIPs to microtubules, thereby affecting microtubule dynamics (Rickard and Kreis, 1991; Choi *et al.*, 2002; Vaughan *et al.*, 2002).

While +TIPs exhibit a dramatic localization to microtubule +ends, the term '+TIP' is somewhat misleading as many localize to other sub-cellular locations, which appears to have functional importance. APC/Kar9 and EB1/Bim1 localize to centrosomes or SPBs independently of astral microtubules in mammals and yeast and EB1/Bim1 is a functional component of both organelles (Berrueta *et al.*, 1998; Liakopoulos *et al.*, 2003; Louie *et al.*, 2004; Cuschieri *et al.*, 2006). XMAP215/Stu2 both localize to centrosomes/SPBs and interact with components of these respective MTOCs in both flies and yeast (Wang and Huffaker, 1997; Chen *et al.*, 1998; Lee *et al.*, 2001; Usui *et al.*, 2003). Stu2 also localizes to kinetochores and works with the kinetochore protein Spc24 to maintain spindle integrity (Ma *et al.*, 2007). CLIP-170 localizes to kinetochores in mammals, (Dujardin *et al.*, 1998; Carvalho *et al.*, 2004; Moore *et al.*, 2005) while Bik1 localizes to SPBs in yeast and has important roles at the SPB in regulating microtubule dynamics and anchorage (Chen *et al.*, 1998; Kosco *et al.*, 2001; Lee *et al.*, 2001; Usui *et al.*, 2003).

In summary, +TIP coordination of microtubule behaviour is a complicated field of study. The function of +TIPs can vary depending on their localization and whether they are in complex with other +TIPs or being regulated. What can be appreciated is that +TIPs work alongside molecular motors in creating local and temporal microenvironments of microtubule organization. These proteins orchestrate and fine-tune the properties of microtubules in order to convert these dynamic polymers into efficient force generating machines.

1.4. Spindle positioning in budding yeast

The previous sections introduced complex protein networks that govern proper spindle placement during asymmetric division. Understanding the interplay between these numerous proteins and how they achieve spindle placement is a complicated task. Yet, many mechanistic details of spindle placement have been worked out in the budding yeast, which has enabled researchers to extrapolate key concepts in the regulation of microtubules and force generation during spindle placement in higher eukaryotes. The studies performed in yeast have identified two key pathways that contribute to spindle placement, of which most of the proteins are conserved. These pathways are genetically distinguishable, but are partially functionally redundant. The best-characterized pathway involves cytoplasmic dynein and facilitates placement of the anaphase spindle into the bud neck. The other pathway functions earlier, to promote spindle placement from a position within the mother to the bud neck, and depends on the +TIPs, Kar9 and Bim1. The major differences between these pathways are the proteins involved and the timing at which each pathway becomes dominant.

1.4.1 Dynein dependent spindle positioning in budding yeast

As was briefly discussed, cytoplasmic dynein is one of the most conserved proteins involved in microtubule-based force generation. Cytoplasmic

dynein is a dimeric, processive –end directed motor protein that participates in many processes involving –end directed motion (Schroer *et al.*, 1989; Vallee *et al.*, 2004; Reck-Peterson *et al.*, 2006). It is the most divergent cytoskeletal motor, with many unique qualities in terms of structure and mechanical movement. For instance, dynein can take forward, backward and lateral steps of various sizes, as well as processively move towards both the microtubule –end and +end in the absence of ATP, when under applied force (Reck-Peterson *et al.*, 2006; Gennerich *et al.*, 2007). Such characteristics make dynein family of motors one of the most versatile and widespread motors in terms of function, localization and conservation across eukaryotes.

Dynein function is heavily dependent on its regulator dynactin (Schroer, 2004). Dynactin is a multisubunit protein complex consisting of the proteins $p150^{glued}$/Nip100, dynamitin/Jnm1, Arp1 and Arp24 and is essential for dynein function during spindle placement (McMillan and Tatchell, 1994; Muhua *et al.*, 1994; Kahana *et al.*, 1998; Amaro *et al.*, 2008; Moore *et al.*, 2008). Dynactin promotes dynein processivity, cargo binding and is important for dynein localization (King and Schroer, 2000; Moore *et al.*, 2008). In budding yeast, dynactin colocalizes with dynein on microtubules, the cell cortex and SPBs (Figure 1.4A) (Moore *et al.*, 2008). In addition to dynactin, other proteins also contribute to dynein processivity and localization including, Pac1 (ortholog of the l lissencephaly disease gene product LIS1) and NudL (ortholog of NudE) (Faulkner *et al.*, 2000; Vallee *et al.*, 2001; Lee *et al.*, 2003; Li *et al.*, 2005).

A role for dynein in spindle placement in budding yeast was first discovered when mutations within the gene encoding for dynein (*DYN1* or *DHC1*) were found to cause defects in spindle and nuclear migration (Eshel *et al.*, 1993; Li *et al.*, 1993). Subsequent genetic analyses revealed that the contribution of dynein in spindle placement was distinct from that of Kar9, supporting the existence of two functional pathways of spindle placement in yeast (Cottingham and Hoyt, 1997; DeZwaan *et al.*, 1997; Miller and Rose, 1998; Lee *et al.*, 1999; Heil-Chapdelaine *et al.*, 2000a). Microscopic analyses that assessed microtubule behaviour during spindle orientation, revealed that

initial movements of the spindle towards the bud neck occurs via microtubule end-on capture and shrinkage events, while spindle placement into the bud neck during anaphase occurs through microtubule sliding events along the bud cortex (Carminati and Stearns, 1997; Adames and Cooper, 2000). Sliding events were found to be dependent on dynein, supporting the requirement for this motor in spindle placement during anaphase (Carminati and Stearns, 1997; Adames and Cooper, 2000).

It was initially thought that dynein was recruited to distinct cortical domains within the bud, where it would then promote microtubule sliding along its anchor site as it traveled towards the microtubule –end (Carminati and Stearns, 1997). However, microscopic analysis of fluorescently tagged dynein revealed that this motor is enriched at the SPB_b and microtubule +ends, suggesting that the majority of dynein is not recruited to the cortex but rather delivered by polymerizing microtubules (Figure 1.4 A) (Xiang *et al.*, 2000; Sheeman *et al.*, 2003; Grava *et al.*, 2006). As previously mentioned, +end recruitment of dynein depends on the kinesin-like motor Kip2, which transports dynein via its association with Bik1, though Kip2 independent mechanisms likely also exist (Figure 1.4 A) (Carvalho *et al.*, 2004; Caudron *et al.*, 2008). Once the microtubule +end reaches the cortex, dynein is off-loaded from the microtubule +end and anchored onto the cortex where it can facilitate microtubule sliding (Sheeman *et al.*, 2003; Carvalho *et al.*, 2004; Lee *et al.*, 2005).

Dynein off-loading and anchorage is dependent on dynactin components, Pac1 as well as the membrane associated protein Num1 (Figure 1.4 A) (Heil-Chapdelaine *et al.*, 2000a; Farkasovsky and Kuntzel, 2001). At the cortex, Num1 acts as an anchorage site for dynein accumulation in the bud and also in the mother cortex during anaphase elongation (Heil-Chapdelaine *et al.*, 2000a; Farkasovsky and Kuntzel, 2001). Num1 also promotes dynein processivity once it is localized to the cortex. Interestingly, it has also been proposed that the PP1 type phosphatase Glc7 and its cortical regulator Bud14 also modulate dynein dependent microtubule interactions with the cortex by regulating dynein off-loading and/or processivity (Knaus *et al.*, 2005). This may be achieved by

regulating the phosphorylation status of specific components of the dynein/dynactin complex, though the targets and the exact mechanism of regulation still require further study.

Figure 1.4 Spindle positioning pathways in budding yeast

(A) The dynein pathway of anaphase spindle placement. **(1)** Dynein/dynactin (violet) is a –end directed motor that is transported to microtubule +ends via interactions with Bik1 (green) and the kinesin Kip2 (blue). **(2)** At the cortex, dynein/dynactin are off-loaded and anchored by various factors including, dynactin, Pacl (yellow) and Num1 (orange). These factors also promote dynein processivity. **(3)** Dynein walks towards the microtubule –end and SPB (red), while remaining tethered to the cortex, and in doing so, mediates microtubule sliding. Presumably once dynein reaches the SPB, the cycle repeats until dynein dependent movements are no longer needed. **(B)** The Kar9 pathway of pre-anaphase spindle placement. **(1)** Kar9 (pink) and Bim1 (orange) are recruited to the SPBs in a Tub4 (blue) dependent manner. The role of phosphorylation via Cdc28/cyclin in this event is unclear but seems to depend on both Tub4 and Bik1 (green). **(2)** Bim1-Kar9-Cdc28/cyclin complexes are then transported to the microtubule +end in a manner that may be dependent on Tub4 and/or phosphorylation. **(3)** Once on microtubule +ends, Kar9 associates with the Myo2 motor (brown) traveling along actin cables towards the bud. This association pulls the microtubule and spindle towards the bud neck. **(4)** Once microtubule +ends reach the cortex, the kinesin Kip3 (blue/red) promotes their +end depolymerization at the cortex, which further pulls the spindle towards the bud neck (dashed line).

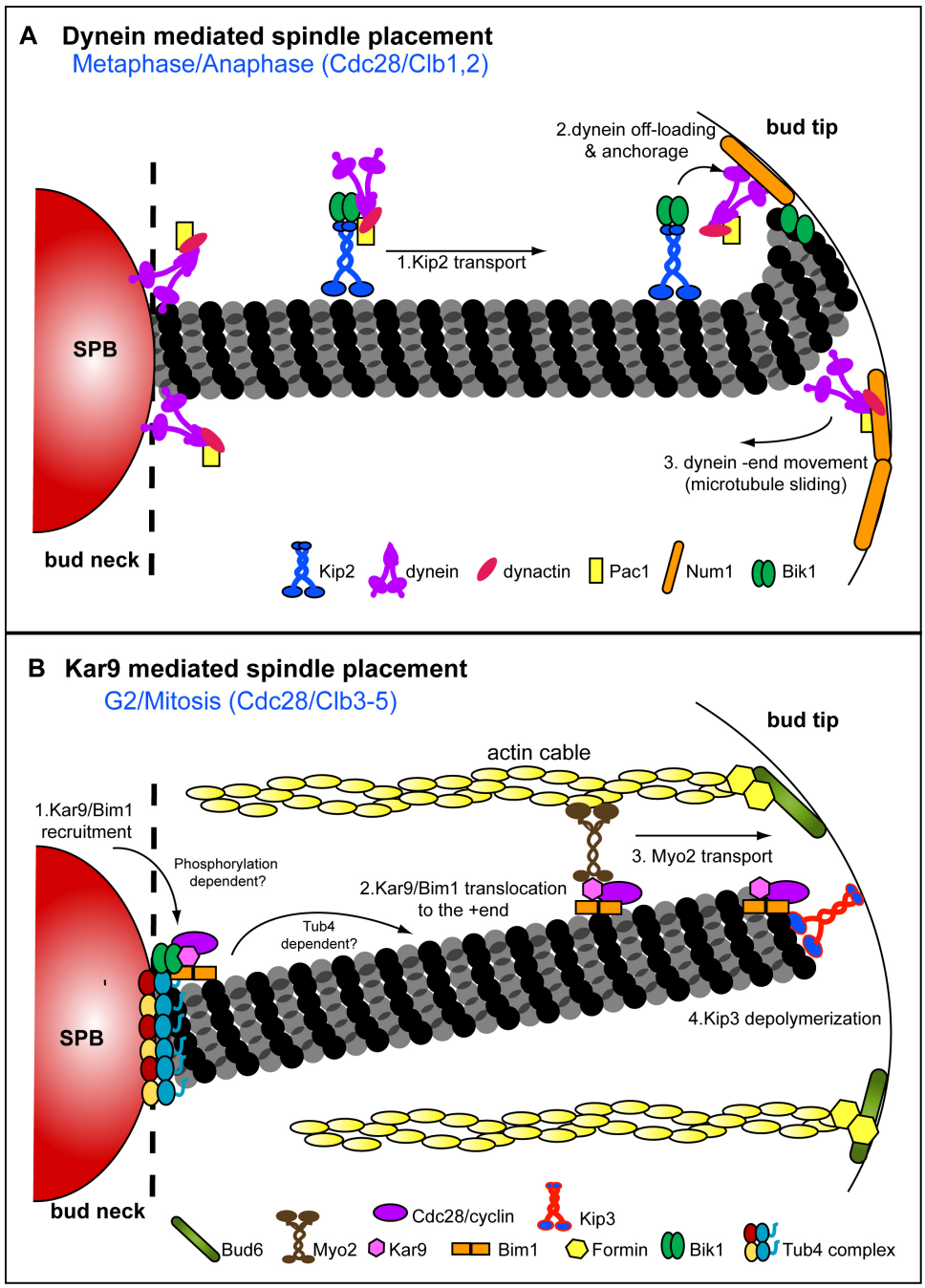
A Dynein mediated spindle placement
Metaphase/Anaphase (Cdc28/Clb1,2)
2.dynein off-loading
& anchorage
bud tip
1.Kip2 transport
SPB
3. dynein -end movement
(microtubule sliding)
bud neck
Kip2
dynein
dynactin
Pac1
Num1
Bik1
B Kar9 mediated spindle placement
G2/Mitosis (Cdc28/Clb3-5)
bud tip
actin cable
1.Kar9/Bim1
recruitment
Phosphorylation
dependent?
3. Myo2 transport
2.Kar9/Bim1 translocation
to the +end
Tub4
dependent?
SPB
4.Kip3 depolymerization
bud neck
Cdc28/cyclin
Kip3
Bud6
Myo2
Kar9
Bim1
Formin
Bik1
Tub4 complex

For dynein to mediate spindle movement into the bud neck, it must be temporally and spatially coordinated with the earlier functioning Kar9 pathway. This coordination appears to happen in several ways. Dynein accumulation to microtubule +ends and cortex is heavily dependent on Bik1 and Kip2, which are upregulated in mitosis (Carvalho *et al.*, 2004). Temporal regulation of Bik1 and Kip2 minimizes the amounts of dynein that associates with astral microtubules +ends prior to mitosis, leaving these microtubule +ends accessible for the Kar9 pathway. Additionally, movement of the spindle into the neck requires an asymmetric localization of dynein to only one side of the spindle, which is regulated by Cdc28 and the late B-type cyclins, Clb1 and Clb2 (Grava *et al.*, 2006). These regulatory complexes appear to act at the SPBs to maintain dynein asymmetry and promote its localization to microtubule +ends (Grava *et al.*, 2006). Also, as the spindle elongates and Clb1 and Clb2 levels begin to decrease, dynein is then symmetrically localized to both the mother and the bud where it facilitates equivalent sliding forces to stabilize spindle placement and elongation during anaphase (Adames and Cooper, 2000; Grava *et al.*, 2006).

Collectively, the research performed in budding yeast has demonstrated the effectiveness of cytoplasmic dynein as a generator of force during anaphase spindle placement. Dynein promotes spindle placement by coupling its movement with astral microtubule sliding along the cortex. As such, spatial and temporal coordination enables the dynein pathway to exert its function at the appropriate time during anaphase.

1.4.2 Kar9 dependent spindle positioning in budding yeast

Prior to the dynein pathway, early spindle placement to the bud neck must be achieved, which is dependent on a less understood pathway involving the +TIP protein Kar9. Kar9 was originally thought to organize microtubules by acting as a cortical capture site for astral microtubule +ends that entered the bud cortex (Miller and Rose, 1998; Miller *et al.*, 1999). Yet microscopic analyses of endogenous Kar9 revealed that it localizes to the $SPB_{\mathbf{b}}$ and to the

+ends of astral microtubules that grow from this pole, rather than at the cortex (Figure 1.4 B) (Liakopoulos *et al.*, 2003; Maekawa *et al.*, 2003). It is unclear how Kar9 is transported from the SPB_b to microtubule +ends. The motor Kip2 may enhance Kar9 accumulation on +ends, though it is not necessary for Kar9 localization to these sites (Maekawa *et al.*, 2003; Moore and Miller, 2007). Alternatively, Kar9 phosphorylation combined with the efforts of SPB components may facilitate the translocation of Kar9 from the SPB to the microtubule +end (Liakopoulos *et al.*, 2003; Cuschieri *et al.*, 2006).

Several studies revealed that Kar9 facilitates spindle placement by linking microtubules and actin cables together through its associations with the actin motor Myo2 (Beach *et al.*, 2000; Yin *et al.*, 2000; Hwang *et al.*, 2003; Liakopoulos *et al.*, 2003; Maekawa *et al.*, 2003). Microtubule +ends that contain Kar9 are pulled along actin cables by Myo2, which results in the proper targeting of these microtubules to the bud neck and bud cortex (Figure 1.4 B) (Kusch *et al.*, 2002). Astral microtubules that are successfully pulled along the bud cortex, are then depolymerized by the +end depolymerase kinesin Kip3 (Gupta *et al.*, 2006). Kip3 appears to promote the depolymerization of these astral microtubules specifically upon cortical contact, which is important to prevent their premature depolymerization prior to reaching the bud (Gupta *et al.*, 2006).

Kar9 has functional similarity to the APC, a protein important for regulating microtubule dynamics and organization in higher eukaryotes (Green *et al.*, 2005). Yet unlike the APC, Kar9 does not bind microtubules directly but rather through interactions with the microtubule +TIP, Bim1 (Schwartz *et al.*, 1997; Miller *et al.*, 2000). Bim1 was originally identified as an interactor of α-tubulin and is important for promoting microtubule dynamics and organization during spindle placement (Schwartz *et al.*, 1997; Tirnauer *et al.*, 1999; Miller *et al.*, 2000). Bim1 is the budding yeast ortholog of the +TIP EB1 and like its higher eukaryotic counterpart, it localizes to centrosomes/SPBs and both spindle and cytoplasmic microtubules, with a preferential localization to the microtubule +end (Su *et al.*, 1995; Schwartz *et al.*, 1997). Bim1 is required to anchor Kar9 to the SPB and astral microtubule +ends, as cells depleted of Bim1 fail to localize

Kar9 to these sites (Liakopoulos *et al.*, 2003). Interestingly, the ability of Kar9 to properly function on microtubule +ends depends largely on its proper associations with Bim1, since mutations that alter the stoichiometry of Bim1-Kar9 complexes affect proper spindle placement and astral microtubule dynamics (Cuschieri *et al.*, 2006). Defects that perturb APC-EB1 interactions in mammalian cells also disrupt proper microtubule dynamics, suggesting that the synergy of these proteins in functioning together as a complex is evolutionarily conserved (Green *et al.*, 2005).

The mechanism of Kar9-dependent spindle placement is coordinated with inherent asymmetries of the two SPBs. The old SPB is normally translocated into the bud (the SPB_b) while the newly duplicated SPB remains in the mother (Pereira *et al.*, 2001). It remains unclear why the newly formed bud inherits the older SPB. It is possible that the old SPB has a type of 'molecular memory' that is important to initiate events within the bud such as spindle formation, following cytokinesis and cleavage. Alternatively, the older SPB may be a more efficient microtubule nucleator and this may be important for the bud, which contains less of the starting material to form a spindle than the mother cell. Further studies are required to fully understand the extent of this phenomenon. The importance of Kar9 to be asymmetrically recruited to the SPB_b is so that it can guide astral microtubules from this pole into the bud (Figure 1.4 B) (Liakopoulos *et al.*, 2003; Maekawa *et al.*, 2003; Maekawa and Schiebel, 2004). This ensures that only one SPB will be inherited by the bud (Liakopoulos *et al.*, 2003).

The ability of Kar9 to asymmetrically localize to the SPB_b is dependent on its phosphorylation status. At SPBs, Kar9 is phosphorylated by Cdc28 in complex with the early B-type mitotic cyclins (Figure 1.4B) (Liakopoulos *et al.*, 2003; Maekawa *et al.*, 2003; Maekawa and Schiebel, 2004; Moore *et al.*, 2005; Moore and Miller, 2007). Kar9 phosphorylation somehow translates into its asymmetric distribution to the old SPB_b and several models have been proposed to explain how this may occur. One model suggests that Cdc28/Clb4 complexes phosphorylate Kar9 at Ser197 and Ser496 at the new SPB destined

to reside in the mother (SPB_m) (Liakopoulos *et al.*, 2003). In this model, phosphorylation is proposed to decrease the affinity of Kar9 for Bim1 at this SPB and therefore promote the relative enrichment of Kar9 at the opposite SPB_b (Liakopoulos *et al.*, 2003). Thus, in this scenario phosphorylation is thought to directly modulate the ability of Kar9 to bind to local SPB factors such as Bim1.

Alternate studies propose that Kar9 asymmetry is largely facilitated via its phosphorylation at the SPB_b by Cdc28/Clb5 complexes and Cdc28/Clb4 (Maekawa *et al.*, 2003; Moore *et al.*, 2005; Moore and Miller, 2007). In contrast to the previous model, this model suggests that Cdc28/Clb5 dependent phosphorylation of Kar9 at Ser496 enables Kar9 to recognize preexisting asymmetries of the two SPBs and enable it to preferentially bind to only the SPB_b. This could occur by either causing phosphorylated Kar9 to be repelled from the SPB_m or attracted to the SPB_b (Moore and Miller, 2007). Furthermore, in the study by Moore et al., 2007, the authors posit that phosphorylation of Kar9 at Ser197 by Cdc28/Clb4 complexes also contributes to maintaining Kar9 asymmetry but is mainly important for releasing Kar9 from the SPB_b and for its proper function in targeting microtubules into the bud. Therefore, in this scenario multiple Kar9 phosphorylation events by different Cdc28/cyclin complexes contribute to Kar9 localization and function (Moore and Miller, 2007).

Taken together, the effects of Kar9 phosphorylation are quite complex and require further study. Though the precise players and mechanisms differ in these models, they highlight a common intriguing theme; that SPBs are hubs of +TIP regulation. Recently my own work, discussed in Chapters 2 and 3, suggests that the conserved centrosome/SPB component γ-tubulin, functions in spindle placement by promoting the proper function, assembly and regulation of Kar9-Bim1 complexes at SPBs, prior to their deployment to microtubule +ends. The next sections introduce the structural components of centrosomes and SPBs with an emphasis on the conserved component γ-tubulin. Furthermore, nucleation and post-nucleation functions of γ-tubulin are also discussed.

1.5 The role of MTOCs in microtubule organization and spindle positioning during asymmetric cell division

Microtubule organizing center (MTOC) is a general term describing a class of specialized structures that direct the assembly and orientation of microtubules in eukaryotic cells. MTOCs include fungal SPBs, protozoan basal bodies, and the higher eukaryotic centrosome. MTOCs provide the nucleation sites on which the initiation of microtubule assembly occurs below the critical concentration of tubulin heterodimers normally required for *de novo* assembly (Mitchison and Kirschner, 1984b). Though the morphologies of MTOCs such as the centrosome and SPBs are quite distinct, these organelles are functionally conserved, especially in regard to their microtubule nucleation function.

The role of MTOCs as a central organizer of the microtubule cytoskeleton has been known for over a century (Stearns and Winey, 1997), yet the mechanism by which MTOCs accomplished this role remained a mystery for some time. A wealth of information has emerged regarding the canonical role of MTOCs in microtubule assembly as well as emerging roles in the control of post-nucleation microtubule organization and dynamics. This is largely due to the landmark discovery of γ-tubulin, a new member of the tubulin superfamily and an evolutionarily conserved component of MTOCs that is required for microtubule nucleation *in vivo* (Oakley and Oakley, 1989; Oegema *et al.*, 1999).

1.5.1 Identification of γ-tubulin; an evolutionarily conserved MTOC component

The primary cellular localization of γ-tubulin is at MTOCs (Oakley and Oakley, 1989; Stearns and Kirschner, 1994; Moritz *et al.*, 1998; Zheng *et al.*, 1998; Oegema *et al.*, 1999). Loss of functional γ-tubulin to these sites causes aberrant mitotic spindle structure, abnormal microtubule curvature and the formation of microtubule bundles in numerous eukaryotic cell types (Oakley *et al.*, 1990; Horio *et al.*, 1991; Stearns *et al.*, 1991; Sobel and Snyder, 1995;

Marschall *et al.*, 1996). These studies revealed the importance of γ-tubulin in microtubule assembly and function and provided the first insight towards the mechanistic understanding of MTOC function in microtubule organization.

γ-tubulin associates to MTOCs as a highly conserved multi-protein complex. This was first identified in centrosomes isolated from *Drosophila* embryos and was found to form a 25 nm open ring structure; the same diameter as a typical 13-protofilament microtubule (Zheng *et al.*, 1995; Moritz *et al.*, 1998). Reconstituted complexes in *Drosophila* and *Xenopus* cells also formed an open ring structure and were designated as γ-tubulin ring complexes (γTuRCs) (Stearns and Kirschner, 1994; Zheng *et al.*, 1995; Moritz *et al.*, 1998). Structurally similar complexes were later identified in centrosomes isolated from oocytes of the surf clam, *Spisula* (Vogel *et al.*, 1997). As purified *Spisula* centrosomes lack mature centrioles, analysis of centrosomal tubulins (α,β,γ) was possible, and revealed that γ-tubulin is the major tubulin constituent of centrosomes (Vogel *et al.*, 1997). γTuRCs are composed of approximately 13 γ-tubulin subunits as well as numerous γTuRC-interacting proteins (GRIPs), and are capable of nucleating the assembly of microtubules *in vitro*. Due to their open ring shape, localization and nucleation capability, γTuRCs have been regarded as the major functional component for microtubule assembly at MTOCs.

The γTuRC structure is evolutionarily conserved across eukaryotes with the exception of unicellular fungi, in which γTuRCs have not yet been identified *in vivo*. However, yeast cells have conserved components of the γTuRC that are assembled into a smaller γ-tubulin complex, known as the γTuSC. In *Drosophila*, the γTuSC is comprised of the three most prominent proteins in the γTuRC; γ–tubulin, Dgrip84 and Dgrip91 (Oegema *et al.*, 1999). This complex was considered primarily as a structural subunit of the γTuRC, due to low levels of detectable nucleation (Oegema *et al.*, 1999). Yet it was recently shown that γ-tubulin is recruited to the MTOC as a γTuSC and centrosomes lacking intact γTuRCs still form microtubules, suggesting that γTuSCs do have some

nucleating capabilities (Verollet *et al.*, 2006). This is consistent with studies in budding yeast, where the sole γ-tubulin complex characterized is most similar to the γTuSC (Knop *et al.*, 1997).

In budding yeast, the γTuSC is composed of two γ-tubulin (Tub4) (Sobel and Snyder, 1995; Marschall *et al.*, 1996; Spang *et al.*, 1996) molecules and one molecule each of the GRIPs, Spc97 and Spc98, orthologs of the Dgrip84 and Dgrip91 respectively (Knop *et al.*, 1997). As γTuRCs have not yet been isolated, the components of the γTuSC appear to be the major effectors of microtubule assembly (Knop *et al.*, 1997). Furthermore, as homologs of Spc97 and Spc98 exist in most organisms, these proteins along with γ-tubulin, likely represent a phylogenetically conserved core complex required for the proper regulation of the γTuRC and other aspects of γTuSC function (Raynaud-Messina and Merdes, 2007).

In budding yeast, SPBs are imbedded within the nuclear envelope and γTuSCs associate to the nuclear and cytoplasmic sides of the SPB. Different receptors on either side of the SPB recruit γTuSCs to these respective faces. On the cytoplasmic side of the SPB, γTuSCs are recruited by the SPB component Spc72, which interacts with Spc98 (Knop and Schiebel, 1998). Conversely, γTuSCs are recruited to the nuclear side via the SPB component Spc110, which interacts with Spc97 and Spc98 (Knop and Schiebel, 1997). γTuSCs are thought to be assembled in the cytoplasm and recruited inside the nucleus by the NLS sequence of Spc98 (Pereira *et al.*, 1998).

1.5.2 The canonical role of γ-tubulin in microtubule nucleation

The canonical role of γ-tubulin is in the coordination of microtubule nucleation. Two models for microtubule nucleation presently exist. The 'template' model suggests that the ring-like γTuRC acts as a template from which microtubules grow (Moritz and Agard, 2001). In this model, γ-tubulins of the γTuRC interact laterally with each other (to maintain their ring formation) and

each γ-tubulin in this ring would form longitudinal associations with α–tubulin at the minus end of the microtubule (Moritz and Agard, 2001). Therefore, each γ-tubulin would nucleate one protofilment. More recently, a modified version of the template model suggests that within the ring, γ-tubulin can also interact with components of the γTuRC other than those in the γTuSC and form longitudinal interactions with α–tubulin and lateral interactions with both α–tubulin and β–tubulin (Moritz and Agard, 2001). This modification explains how an even number of γ-tubulins in the γTuRC (since there are two γ-tubulins in each γTuSC) could generate a microtubule comprised of 13 protofilaments. The second model, known as the 'protofilament' model posits that γ-tubulins of the γTuRC unwind from the ring-like structure and interact longitudinally similar to a protofilament. The γ-tubulins of this protofilament would interact laterally with both α– and β–tubulin to form a sheet that eventually folds into the microtubule (Moritz and Agard, 2001).

To distinguish between these possibilities, localization studies of γ-tubulin were performed which suggested that γ-tubulin is confined to a zone at the end of the microtubule, consistent with the template model (Keating and Borisy, 2000; Wiese and Zheng, 2000). Furthermore, the recently solved crystal structure of γ-tubulin (Aldaz *et al.*, 2005) revealed that γ-tubulin exists mostly in a curved confirmation that is conducive to forming lateral interactions with other γ-tubulins, which would be consistent with the formation of a ring. Therefore, recent work favours the template model as the dominant mechanism of microtubule nucleation.

Interestingly, in addition to its role in microtubule nucleation, a number of studies have identified novel functions for γ-tubulin in the control of microtubule dynamics during spindle placement, cell cycle control and checkpoint response (Cuschieri *et al.*, 2007). Furthermore, it was shown that γ-tubulin is phosphorylated and that phosphroylation influences microtubule organization, dynamics and other possible functions (Vogel *et al.*, 2001). As such, it is becoming widely accepted that γ-tubulin is integral for cellular viability due to its

microtubule nucleation and more recently identified post-nucleation functions.

1.5.3 Post-nucleation functions of γ-tubulin

Numerous studies conducted in various organisms indicate that γ-tubulin has additional functions other than regulating microtubule assembly and structure. For example, several studies suggest that γ-tubulin is involved in the coordination of proper cell cycle progression. In *Aspergillus nidulans*, a mutation within γ-tubulin resulted in a failure to coordinate late mitotic events such as, anaphase A, anaphase B and chromosome disjunction (Prigozhina *et al.*, 2004). In the plant *Arabidopsis thaliana*, a reduction in γ-tubulin levels was previously shown to perturb the completion of cytokinesis (Binarova *et al.*, 2006).

Other studies have implicated γ-tubulin in functioning during checkpoint response. Alanine-scanning mutagenesis of human γ-tubulin identified a subset of mutations that allowed cells to undergo inappropriate mitotic progression in the presence of abnormal spindles (Hendrickson *et al.*, 2001). In healthy cells, when spindle formation is perturbed, cells are arrested in G2/M through activation of the spindle assembly checkpoint (SAC). Mutations within genes that encode components of the SAC typically enable cells to bypass this arrest in the presence of perturbed spindle formation, thus explaining the possible role for γ-tubulin in this checkpoint. A more recent and controversial study proposes that γTuRC components are direct members of the SAC that trigger an arrest when spindle assembly is compromised (Muller *et al.*, 2006).

In addition to these novel roles of γ-tubulin, mutations within the budding yeast γ-tubulin, Tub4, were found to perturb microtubule organization and dynamics during spindle placement, but not inhibit the assembly of microtubules (Vogel and Snyder, 2000; Vogel *et al.*, 2001). This implies a functional overlap in the coordination of microtubule dynamics during spindle placement between γ-tubulin and +TIPs. As such, we were intrigued in understanding how a protein localized to MTOCs, could affect microtubule dynamics and spindle positioning. To investigate this, I characterized defects of a Tub4 mutant that was previously

shown to have perturbed microtubule organization and defective spindle placement (Vogel and Snyder, 2000). The results of this study are presented in Chapter 2 and collectively they demonstrate a role for Tub4 in the Kar9 pathway of spindle placement. Specifically, the data presented in Chapter 2 suggests that Tub4 promotes the proper assembly of Kar9-Bim1 complexes at SPBs prior to their deployment and function on microtubule +ends.

Chapter 2: γ-tubulin Is Required For Proper Recruitment And Assembly Of Kar9-Bim1 Complexes In Budding Yeast

2.1 Summary

During asymmetric division, placement of the mitotic spindle perpendicular to the future division plane is essential for the accurate partitioning of the DNA. In budding yeast, the microtubule plus end interacting proteins (+TIPs) Bim1 and Kar9 promote dynamic interactions between the plus ends (+ends) of astral microtubules and cortical actin to facilitate early spindle placement to the bud neck. While both proteins are thought to function primarily on microtubule +ends, they also associate with spindle pole bodies (SPBs), the fungal equivalent to centrosomes. Yet, the functional relevance of this localization has remained unclear. We have found that a mutant form of the conserved centrosome/SPB component γ-tubulin or Tub4 (*tub4-Δdsyl*) perturbs the localization of Bim1 and Kar9 to SPBs and disrupts early spindle placement. In *tub4-Δdsyl* cells, Kar9 localization to microtubule +ends remains intact yet these microtubules still fail to position the spindle. In addition, microscopic and biochemical analyses suggest that Kar9 complexes in *tub4-Δdsyl* cells contain reduced levels of Bim1. Furthermore, astral microtubule dynamics are suppressed in *tub4-Δdsyl* cells, but are restored when Kar9 is deleted from the cell or when microtubule attachments mediated via Kar9 to the bud cortex are inhibited. This suggests that defective Kar9 complexes tether microtubule +ends to the cortex in *tub4-Δdsyl* cells, resulting in perturbed spindle placement. Our results suggest that SPBs via Tub4, promote the proper assembly of functional Bim1-Kar9 complexes prior to their deployment to microtubule +ends.

2.2 Introduction

In budding yeast, the EB1 ortholog Bim1 and the APC–like protein Kar9 are +TIPs that link astral microtubules to the cortex and facilitate spindle placement at the bud neck prior to anaphase (Carminati and Stearns, 1997; Tirnauer *et al.*, 1999; Beach *et al.*, 2000; Lee *et al.*, 2000; Miller *et al.*, 2000; Yin *et al.*, 2000; Liakopoulos *et al.*, 2003; Maekawa *et al.*, 2003). Paradoxically, EB1/Bim1 and APC/Kar9 also localize to microtubule organizing centers (MTOCs); centrosomes or SPBs in yeast, independently of astral microtubules when in the presence of the microtubule destabilizing drug nocodazole (Liakopoulos *et al.*, 2003; Louie *et al.*, 2004; Maekawa and Schiebel, 2004). The asymmetric localization of Kar9 to the SPB destined to enter the bud ("old" SPB or $SPB_{\mathbf{b}}$) and to astral microtubules that emanate from the $SPB_{\mathbf{b}}$ is critical for proper spindle placement and orientation (Liakopoulos *et al.*, 2003; Maekawa *et al.*, 2003; Maekawa and Schiebel, 2004; Moore *et al.*, 2005). However, any functional significance between the SPB localization of +TIP proteins and their subsequent function on astral microtubule +ends has not been clearly demonstrated. It has been proposed that SPB components may promote the assembly of +TIP complexes at the SPB prior to their deployment onto the microtubule +end (Liakopoulos *et al.*, 2003). Thus, mutations in SPB components that perturb the localization of Bim1 and/or Kar9 at SPBs, but do not block the assembly of astral microtubules, may reveal additional functional significance of their initial localization to these organelles.

γ-Tubulin (Tub4) localizes specifically to SPBs and initiates microtubule nucleation solely from these organelles in budding yeast (Sobel and Snyder, 1995; Marschall *et al.*, 1996; Spang *et al.*, 1996). Significantly, mutations in the carboxyl terminal (c-terminal) tail of Tub4 do not perturb the assembly of astral microtubules but instead affect their organization (Vogel and Snyder, 2000; Vogel *et al.*, 2001). In particular, an internal deletion of the DSYLD residues of the acidic c-terminal tail of Tub4 (*tub4-*Δ*dsyld*) was previously shown to promote the formation of stable astral microtubules that terminated in the cortex of the

bud (Vogel and Snyder, 2000). In addition, pre-anaphase spindles in *tub4-*Δ*dsyld* cells were frequently found displaced from the bud neck and associated with stabilized astral microtubules that terminated at the bud cortex (Vogel and Snyder, 2000). The effect of the *tub4-*Δ*dsyld* mutation on astral microtubule organization was specific to astral microtubules that entered the bud, suggesting the cortex may play a role in the formation of these stable arrays. Consistent with this possibility, astral microtubules that projected to the bud cortex persisted in the presence of microtubule destabilizing drugs, while astral microtubules that projected into the mother were de-polymerized (Vogel and Snyder, 2000). These observations, in combination with the previously described SPB localization of Kar9 and Bim1 (Liakopoulos *et al.*, 2003; Maekawa *et al.*, 2003; Maekawa and Schiebel, 2004) led us to investigate if Tub4 might be important for the localization of Kar9 and Bim1 to SPBs, and ultimately for their function in regulating astral microtubule +end dynamics during spindle positioning. Moreover, we speculated that the DSYL residues, which lie in the highly unstructured and acidic tail of γ-tubulin (Aldaz *et al.*, 2005), might be important for this novel aspect of Tub4 function.

Here, we demonstrate that the localization of Bim1 and Kar9 to SPBs is defective in *tub4-*Δ*dsyl* cells, and that the *tub4-*Δ*dsyl* mutation perturbs the function of the Kar9 pathway. We demonstrate that this defect is not due to a failure of Kar9 to localize to +ends, but rather due to defective Kar9 complexes on astral microtubules that enter the bud and fail to position the spindle. These Kar9 complexes contain reduced Bim1 and appear to stabilize the +ends of astral microtubules in the bud, resulting in long astral microtubules and increased dwell time of Kar9 at the bud cortex. Finally, we show that over-production of Bim1 in *tub4-*Δ*dsyl* cells restores Bim1-Kar9 physical interactions, spindle placement, and dynamic interactions between Kar9-loaded microtubule +ends and the bud cortex. Our analysis reveals that Tub4 is required for the proper loading and/or assembly of functional Bim1-Kar9 complexes at SPBs prior to their deployment to astral microtubule +ends.

2.3 Materials and methods

2.3.1 Strain construction and plasmids

Strains (for strain list see Table 2.3.1) were created through PCR-based transformation, standard non-integrative plasmid transformation and mating procedures as previously described (Christianson *et al.*, 1992; Longtine *et al.*, 1998). Media (rich media; yeast extract, peptone, adenine sulfate, dextrose (YPAD) and synthetic complete, SC) and general yeast methods are described (Guthrie, 1991). The *tub4-Δdsyl* mutation removes the N-terminal Asp and hydrophobic SYL residues of the previously described DSYLD domain (Vogel and Snyder, 2000). Homologous recombination was used to replace the *TUB4* ORF with the *tub4-Δdsyl* allele as previously described for *tub4-Y445D* (Vogel et al. 2001).

2.3.2 Genetic (synthetic lethality) analysis

For synthetic lethality analysis, heterozygous diploid strains were sporulated in low nitrogen liquid medium and meiotic products (tetrads) obtained (Guthrie, 1991). Tetrads were dissected on a Nikon E400 micromanipulator. For each analysis, meiotic products of 40 tetrads (spores) were grown on rich medium (YPAD) at 25˚C, and the segregation of alleles determined by re-plating spores on appropriate selection media at permissive (25˚C) and restrictive (30˚C, 37˚C) temperatures. The segregation of *tub4* alleles was confirmed by growth on minimal medium lacking tryptophane and by suppression of growth on rich medium at 37˚C as previously described (Vogel *et al.*, 2001). The segregation of array mutations (*geneΔ::KanMX*) was confirmed on YPAD containing G418.

TABLE 2.3.I. Yeast strains and plasmids used in Chapter 2

Strain	Genotype†	Source
YJV153	*MAT**a** TUB4::TRP1, URA3::GFP::TUB1*	(Vogel *et al.*, 2001)
YJV155	*MAT**a** tub4-Y445d::TRP1, URA3::GFP::TUB1*	(Vogel *et al.*, 2001)
YJV157	*MAT**a** tub4-Δdsyl::TRP1, URA3::TUB1::GFP*	This study
YJV149	*MAT**a** TUB4:TRP1*	(Vogel *et al.*, 2001)
YJV126	*MAT**a** tub4-Y445D::TRP1*	(Vogel *et al.*, 2001)
YLC11	*MAT**a** tub4-Δdsyl::TRP1*	This study
YJV148	*MAT**a** TUB4::TRP1*	(Vogel *et al.*, 2001)
YJV129	*MAT**a** tub4-Y445D::TRP1*	(Vogel *et al.*, 2001)
YLC15	*MAT**a** tub4-Δdsyl::TRP1*	This study
Y00147	*MAT**a** bim1::kan*MX6, *TRP1*, *leu2-3,112*	(Brachmann *et al.*, 1998)
Y01023	*MAT**a** kar9::kan*MX6 *TRP1*, *leu2-3,112*	(Brachmann *et al.*, 1998)
Y05556	*MAT**a** kar3::kan*MX6 *TRP1*, *leu2-3,112*	(Brachmann *et al.*, 1998)
Y01039	*MAT**a** vik1::kan*MX6 *TRP1*, *leu2-3,112*	(Brachmann *et al.*, 1998)
Y04582	*MAT**a** kip3::kan*MX6 *TRP1*, *leu2-3,112*	(Brachmann *et al.*, 1998)
Y03089	*MAT**a** kip1::kanMX6 TRP1*, *leu2-3,112*	(Brachmann *et al.*, 1998)
Y01957	*MAT**a** arp1::kanMX6 TRP1*, *leu2-3,112*	(Brachmann *et al.*, 1998)
Y00784	*MAT**a** cik1::kanMX6 TRP1*, *leu2-3,112*	(Brachmann *et al.*, 1998)
Y00147	*MAT**a** cin8::kanMX6 TRP1*, *leu2-3,112*	(Brachmann *et al.*, 1998)
Y02097	*MAT**a** kip2::kanMX6 TRP1*, *leu2-3,112*	(Brachmann *et al.*, 1998)
Y01392	*MAT**a** mad2::kanMX6 TRP1*, *leu2-3,112*	(Brachmann *et al.*, 1998)
Y05125	*MAT**a** dhc1::kanMX6 TRP1*, *leu2-3,112*	(Brachmann *et al.*, 1998)
Y03436	*MAT**a** bik1::kanMX6 TRP1*, *leu2-3,112*	(Brachmann *et al.*, 1998)
ABY536	*MAT**a** myo2-16::HIS3, hi3Δ200, trp1-Δ63*	(Schott *et al.*, 1999)
ABY537	*MAT**a** myo2-17::HIS3, hi3Δ200, trp1-Δ63*	(Schott *et al.*, 1999)
CUY1070	*MAT**a** stu2-10:LEU2, leu2-3,112*	(Kosco *et al.*, 2001)
YLC204	*MAT**a** DHC1::VFP::natR, URA3::TUB1::CFP, TUB4::TRP1*	This study
YLC205	*MAT**a** DHC1::VFP::natR, URA3::TUB1::CFP, tub4-Δdsyl::TRP1*	This study
TSY502	*MAT**a** tub4-34, leu2-3,112*	(Marschall *et al.*, 1996)
YLC162	*MAT**a** TUB4::TRP1,BIM1::GFP::kanMX6, SPC42::CFP::kanMX6,*	This study
YLC182	*MAT**a** tub4-Y445D::TRP1, BIM1::GFP::kanMX6, SPC42::CFP::kanMX6,*	This study
YLC183	*MAT**a** tub4-Δdsyl::TRP1,BIM1::GFP::kanMX6, SPC42::CFP::kanMX6*	This study
YLC159	*MAT**a** TUB4::TRP1, KAR9::GFP::TRP1, SPC42::CFP::kanMX6*	This study
YLC178	*MAT**a** tub4-Δdsyl::TRP1, KAR9::GFP::TRP1, SPC42::CFP::kanMX6*	This study
YLC223	*MAT**a** TUB4::TRP1, KAR9::ProA::kanMX6*	This study
YLC227	*MAT**a** tub4-Δdsyl::TRP1, KAR9::ProA::kanMX6*	This study
YLC217	*MAT**a** TUB4::TRP, BIM1::CFP::KAN, KAR9::GFP::TRP*	This study
YLC222	*MAT**a** tub4-Δdsyl::TRP, BIM1::CFP::KAN, KAR9::GFP::TRP*	This study
YLC130	*MAT**a** tub4-Δdsyl::TRP, URA3::GFP::TUB1,* pRS423	This study
YLC135	*MAT**a** tub4-Δdsyl::TRP, URA3::GFP::TUB1,* pLC1	This study
YLC119	*MAT**a** TUB4::TRP,URA3::GFP::TUB1,* pRS423	This study
YLC133	*MAT**a** TUB4::TRP,URA3::GFP::TUB1,* pLC1	This study
YLC240	*MAT**a** TUB4::TRP1, KAR9::ProA::kanMX6[pRS423]*	This study
YLC238	*MAT**a** TUB4::TRP1, KAR9::ProA::kanMX6[pLC1]*	This study
YLC244	*MAT**a** tub4-Δdsyl::TRP1,KAR9::ProA::kanMX6, [pRS423]*	This study
YLC246	*MAT**a** tub4-Δdsyl::TRP1,KAR9::ProA::kanMX6, [pLC1]*	This study
YLC242	*MAT**a**, dhc1::kanMX, [pPRS423]*	This study
YLC248	*MAT**a**, dhc1::kanMX, [pLC1]*	This study
YLC251	*MAT**a**, dhc1::kanMX, [pRM515]*	This study
YLC253	*MAT**a** TUB4::TRP, BIM1::CFP::KAN, KAR9::GFP::TRP [pRS423]*	This study
YLC254	*MAT**a** TUB4::TRP, BIM1::CFP::KAN, KAR9::GFP::TRP [pLC1]*	This study
YLC255	*MAT**a** tub4-Δdsyl::TRP, BIM1::CFP::KAN, KAR9::GFP::TRP [pRS423]*	This study
YLC256	*MAT**a** tub4-Δdsyl::TRP, BIM1::CFP::KAN, KAR9::GFP::TRP [pLC1]*	This study

Plasmid	Description	Source
pRS423	PCEN; HIS3 2μ	Christianson and Heiter,1992
pBIM1	*BIM1* ORF + 600 bp of 5' UTR and 200 bp of 3'UTR inserted in pRS423 at ClaI and SacI sites	This study
pRM515	*KAR9* ORF inserted in pMR1869 at ApaI and SacI sites	R. Miller

†All strains are S288C (*his3-Δ200, lys2-801, ura3-52, trp1-Δ1, ade2-101)*

2.3.3 Statistical Analysis

Data from 3 independent experiments were used for measuring astral microtubule dynamics and quantitative analysis of fluorescence intensity. The average value for each analysis was determined and the standard error of the mean calculated (y-error bars, representing the precision of the measurement) using Excel. Where indicated, significance (defined as a $p<0.01$) was determined using the standard deviation of the samples (population) for a 2-tailed homoscedastic Student's t-test. All calculations were performed with Excel.

2.3.4 Fluorescent microscopy methods

For time-lapse imaging, overnight cultures were grown in either YPAD or fluorescent protein media (FPM: (Pot *et al.*, 2005) at the permissive temperature of 25˚C, diluted to a cell density of ~0.1 OD units ml^{-1}, then re-grown to a density of ~0.4 OD units ml^{-1}. Yeast cells were collected by centrifugation, washed twice with fresh FPM and mounted on 2% agarose/FPM pads sealed with Valap. All microscopic analysis was performed at 25˚C unless otherwise indicated. For analysis of microtubule guidance, live cells were examined using a deconvolution imaging system mounted on a Nikon TE2000-U (Pot *et al.*, 2005). Optical sections were acquired at 0.5 μm intervals in 6.0 μm stack using Openlab Automator Pro (Improvision, UK).

Single-channel imaging of astral microtubule dynamics (GFP-Tub1) and multi-channel 4D imaging of Spc42-RFP, CFP-Tub1, Bim1-CFP, Bim1-GFP Kar9-GFP and Kar9-YFP fluorescent fusion proteins was performed using a WaveFX spinning disc confocal system (Quorum Technologies Inc., Guelph, ON) mounted on a Leica DM 5000 upright motorized microscope equipped with a Synapse Diode Laser merge module (Quorum Technologies Inc., Guelph, ON) with lines for 440nm (14 mW coupled output) and 491nm (13 mW coupled output) excitation, a modified Yokagawa CSU10 Nipkow Disc scan head, and a

Hamamatsu C9100-12 Back Thinned EMCCD camera. An Exfo light source and appropriate excitation and emission filters were used for detection of RFP. Optical sections (0.5 or 0.75 μm) were acquired through a 4.0 μm stack, either continuously or at 5 sec intervals using Volocity 3DM (Improvision, UK). For microtubule dynamics, optical sections (0.3 μm) were acquired through a 4.0 μm stack at 10 sec intervals for a total time of 5 minutes.

2.3.5 Calculation of microtubule dynamics

Microtubule dynamics (elongation rates, shrinkage rates, pauses) were determined by measuring microtubule lifetime lengths using Volocity 3DM (Improvision, UK). Microtubule lengths were measured in triplicate and the average value for each time point used for calculations. Elongation were defined as 3 consecutive points on a regression line in which the increased change in length of a microtubule ($\Delta length_{increase}$) was ≥ 0.3 μm. Shrinkage was defined as 3 consecutive points on a regression line in which the decreased change in length of a microtubule ($\Delta length_{decrease}$) was ≥ 0.3 μm. Microtubule pausing was defined as a change in length spanning 3 points on a regression line that was ≤ 0.3 μm.

2.3.6 Kar9-GFP +end tracking method

Dynamic movement of Kar9-GFP on microtubule +ends was tracked using Volocity Classification module (Improvision, UK). To track Kar9-GFP movements in the conditional *myo2-16* allele, cells were grown in rich medium at a restrictive temperature for *myo2-16* (Schott *et al.*, 1999) that is not restrictive for the *tub4-*Δ*dsyl* allele (30˚C). A Kar9 classifier (classifier: a representative 3-dimensional volume for a given fluorophore) was created based on the shape and size defined by Kar9-GFP associated with astral microtubules in wild-type cells. This classifier was used to track Kar9-GFP on +ends in space and time for representative small budded cells of each strain

from 3 independent experiments. The classifier was defined to automatically join broken tracks and fill empty holes of fluorescence. In addition, the classifier was restricted to track Kar9-GFP between an average minimum and maximum fluorescent intensity per cell. In time-points where the Kar9-GFP intensity either exceeded or failed to meet the intensity requirements of the classifier, manual tracking was used. Finally, tracks were confirmed manually using frames from the original image sequence.

2.3.7 Quantitative fluorescence

For quantitative fluorescence measurements, image stacks were acquired with a WaveFX confocal system using the following exposures: Kar9-GFP (300 msec), Kar9-YFP (co-localization experiments; 500 msec), Bim1-CFP (100 msec). Image series were de-convolved to 90% confidence or 25 iterations using the Volocity Restoration module (Improvision). For each analysis, fluorescence intensities were measured in >100 cells per strain and/or condition in 3 independent experiments. An 8.0 voxel volume was used for each measurement. Background signal was calculated as the averaged intensity of 4 equivalent volumes located inside of the cell. Fluorescent intensities (average/volume for the de-convolved image) were calculated using the Volocity Visualization module (Improvision) and background subtracted, resulting in corrected fluorescence units (FU).

2.3.8 Protein methods and co-immunoprecipitation

All steps were performed at 4˚C unless indicated otherwise. Whole cell extracts were prepared as previously described (Vogel *et al.*, 2001). Extracts were clarified by centrifugation for 10 minutes at 14,000 xg. For IPs, 900 μl of 1x IP buffer (lysis buffer + 0.1% NP-40) was added to clarified extracts. An aliquot of undiluted extract (input) was diluted 1:1 with 2x sample buffer (SB) for analysis. Diluted extracts were incubated with pre-equilibrated IgG sepharose

(25µl; 50% slurry) for 2 hours. Beads were washed 6 times with IP buffer, pelleted at 2000 xg for 1 minute and the supernatant aspirated. Bound proteins were recovered from the beads by incubating in 25 µl of 2x SB for 7 minutes at 90˚C.

2.3.9 Electrophoresis and immunoblotting

SDS-polyacrylamide gel electrophoresis and immunoblotting was performed as previously described (Vogel *et al.*, 2001). Anti-TAP (ProA detection; Open Biosystems, Huntsville AL) was used at 1:7000 in TBS-0.20% tween-20 (TBS-T). A polyclonal anti-Bim1 antibody was used at 1:4000. Monoclonal anti-actin (MP Biomedicals, Irvine CA) was used at 1:5000 in TBS-T. Anti-rabbit (anti-TAP and anti-Bim1) or mouse (anti-actin) HRP-conjugated secondary antibodies were used at 1:10,000 in TBS/T-20 (Amersham Arlington Heights, IL) Protein/antibody complexes were detected using ECL (Amersham).

2.3.10 Latrunculin B (LatB), phalloidin and nocodazole (NZ) treatment

Cells were grown overnight in FP medium, diluted to a cell density of ~0.1 OD units ml^{-1}, then re-grown to a density of ~0.4 OD units ml^{-1}**.** Cells were incubated in FP medium containing 200 µM LatB (Sigma) for 30-60 minutes at 25˚C to de-polymerize actin structures. Disruption of F-actin in LatB treated cells was confirmed by staining an aliquot of fixed, treated cells with Alexa 488-phalloidin (Molecular Probes). To de-polymerize microtubules, cells were incubated in FP medium containing 30 µg/ml NZ for 30 minutes at 18˚C. Disruption of astral microtubules and spindle collapse was confirmed by imaging CFP-tubulin labeled microtubules.

2.4 Results

2.4.1 Bim1 and Kar9 localization to SPBs is defective in *tub4-*Δ*dsyl* cells

Tub4 is known to localize exclusively to SPBs in budding yeast (Sobel and Snyder, 1995; Marschall *et al.*, 1996). Surprisingly, *tub4-Y445D* and *tub4-*Δ*dsyl* mutants exhibit defects in microtubule organization and dynamics (Vogel and Snyder, 2000; Vogel *et al.*, 2001). We confirmed that these defects were not due to a failure of Tub4 to localize to SPBs in either mutant background (unpublished results), suggesting that proteins associated specifically with SPBs can influence the behavior of the microtubule +end. We asked if *tub4* mutants might exert their effect on microtubule +ends by influencing the localization of Bim1 and/or Kar9 to SPBs, which have been shown to localize to SPBs independently of their association with microtubules (Liakopoulos *et al.*, 2003). As it has previously been proposed that +TIPs assemble into complexes at SPBs (Liakopoulos *et al.*, 2003), a failure of Bim1 and/or Kar9 to localize to these organelles may perturb their subsequent localization to microtubule +ends and/or functions at these sites.

To begin testing whether Bim1 and Kar9 fail to localize to SPBs in *tub4* mutants, wild-type, *tub4-Y455D* and *tub4-*Δ*dsyl* cells expressing Bim1-GFP and CFP-Tub1 were treated with the microtubule destabilizing drug nocodozole (NZ; 30 µg/ml) and small-budded cells were scored for Bim1-GFP co-localization to the collapsed spindle (seen as single focus of CFP-tubulin following NZ treatment). We found that Bim1-GFP localized to the collapsed spindle in the majority of wild-type (82%; n=141 cells) and *tub4-Y445D* cells (77%; n=119) lacking astral microtubules (Figure 2.4.1 A,B). However, Bim1-GFP was rarely detected in *tub4-*Δ*dsyl* cells (24%; n=115 cells) lacking astral microtubules (Figure 2.4.1 A,B). This suggested that the localization of Bim1 to SPBs is perturbed by the *tub4-*Δ*dsyl* mutation but not the *tub4-Y445D* mutation.

Figure 2.4.1. The localization of Bim1 and Kar9 to SPBs is defective in *tub4-*∆*dsyl* cells.

(A) Microscopic analysis of Bim1 SPB localization in nocodazole (NZ) treated cells. *TUB4* and *tub4-Y445D* cells treated with NZ (30 µg/ml) had detectable Bim1-GFP foci associated with the collapsed spindle (single focus of CFP-Tub1) while the majority of *tub4-*∆*dsyl* cells treated with NZ did not. **(B)** Histogram showing the percentage of *TUB4, tub4-Y445D* and *tub4-*∆*dsyl* cells with detectable Bim1-GFP foci at collapsed spindles following NZ treatment. **(C)** Microscopic analysis of Kar9 SPB localization in NZ treated cells. *TUB4* and *tub4-Y445D* cells treated with NZ had Kar9-GFP foci localized to the $SPB_{\mathbf{b}}$. In contrast, the majority of *tub4-*∆*dsyl* cells lacked detectable Kar9-GFP foci associated with $SPB_{\mathbf{b}}$. Spc42-RFP marks the 'old SPB' or $SPB_{\mathbf{b}}$. Microtubules are labeled with CFP-Tub1. **(D)** Histogram indicating the percentage of *TUB4, tub4-Y445D* and *tub4-*∆*dsyl* cells exhibiting Kar9-GFP foci at the $SPB_{\mathbf{b}}$.

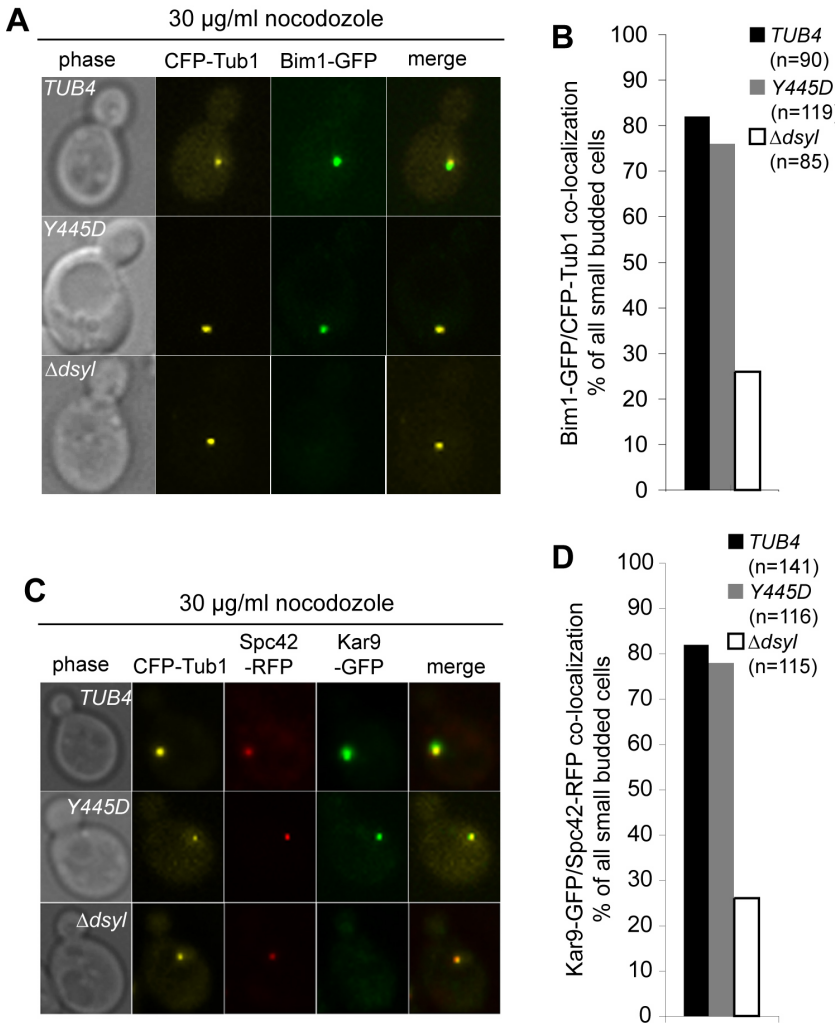
A
30 µg/ml nocodozole
phase
CFP-Tub1
Bim1-GFP
merge
TUB4
Y445D
Δdsyl
B
Bim1-GFP/CFP-Tub1 co-localization
% of all small budded cells
100
90
80
70
60
50
40
30
20
10
0
TUB4
(n=90)
Y445D
(n=119)
Δdsyl
(n=85)
C
30 µg/ml nocodozole
phase
CFP-Tub1
Spc42
-RFP
Kar9
-GFP
merge
TUB4
Y445D
Δdsyl
D
Kar9-GFP/Spc42-RFP co-localization
% of all small budded cells
100
90
80
70
60
50
40
30
20
10
0
TUB4
(n=141)
Y445D
(n=116)
Δdsyl
(n=115)

We next tested if Kar9 SPB_b localization was also defective in *tub4-Δdsyl* cells by treating wild-type, *tub4-Y445D* and *tub4-Δdsyl* cells expressing Kar9-GFP, CFP-Tub1, and the SPB_b specific marker Spc42-RFP (Pereira *et al.*, 2001) with NZ and assessing for co-localization of Kar9-GFP with Spc42-RFP. We found Kar9-GFP co-localized with Spc42-RFP in the majority of wild-type (84%; n=90 cells) and *tub4-Y445D* (78%, n=116 cells) cells lacking astral microtubules (Figure 2.4.1 C, D). However, Kar9-GFP was rarely detected at the SPB_b in *tub4-Δdsyl* cells (24%; n=85 cells; Figure 2.4.1 C, D). This analysis suggested that Bim1 and Kar9 SPB localizations are defective in *tub4-Δdsyl* cells, and that the DSYL residues are important for the association of these +TIPs with SPBs.

2.4.2 The DSYL residues are required for the function of the Kar9 pathway

The reduced localization of Bim1 and Kar9 to SPBs in *tub4-Δdsyl* cells suggested that this mutation perturbs the function of the Kar9 pathway. To test this, we assessed if the *tub4-Δdsyl* mutation is lethal with mutations in genes acting in the dynein pathway. Genes acting in dynein-dependant spindle positioning are essential for life when the Kar9 pathway is disrupted (Miller and Rose, 1998). Correspondingly, mutations disrupting Kar9 function are lethal in combination with mutations in the dynein pathway (Miller and Rose, 1998). Based on this, if the Tub4 DSYL residues are important for the Kar9 pathway, then the *tub4-Δdsyl* mutation should be lethal with mutations perturbing dynein function. As a control, we tested for synthetic lethality with the *tub4-Y445D* mutation, which did not alter the localization of Kar9 or Bim1 to SPBs.

As expected, we observed that mutations in the dynein pathway were synthetically lethal in combination with only the *tub4-Δdsyl* allele and not the *tub4-Y445D* allele (Figure 2.4.2 B; representative tetrads shown in C). Consistent with a defect in the Kar9 pathway, we found that mutations in the majority of genes acting in the Kar9 pathway were not synthetically lethal with either *tub4* allele (Figure 2.4.2 B & C).

Figure 2.4.2 The DSYL residues are required for function of the Kar9 pathway.

(A) Cartoon of spindle positioning pathways in budding yeast. Early spindle placement is dependent on the Kar9 pathway while the maintenance of spindle placement during anaphase requires the dynein pathway. **(B)** Query alleles (*tub4-Y445D* and *tub4-*Δ*dsyl*) were analyzed for synthetic lethal interactions with mutations that disrupt either Kar9 or Dhc1 function. Synthetic lethal (+) and viable interactions (-) are indicated. The *tub4-*Δ*dsyl* allele was synthetically lethal with mutations that disrupt Dhc1 function but not Kar9 function. **(C)** Representative tetrads for the analysis in **B**. Double mutant spores are circled. *tub4-*Δ*dsyl dhc1*Δ double mutants failed to grow while *tub4-*Δ*dsyl kar9*Δ double mutants were viable. N=40 tetrads for each cross. The allele segregation for each tetrad is indicated (NPD = non-parental ditype; TT = tetratype; PDT = parental ditype). **(D)** The frequency of astral microtubule misguidance (visualized by GFP-Tub1) that occurred from the mother-bound SPB ($SPB_{\mathbf{m}}$) or bud-bound SPB ($SPB_{\mathbf{b}}$) was measured in *TUB4* and *tub4-*Δ*dsyl* cells. *tub4-*Δ*dsyl* cells had a higher frequency of microtubule misguidance relative to wild-type. N = 300. **(E)** Analysis of spindle placement in *TUB4* and *tub4-*Δ*dsyl* cells. *tub4-*Δ*dsyl* cells had a higher frequency of spindles that were positioned far from the bud neck relative to *TUB4* cells. N=300. Categories of spindle placement assessed are represented in the cartoon image.

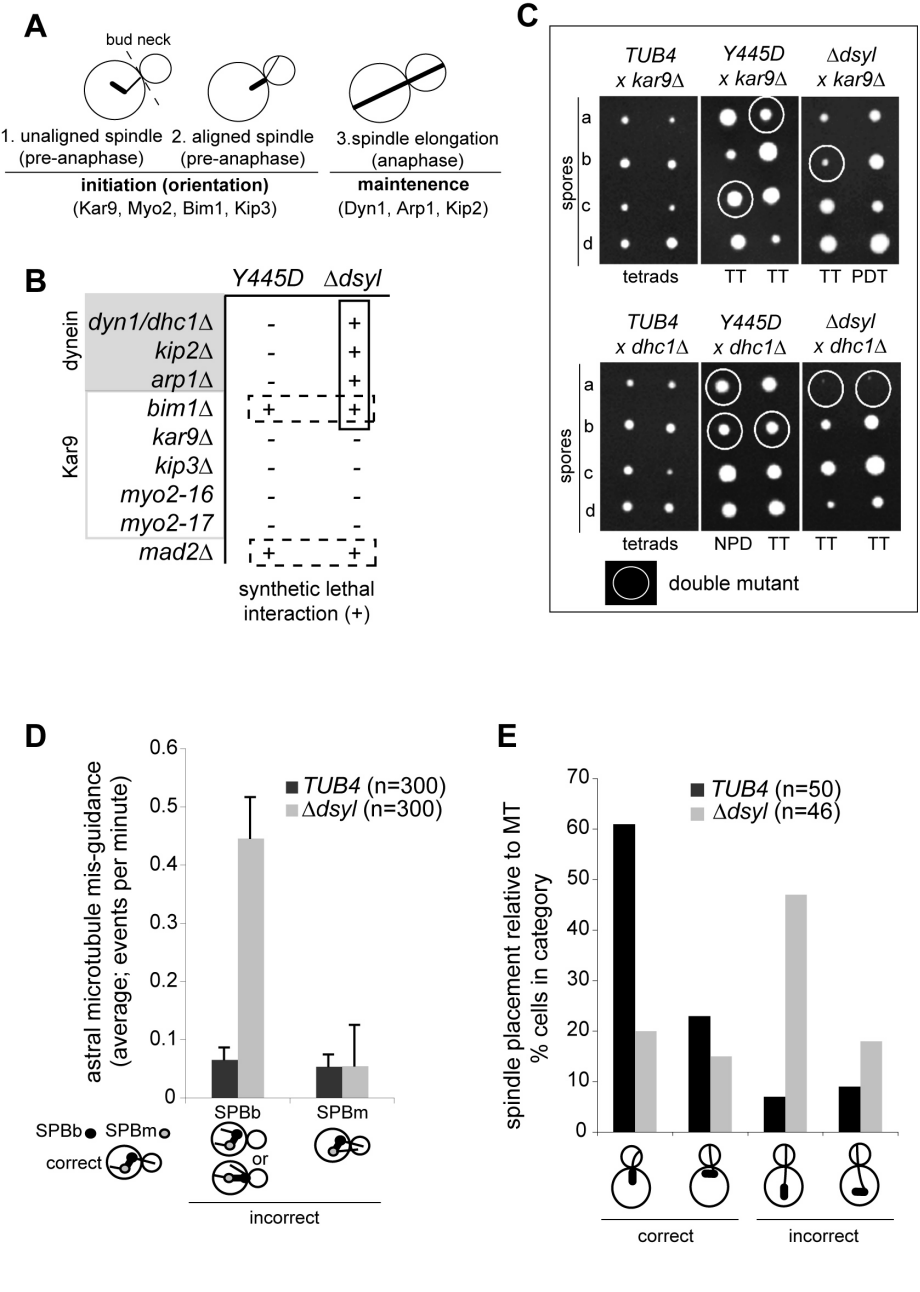
A
bud neck
1. unaligned spindle (pre-anaphase)
2. aligned spindle (pre-anaphase)
3.spindle elongation (anaphase)
initiation (orientation)
(Kar9, Myo2, Bim1, Kip3)
maintenence
(Dyn1, Arp1, Kip2)
B
Y445D
Δdsyl
dynein
Kar9
dyn1/dhc1Δ
kip2Δ
arp1Δ
bim1Δ
kar9Δ
kip3Δ
myo2-16
myo2-17
mad2Δ
synthetic lethal interaction (+)
C
TUB4 x kar9Δ
Y445D x kar9Δ
Δdsyl x kar9Δ
spores
a
b
c
d
tetrads
TT TT
TT PDT
TUB4 x dhc1Δ
Y445D x dhc1Δ
Δdsyl x dhc1Δ
tetrads
NPD TT
TT TT
double mutant
D
astral microtubule mis-guidance (average; events per minute)
TUB4 (n=300)
Δdsyl (n=300)
SPBb
SPBm
correct
or
incorrect
E
spindle placement relative to MT % cells in category
TUB4 (n=50)
Δdsyl (n=46)
correct
incorrect

One exception we found was a null mutation in *BIM1 (bim*Δ*).* Bim1 has a complex genetic interaction network that is not restricted to Kar9 function and may include a role in chromosome segregation (Tong *et al.*, 2001; Gardner *et al.*, 2008). Consistent with this possibility, the *tub4-*Δ*dsyl* and *tub4-Y445D* mutations were lethal in combination with deletion of the spindle checkpoint protein Mad2 (*mad2*Δ). Therefore, the observed pattern of synthetic lethal interactions for the *tub4-*Δ*dsyl* mutant indicates that the dynein pathway is essential in *tub4-*Δ*dsyl* cells, and is consistent with the hypothesis that the *tub4-*Δ*dsyl* mutation perturbs Kar9 pathway function.

In order to further confirm that Kar9 function is perturbed by the *tub4-*Δ*dsyl* mutation, we tested if spindle placement was disrupted in *tub4-*Δ*dsyl* cells due to astral microtubule mis-targeting. The rational being that in wild-type cells, Kar9 promotes spindle placement by properly targeting astral microtubule +ends into the bud, via associations with Myo2 (Liakopoulos *et al.*, 2003). Wild-type and *tub4-*Δ*dsyl* cells expressing GFP-Tub1 (Straight *et al.*, 1997) were examined for this analysis. We found that microtubule mis-targeting was rare in wild-type cells (0.07 events/minute, n=300 cells) but increased 5-fold in *tub4-*Δ*dsyl* cells (0.45 events/minute, n=300 cells; p>0.01; Figure 2.4.2 D). Thus, microtubule mis-targeting is more frequent in *tub4-*Δ*dsyl* cells.

Strangely, during this analysis we noticed that the majority of displaced spindles (ie. spindles positioned far from the bud neck) in *tub4-*Δ*dsyl* cells were associated with an astral microtubule that was properly targeted into the bud. More specifically, a larger percentage of small budded cells containing an oriented spindle near the bud neck with a microtubule targeted into the bud were observed in the wild-type strain (61%, n=300 cells) relative to the *tub4-*Δ*dsyl* mutant (20%, n=300 cells; Figure 2.4.2 E). Also, the percentage of cells with an un-aligned spindle positioned near the bud neck (a characteristic intermediate of normal spindle positioning) was also greater in wild-type cells (23%, n=300 cells) relative to the *tub4-*Δ*dsyl* mutant (15%, n=300 cells; Figure 2.4.2 E). In contrast, the percentage of cells with a bud-directed microtubule that was associated with a spindle positioned far from the bud neck was dramatically

increased in the *tub4-*Δ*dsyl* mutant (65%) relative to the wild-type background (<10%; Figure 2.4.2 E). This analysis indicated that though microtubule mistargeting is more frequent in *tub4-*Δ*dsyl* cells it is not likely the major cause of displaced spindles in this mutant, and while many astral microtubules are properly targeted into the bud in *tub4-*Δ*dsyl* cells, the ability of these microtubules to mediate proper spindle placement is perturbed.

2.4.3 Kar9 preferentially localizes to astral microtubule +ends in *tub4-*Δ*dsyl* cells

Kar9 normally localizes to the SPB_b and to the +ends of astral microtubules associated with this pole (Liakopoulos *et al.*, 2003; Maekawa *et al.*, 2003). We predicted that spindle positioning to the bud neck is defective in *tub4-*Δ*dsyl* cells because Kar9 fails to localize to targeted astral microtubule +ends, as a consequence of not localizing to the SPB_b. We examined the localization of Kar9-GFP in wild-type and *tub4-*Δ*dsyl* cells co-expressing CFP-Tub1. Unexpectedly, we found that Kar9-GFP does still localize to the +ends of astral microtubules projecting from the SPB_b in *tub4-*Δ*dsyl* cells (Figure 2.4.3 A). Quantitative fluorescence analysis suggested that the amount of Kar9-GFP associated with microtubule +ends was significantly increased in *tub4-*Δ*dsyl* cells (658.1± 73.24 FU) relative to wild-type cells (396.2±101.72 FU, $p<0.01$; Figure 2.4.3 B). Additionally, Kar9-GFP localization at the SPB_b was reduced in *tub4-*Δ*dsyl* cells (21.4%, n=200 cells) relative to wild-type cells (51.5%, n=200 cells; Figure 2.4.3 C). Therefore, though Kar9-GFP localization to the SPB_b is defective in *tub4-*Δ*dsyl* cells, its localization to microtubule +ends is maintained.

We were curious why spindle positioning is defective in *tub4-*Δ*dsyl* cells despite Kar9 still localizing to microtubule +ends. One possibility is that Kar9 does not typically localize to the +ends of microtubules that enter the bud but rather to those that are mis-targeted. We tested this, by examining the localization of Kar9-GFP in wild-type and *tub4-*Δ*dsyl* cells with CFP labeled microtubules. As expected, in wild-type cells most microtubules loaded with

Kar9-GFP were properly targeted into the bud. Additionally, in *tub4-*Δ*dsyl* cells the majority of microtubules loaded with Kar9-GFP were also properly targeted into the bud, suggesting that the spindle positioning defects are not a consequence of Kar9 loading onto mis-targeted microtubules (Figure 2.4.3 D).

We further confirmed this result by examining if the targeted astral microtubules containing Kar9-GFP in *tub4-*Δ*dsyl* cells were also the same microtubules that were attached to a displaced spindle (>2 μm from the neck). Our analysis revealed that Kar9-loaded microtubules directed into the bud were attached to a displaced spindle positioned far from the bud neck in the mother in 72.7% of *tub4-*Δ*dsyl* cells (n=55) but only 13.3% of wild-type cells (n=90; Figure 2.4.3E). These findings suggested that in *tub4-*Δ*dsyl* cells, Kar9 complexes that load onto microtubule +ends are incapable of positioning the spindle. Therefore, while the +end localization of Kar9 is maintained in *tub4-*Δ*dsyl* cells, its function with respect to promoting microtubule dynamics and spindle placement is seemingly perturbed.

Figure 2.4.3 Kar9 preferentially localizes to astral microtubule +ends in *tub4-*Δ*dsyl* cells.

(A) Microscopic analysis of Kar9 localization. In wild-type and *tub4-*Δ*dsyl* cells, Kar9-GFP localizes to the +ends of astral microtubules. CFP-Tub1 was used to visualize microtubules. Dashed line indicates the position of the bud neck. Scale bar = 2 μm. **(B)** Histogram indicating the fluorescent intensities of Kar9-GFP foci associated with microtubule +ends in *TUB4* and *tub4-*Δ*dsyl* cells. *tub4-*Δ*dsyl* cells (n=300 $p<0.01$) have a higher average fluorescent intensity of Kar9-GFP associated with microtubule +ends relative to those of *TUB4* (n=300, $p<0.01$) cells. **(C)** Quantification of Kar9 localization in *TUB4* and *tub4-*Δ*dsyl* cells. The majority of *tub4-*Δ*dsyl* cells have Kar9-GFP foci associated with microtubule +ends but not the SPB_b. **(D)** Histogram indicating the localization of Kar9-GFP foci in *TUB4* and *tub4-*Δ*dsyl* cells. The majority of Kar9-GFP foci are properly targeted into the bud for both cell types. **(E)** Spindle positioning relative to Kar9-GFP foci was analyzed in *TUB4* and *tub4-*Δ*dsyl* cells. In *tub4-*Δ*dsyl* cells, spindles remain mis-positioned (in the mother) when a Kar9-loaded astral microtubule is properly targeted into the bud. Categories of spindle placement assessed are represented in the cartoon images.

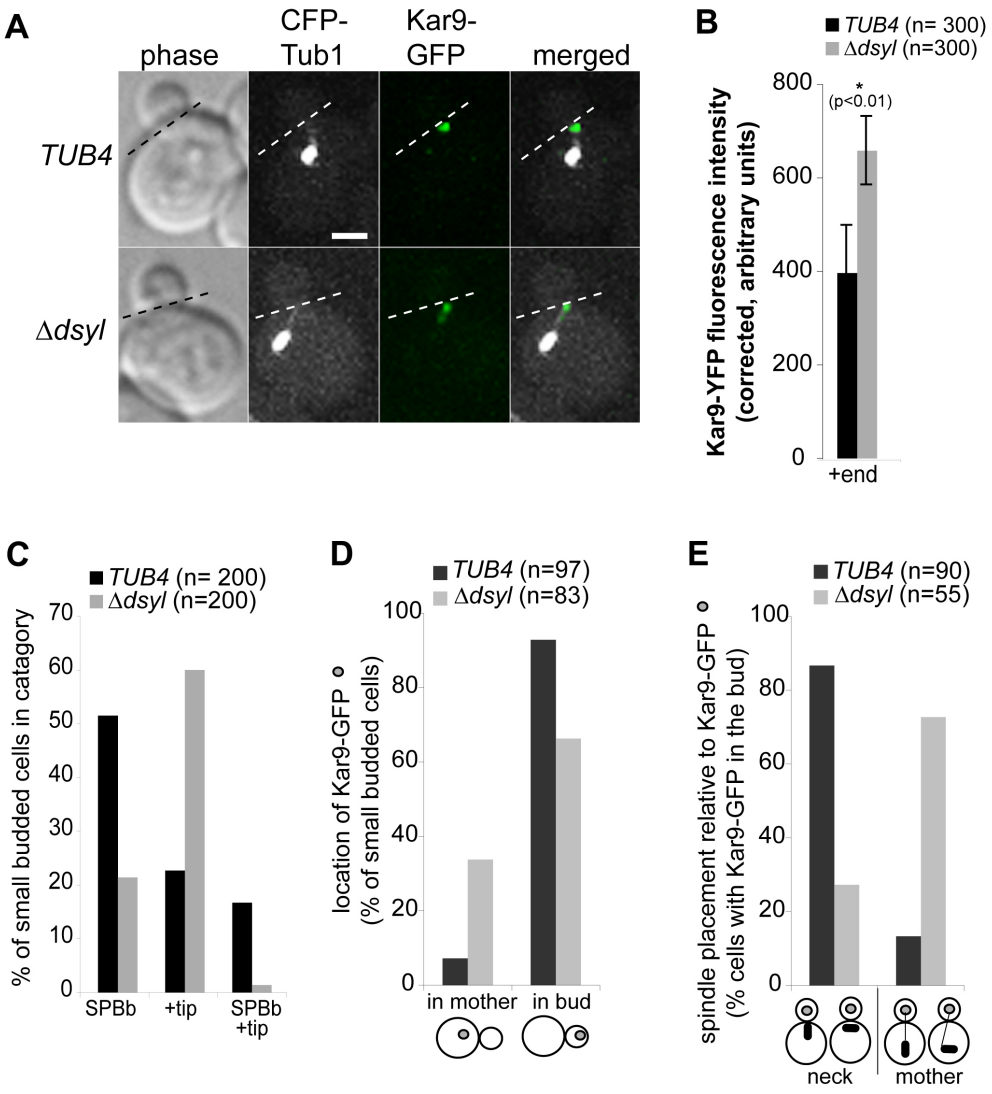
A
phase
CFP-Tub1
Kar9-GFP
merged
TUB4
Δdsyl
B
TUB4 (n= 300)
Δdsyl (n=300)
Kar9-YFP fluorescence intensity (corrected, arbitrary units)
800
600
400
200
0
*
(p<0.01)
+end
C
TUB4 (n= 200)
Δdsyl (n=200)
% of small budded cells in catagory
70
60
50
40
30
20
10
0
SPBb
+tip
SPBb +tip
D
TUB4 (n=97)
Δdsyl (n=83)
location of Kar9-GFP
(% of small budded cells)
100
80
60
40
20
0
in mother
in bud
E
TUB4 (n=90)
Δdsyl (n=55)
spindle placement relative to Kar9-GFP
(% cells with Kar9-GFP in the bud)
100
80
60
40
20
0
neck
mother

2.4.4 Bim1-Kar9 stoichiometry is reduced in *tub4-*Δ*dsyl* cells

Bim1 is required for Kar9 localization to the SPB_b and microtubule +ends (Miller *et al.*, 2000; Liakopoulos *et al.*, 2003). As Kar9 maintained its localization to microtubule +ends in *tub4-*Δ*dsyl* cells, we expected that Bim1 would exhibit a similar localization pattern. Co-localization of Bim1 and Kar9 on +ends was assessed in *TUB4* and *tub4-*Δ*dsyl* cells expressing Bim1-CFP and Kar9-YFP (Figure 2.4.4 A). To our surprise, this analysis indicated that unlike Kar9, the amount of Bim1-CFP that localized to microtubule +ends was decreased in *tub4-*Δ*dsyl* cells (208.5±27.95 FU; $p<0.01$) relative to wild-type cells (394.1±52.73 FU; $p<0.01$; Figure 2.4.4 A,B). Consistently, the ratio of Bim1-CFP/Kar9-GFP fluorescence intensities co-localizing on microtubule +ends was also decreased in *tub4-*Δ*dsyl* cells (0.38±0.078 FU) relative to wild-type cells (0.96±0.224 FU, $p< 0.01$; Figure 2.4.4 C).

Levels of Bim1 and Kar9-ProA protein were similar in whole cell extracts prepared from wild-type and *tub4-*Δ*dsyl* cells, indicating that the altered localization of these proteins was not due to their decreased stability in *tub4-*Δ*dsyl* cells (Figure 2.4.4 D,E). Instead, this analysis suggested physical interactions between Kar9 and Bim1 might be defective in the *tub4-*Δ*dsyl* mutant. To test this possibility, the amount of Bim1 co-purifying with Kar9-ProA was measured in wild-type and *tub4-*Δ*dsyl* extracts. Kar9-ProA was isolated from whole cell extracts by IgG-sepharose affinity purification (Puig *et al.*, 2001) and the amount of co-purifying Bim1 detected with an anti-Bim1 polyclonal antibody. This analysis revealed reduced levels of Bim1 co-purifying with Kar9-ProA isolated from *tub4-*Δ*dsyl* cells relative to wild-type (Figure 2.4.4 F). The amount of co-purifying Bim1 (arbitrary units) normalized to the Kar9-ProA input from 3 independent experiments was averaged for the wild-type and *tub4-*Δ*dsyl* strains and is shown in Figure 2.4.4 G. Taken together, these results suggest that the ratio of Bim1 and Kar9 on microtubule +ends is decreased as a consequence of the *tub4-*Δ*dsyl* mutation.

Figure 2.4.4 Stoichiometry of Bim1-Kar9 complexes is reduced in *tub4-*Δ*dsyl* cells

(A) Microscopic analysis of Bim1 and Kar9 localization in wild-type and *tub4-*Δ*dsyl* cells. In *TUB4* cells, Bim1-CFP and Kar9-YFP are observed on microtubule +ends (white arrows). In contrast, Kar9-YFP foci are detected on +ends lacking detectable Bim1-CFP (white arrows) in the majority of *tub4-*Δ*dsyl* cells. White dashed line indicates bud neck and white line outlines the mother and bud. Scale bar, 2μm. **(B)** Quantification of Bim1-CFP fluorescence indicated that the amount of Bim1 localized to microtubule +ends is significantly reduced in *tub4-*Δ*dsyl* cells relative to wild-type ($p < 0.01$). **(C)** The ratio of Bim1-CFP/Kar9-YFP fluorescence is greater in *TUB4* cells (0.958±0.224 arbitrary fluorescent units) relative to *tub4-*Δ*dsyl* cells (0.377±0.078 arbitrary fluorescent units). **(D & E)** Bim1 and Kar9 protein levels in *tub4-*Δ*dsyl* cells are similar to those in *TUB4* cells. Actin is shown as a loading control. **(F)** Bim1 co-purifies with Kar9-ProA in wild-type and *tub4-*Δ*dsyl* cells, but the level of Bim1 co-purification is reduced in *tub4-*Δ*dsyl* cells. **(G)** Histogram showing the averaged amount of co-purifying Bim1 (arbitrary units normalized to the Kar9-ProA input) in 3 independent experiments for wild-type and *tub4-*Δ*dsyl* strains.

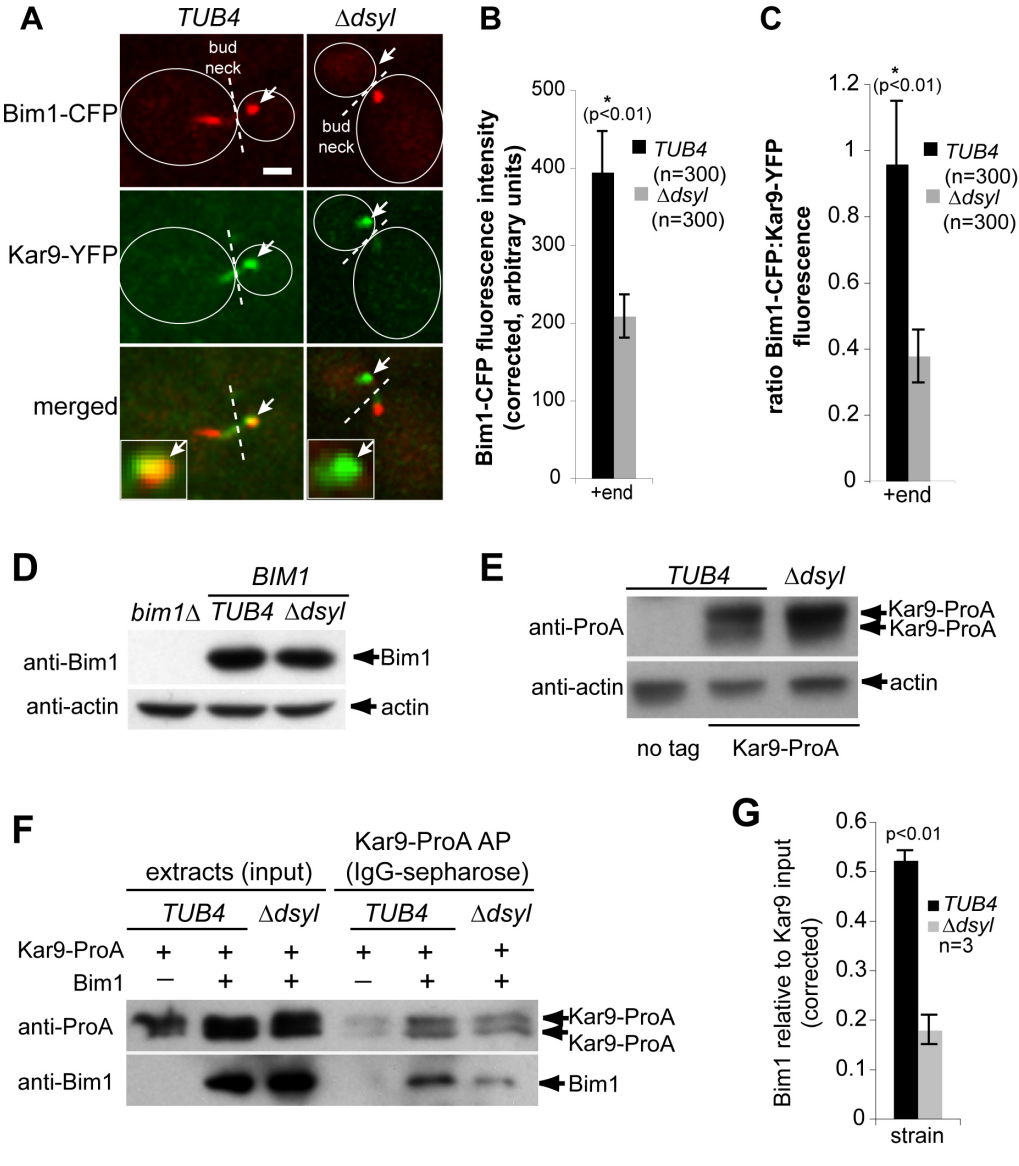
A
TUB4
Δdsyl
bud neck
bud neck
Bim1-CFP
Kar9-YFP
merged
B
Bim1-CFP fluorescence intensity (corrected, arbitrary units)
500
400
300
200
100
0
*
(p<0.01)
TUB4 (n=300)
Δdsyl (n=300)
+end
C
ratio Bim1-CFP:Kar9-YFP fluorescence
1.2
1
0.8
0.6
0.4
0.2
0
*
(p<0.01)
TUB4 (n=300)
Δdsyl (n=300)
+end
D
BIM1
bim1Δ
TUB4
Δdsyl
anti-Bim1
Bim1
anti-actin
actin
E
TUB4
Δdsyl
anti-ProA
Kar9-ProA
Kar9-ProA
anti-actin
actin
no tag
Kar9-ProA
F
extracts (input)
Kar9-ProA AP (IgG-sepharose)
TUB4
Δdsyl
TUB4
Δdsyl
Kar9-ProA + + + + + +
Bim1 − + + − + +
anti-ProA
Kar9-ProA
Kar9-ProA
anti-Bim1
Bim1
G
Bim1 relative to Kar9 input (corrected)
0.6
0.5
0.4
0.3
0.2
0.1
0
p<0.01
TUB4
Δdsyl
n=3
strain

2.4.5 Kar9 suppresses microtubule dynamics in *tub4-Δdsyl* cells

Spindle positioning defects in *tub4-Δdsyl* cells may result from defective Kar9 complexes that tether microtubule +ends to the cortex and suppress dynamics, or from an alteration of the microtubule lattice that perturbs microtubule dynamics. To distinguish between these possibilities, we tested if deletion of Kar9 would affect the rates of elongation, shrinkage and pause time of astral microtubules in *tub4-Δdsyl* cells. These parameters were analyzed in *TUB4, tub4-Δdsyl, kar9Δ* and *tub4-Δdsyl kar9Δ* cells expressing GFP-Tub1. We reasoned that if spindle positioning defects in *tub4-Δdsyl* cells result from an altered microtubule lattice, then deleting Kar9 should not affect these parameters and the rates of elongation, shrinkage and pause time should be similar in *tub4-Δdsyl* and *tub4-Δdysl kar9Δ* cells.

We found astral microtubules were dynamic in *TUB4* and *kar9Δ* cells, with periodic phases of elongation and shrinkage, while those in *tub4-Δdsyl* cells were less dynamic (Figure 2.4.5 A). Significantly, deletion of Kar9 in *tub4-Δdsyl* cells (*tub4-Δdsyl kar9Δ*) resulted in near wild-type dynamics (Figure 2.4.5 A). Microtubule elongation rate, shrinkage rate and the time a microtubule spent in the paused state were calculated for each cell type (Figure 2.4.5B). *tub4-Δdsyl* cells had a decreased elongation rate (0.92 ± 0.19μm·min^{-1}, p<0.01) relative to *TUB4* (1.35 ± 0.03μm·min^{-1}, p<0.01), *kar9Δ* (1.27 ± 0.07μm·min^{-1}, p<0.01) and *tub4-Δdsyl kar9Δ* cells (1.27 ± 0.05μm·min^{-1}, p<0.01). The shrinkage rate of *tub4-Δdsyl* cells was similar to that of the wild-type strain, however the time a microtubule spent in a paused state was greatly increased in *tub4-Δdsyl* cells (88.6sec ± 10.4; P<0.01) relative to *TUB4* (32.4 sec ± 5.3), *kar9Δ* (35.0 sec ± 5.3) and *tub4-Δdsyl kar9Δ* cells (27.2 sec ± 5.3) (Figure 2.4.5 B). Thus, the affect of the *tub4-Δdsyl* mutation on the dynamic properties of astral microtubules is unlikely to be the result of an alteration of microtubule structure. Instead, this analysis is in agreement with defective Kar9 complexes on +ends that suppress microtubule dynamics in *tub4-Δdsyl* cells.

Figure 2.4.5 Preferential localization of Kar9 on microtubule +ends in *tub4-*∆*dsyl* cells alters astral microtubule dynamics

(A & B) Microtubule lifetime lengths were measured in *TUB4*, *tub4-*∆*dsyl, kar9*∆ and *tub4-*∆*dsyl kar9*∆ cells containing a GFP-Tub1 fusion protein (see materials and methods for experimental details). Microtubule lengths (µm) were measured in triplicate at 10 sec intervals (total time = 310 seconds) and the averaged length plotted relative to time (seconds). **(B)** Astral microtubules in *tub4-*∆*dsyl* cells were less dynamic relative to *TUB4* and *kar9*∆ cells with an increase in the duration of pause event. Dynamics are restored in *tub4-*∆*dsyl kar9*∆ double mutant cells.

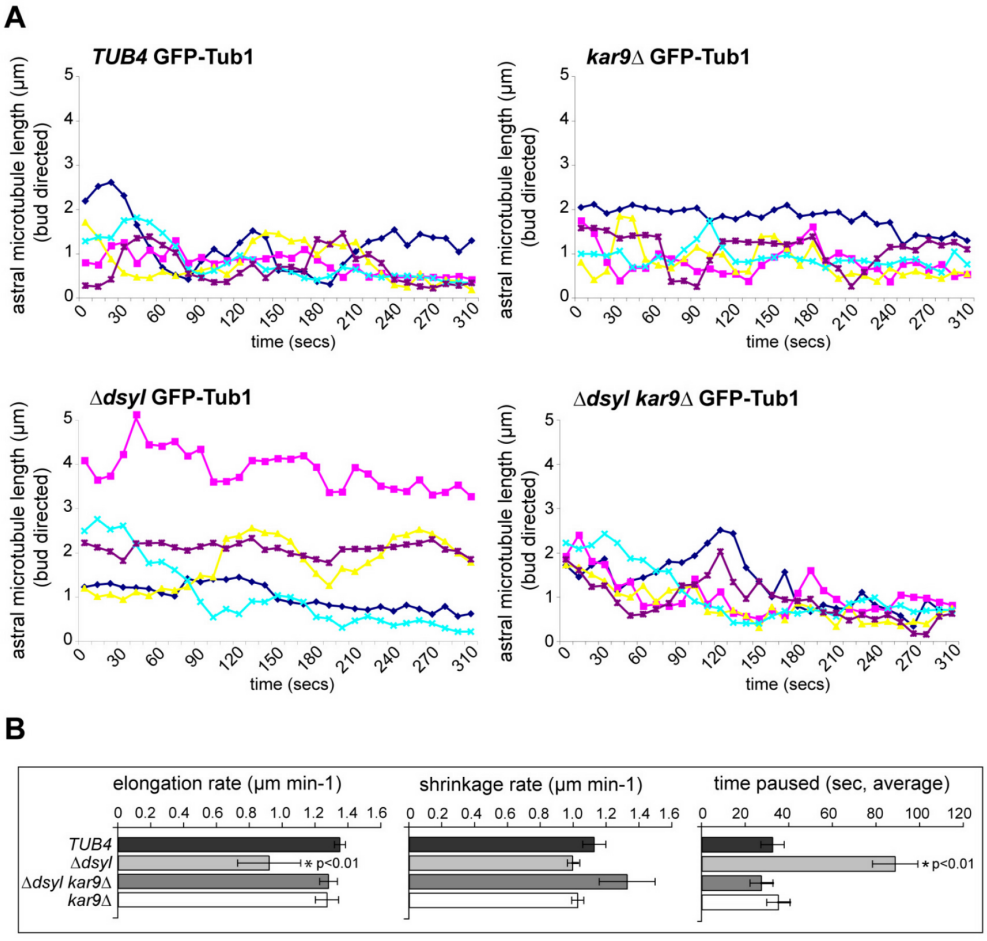
A
TUB4 GFP-Tub1
kar9Δ GFP-Tub1
ΔdsyI GFP-Tub1
ΔdsyI kar9Δ GFP-Tub1
astral microtubule length (μm) (bud directed)
time (secs)
B
elongation rate (μm min-1)
shrinkage rate (μm min-1)
time paused (sec, average)
TUB4
ΔdsyI
ΔdsyI kar9Δ
kar9Δ
* p<0.01
* p<0.01

2.4.6 Kar9 interactions with Myo2 are stabilized in *tub4-*Δ*dsyl* cells

Typically during spindle placement, Bim1-Kar9 loaded microtubules dynamically probe the bud neck and cortex and then retract back to the SPB_b until associations with Myo2 are achieved (Kusch *et al.*, 2002; Liakopoulos *et al.*, 2003; Maekawa *et al.*, 2003). However in *tub4-*Δ*dsyl* cells, it appeared that altered Kar9 complexes containing reduced Bim1 were not efficiently releasing from the cortex back to the SPB_b and rather exhibited prolonged interactions with the cortex. We examined this by assessing the localization of Kar9 relative the SPB_b in wild-type and *tub4-*Δ*dsyl* cells expressing Kar9-GFP and the SPB marker, Spc42-CFP. As expected, in wild-type cells Kar9-GFP foci probe the bud neck and retract back to the SPB_b (Figure 2.4.6 A). During this time, the spindle remains close to the bud neck (Figure 2.4.6 A; the distances of Kar9-GFP relative to SPBs in μm are shown above each frame of A). Conversely, in *tub4-*Δ*dsyl* cells Kar9-GFP dwell either at the cortex or at the bud neck, and rarely retract back to the SPB_b (Figure 2.4.6 A).

A summary indicating the distribution of Kar9-GFP localization and movements in the bud, relative to the SPB_b for each strain/condition are shown in Figure 2.4.6 B and C. The cumulative distribution of Kar9-GFP foci in all wild-type cells assessed, ranges from the SPB_b and the bud neck, to the bud cortex (Figure 2.4.6 B, panel i). This suggests that Kar9-GFP foci in these cells are dynamic and localize throughout this entire volume between the SPB and the bud tip. Additionally, Kar9-GFP movements in wild-type cells consist of periodic movements away from and towards the SPB (Figure 2.4.6 B, panel ii). In contrast, the cumulative distribution of Kar9-GFP foci in *tub4-*Δ*dsyl* cells assessed was restricted between the neck and the bud tip, >1.0 μm from the SPB_b (Figure 2.4.6 C, panel i). This suggests that Kar9 loaded microtubules are not dynamic and remain far away from the SPB_b. Consistently, the movement of Kar9-GFP foci in the bud was less dynamic in *tub4-*Δ*dsyl* cells, with minor movements relative to the position of the SPB (Figure 2.4.6 C, panel ii).

Figure 2.4.6 Kar9 interactions with Myo2 are stabilized in *tub4-*Δ*dsyl* cells

(A) In *TUB4* cells microtubules loaded with Kar9-GFP (green arrows) are dynamic and retract quickly from the cortex and bud neck (dashed line) to the SPB_b (red arrows). In *tub4-*Δ*dsyl* cells, Kar9-associated microtubules are less dynamic and rarely de-polymerize back to the SPB_b or bud neck. Mother and bud are outlined (white) in the first frame of the montage. For each strain, distance (μm) of Kar9-GFP relative to SPB and the Δ of distance relative to the previous time-point are indicated above each panel. A (+Δ) reflects microtubule growth, while (-Δ) reflects microtubule shrinkage as a read-out of Kar9-GFP localization relative to the previous frame. **(B)** In wild-type cells, Kar9-GFP foci distribute near and far from the SPB_b **(B, panel i).** Kar9-GFP foci are highly dynamic and are associated with both growing and shrinking microtubules **(B, panel ii)**. **(C)** In *tub4-*Δ*dsyl* cells **(C, panel i)**, the Kar9-GFP foci to not cluster near the SPB_b but rather to a region approximately 1.5-3 μm in length from the SPB_b. Furthermore, Kar9-GFP foci are not dynamic and are associated with microtubules that do not move towards and away from the SPB_b **(C, panel ii)**. **(D)** Montage (t<30 min) of Kar9-foci in *myo2-16* cells and *tub4-*Δ*dsyl myo2-16* double mutants revealed that Kar9 is dynamic in both cell types. **(E)** In *myo2-16* Kar9-GFP foci have a large distribution due to the growth and shrinkage of dynamic microtubules **(E, panel i).** Microtubules in the *myo2-16* cells are dynamic due to short interactions with the cortex **(E, panel ii). (F)** In *myo2-16*, *tub4-*Δ*dsyl* double mutants, Kar9-GFP foci are distributed near the SPB_b and the bud cortex **(F, panel i)** while Kar9 dynamics are restored **(F, panel ii)**.

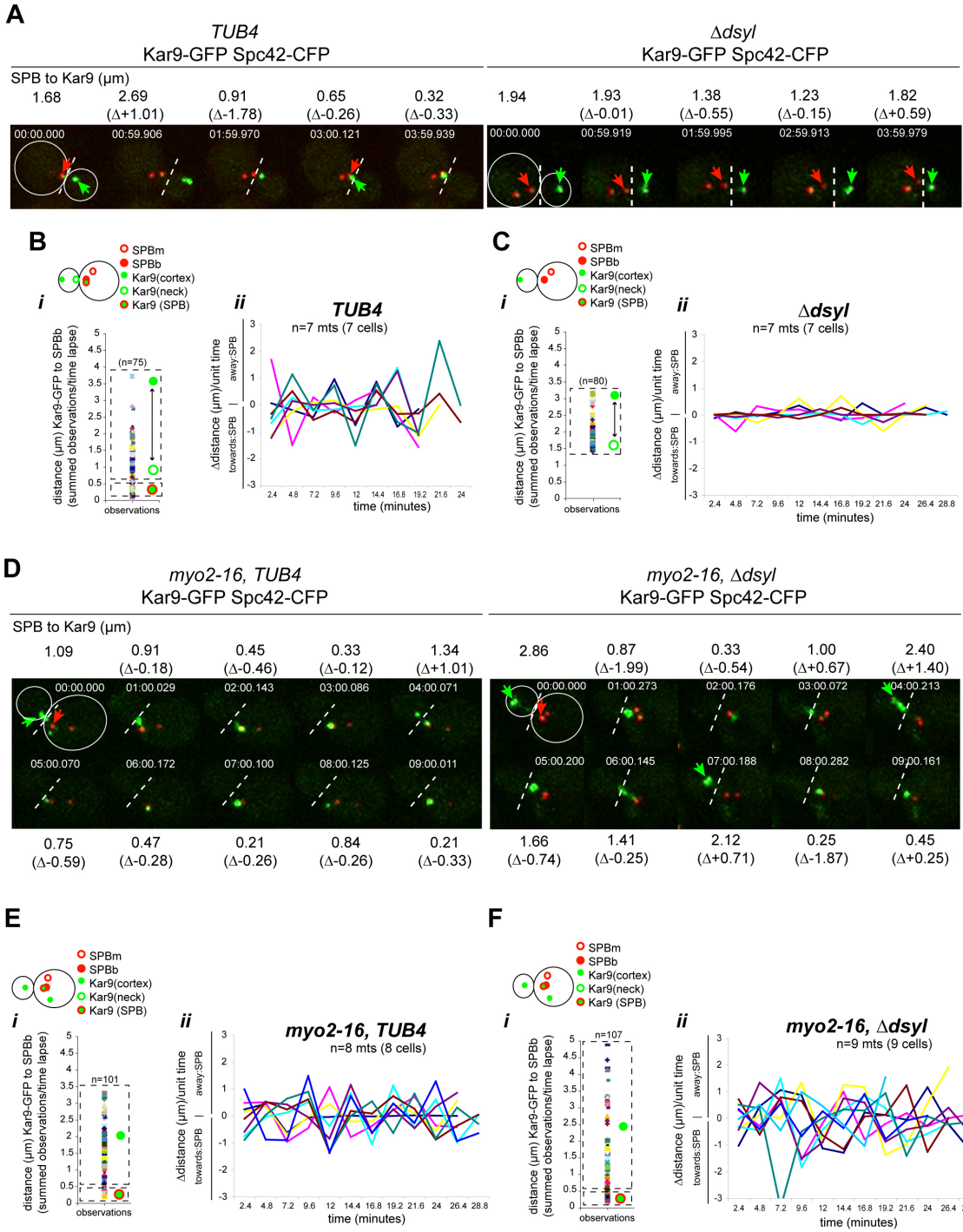
A
TUB4
Kar9-GFP Spc42-CFP
Δdsyl
Kar9-GFP Spc42-CFP
SPB to Kar9 (μm)
1.68
2.69 (Δ+1.01)
0.91 (Δ-1.78)
0.65 (Δ-0.26)
0.32 (Δ-0.33)
1.94
1.93 (Δ-0.01)
1.38 (Δ-0.55)
1.23 (Δ-0.15)
1.82 (Δ+0.59)
00:00.000
00:59.906
01:59.970
03:00.121
03:59.939
00:00.000
00:59.919
01:59.995
02:59.913
03:59.979
B
C
SPBm
SPBb
Kar9(cortex)
Kar9(neck)
Kar9 (SPB)
i
ii
distance (μm) Kar9-GFP to SPBb (summed observations/time lapse)
observations
(n=75)
(n=80)
Δdistance (μm)/unit time
towards:SPB
away:SPB
time (minutes)
TUB4
n=7 mts (7 cells)
Δdsyl
n=7 mts (7 cells)
D
myo2-16, TUB4
Kar9-GFP Spc42-CFP
myo2-16, Δdsyl
Kar9-GFP Spc42-CFP
SPB to Kar9 (μm)
1.09
0.91 (Δ-0.18)
0.45 (Δ-0.46)
0.33 (Δ-0.12)
1.34 (Δ+1.01)
2.86
0.87 (Δ-1.99)
0.33 (Δ-0.54)
1.00 (Δ+0.67)
2.40 (Δ+1.40)
00:00.000
01:00.029
02:00.143
03:00.086
04:00.071
05:00.070
06:00.172
07:00.100
08:00.125
09:00.011
00:00.000
01:00.273
02:00.176
03:00.072
04:00.213
05:00.200
06:00.145
07:00.188
08:00.282
09:00.161
0.75 (Δ-0.59)
0.47 (Δ-0.28)
0.21 (Δ-0.26)
0.84 (Δ-0.26)
0.21 (Δ-0.33)
1.66 (Δ-0.74)
1.41 (Δ-0.25)
2.12 (Δ+0.71)
0.25 (Δ-1.87)
0.45 (Δ+0.25)
E
F
SPBm
SPBb
Kar9(cortex)
Kar9(neck)
Kar9 (SPB)
i
ii
distance (μm) Kar9-GFP to SPBb (summed observations/time lapse)
observations
(n=101)
(n=107)
Δdistance (μm)/unit time
towards:SPB
away:SPB
time (minutes)
myo2-16, TUB4
n=8 mts (8 cells)
myo2-16, Δdsyl
n=9 mts (9 cells)

Kar9 interacts with cortical actin via its association with the tail domain of the type V myosin Myo2, which guides microtubules loaded with Kar9 along polarized actin filaments during spindle positioning (Beach *et al.*, 2000; Yin *et al.*, 2000; Hwang *et al.*, 2003). We speculated that the static localization of Kar9 in the bud and defect in Kar9 function was due to an inappropriately stable interaction between Kar9 and Myo2. To test this possibility, we analyzed Kar9-GFP movements in the *myo2-16* mutant, which is defective for Myo2-Kar9 interactions at 30˚C in rich medium (Schott *et al.*, 1999).

Kar9-GFP movements were extremely dynamic in *myo2-16* cells, however microtubules frequently failed to enter the bud and spindle positioning was defective (Figure 2.4.6 D). Next, we tested whether the *myo2-16* mutation would increase Kar9-GFP dynamics in *tub4-*Δ*dsyl* cells and eliminate cortical dwelling. Our analysis revealed that Kar9-GFP movements in *tub4-*Δ*dsyl* cells were highly dynamic, though as in *myo2-16* cells, microtubule +end targeting into the bud and spindle positioning remained defective (Figure 2.4.6 D). Kar9-GFP localization in the bud relative to the SPB and movements were monitored for each condition (*TUB4 myo2-16*, n=8; *tub4-*Δ*dsyl myo2-16*, n=9; Figure 2.4.6 E, F). In *TUB4 myo2-16* cells, Kar9-GFP was detected at the bud neck, bud cortex and SPB_b (Figure 2.4.6 E, panel i). Kar9-GFP movements in the bud were highly dynamic, characterized by movements away from and towards the SPB (Figure 2.4.6 E, panel ii). Similarly, Kar9-GFP localized to the bud neck, bud cortex and SPB_b in *myo2-16 tub4-*Δ*dsyl* cells (Figure 2.4.6 F, panel i). Moreover, Kar9-GFP movements in the bud were highly dynamic (Figure 2.4.6 F, panel ii). Taken together, this data suggests that the stable interaction between Kar9 and the cortex in *tub4-*Δ*dsyl* cells is a result of inappropriately stable interactions between Kar9 and Myo2 and is consistent with the restoration of microtubule dynamics observed in *tub4-*Δ*dsyl kar9*Δ double mutants.

2.4.7 Kar9 dwelling in the bud requires cortical actin

In order to confirm that stable interactions between Kar9 and Myo2 were dependent on cortical actin, we tested whether disruption of cortical F-actin by latrunculin B (LatB) would similarly restore dynamic Kar9-GFP movements in *tub4-*Δ*dsyl* cells. Wild-type and *tub4-*Δ*dsyl* cells expressing Kar9-GFP and Spc42-CFP were treated with 200 mM LatB for 30-60 minutes. Cells were stained with Alexa 488-phalloidin to confirm that F-actin was similarly disrupted in both strains (Figure 2.4.7 A). Kar9-GFP localization was distributed between the cortex and SPB_b in wild-type cells treated with LatB (Figure 2.4.7 B, panel i) characterized by highly dynamic movements between the SPB_b and bud cortex (Figure 2.4.7 B, panel ii). Similarly, *tub4-*Δ*dsyl* cells also exhibited a distribution of Kar9-GFP foci between the SPB_b and cortex (Figure 2.4.7 C, panel i) and dynamic movements within the bud (Figure 2.4.7 C, panel ii).

We next tested if the dynamic movements of Kar9 in *tub4-*Δ*dsyl* cells treated with LatB correlated with a restoration of Bim1 and/or Kar9 SPB localization. If the failure of these proteins to localize to SPB is due to the loss of the DSYL residues, then releasing Kar9 complexes from the cortex should not restore their localization to SPBs. We analyzed the SPB localization of Bim1-GFP in wild-type and *tub4-*Δ*dsyl* cells treated with LatB to disrupt F-actin, and NZ to de-polymerize astral microtubules. CFP-Tub1 was used to visualize the collapsed spindle and Alexa 488-phallodin to confirm the disruption of the actin cytoskeleton. As before we found the majority of wild-type cells (87.7%, n=65) treated with LatB and NZ had detectable Bim1-GFP associated with the collapsed spindle (Figure 2.4.7 D,F). In contrast relatively few *tub4-*Δ*dsyl* cells treated with LatB and NZ (37.7%, n=69) had detectable Bim1-GFP (Figure 2.4.7 D,F). Similarly, the localization of Kar9-GFP in *tub4-*Δ*dsyl* cells treated with LatB and NZ was reduced; 31.3% of *tub4-*Δ*dsyl* cells (n=67) had detectable Kar9-GFP compared to 78% of wild-type cells (n=70; Figure 2.4.7 E,F). This analysis suggests that the defect in Bim1 and Kar9 localization at SPBs in *tub4-*Δ*dsyl* cells is independent of the interaction between Kar9 and the cortex.

Figure 2.4.7 Stable localization of Kar9 in the bud depends on cortical actin.

(A) Actin staining of *TUB4* and *tub4-*Δ*dsyl* cells with and without treatment of 200μm latrunculin B (LatB). Treatment with LatB resulted in the depolymerization of the actin cytoskeleton in *TUB4* and *tub4-*Δ*dsyl* cells. Respective phase images shown. Scale bar=2μm. (**B, panel i)** In wild-type cells treated with LatB, Kar9-GFP foci distributed to the bud cortex as well as the SPB. Following latrunculin treatment, microtubules (Kar9-GFP foci) in wild-type cells were highly dynamic. In *tub4-*Δ*dsyl* cells treated with latrunculin, the distribution of Kar9-GFP foci relative to the SPB were rescued to near wild-type levels **(C, panel i).** Kar9 dynamics were also rescued to near wild-type levels **(C, panel ii). (D-F)** Analysis of Bim1 and Kar9 SPB localization in cells treated with 200μM LatB (to disrupt F-actin) and 30μg/ml NZ (to de-polymerize astral microtubules). CFP-Tub1 was used to visualize the collapsed spindle and Alexa 488-phallodin to confirm the disruption of the actin cytoskeleton in the presence or absence of latrunculin and NZ. The majority of wild-type cells (87.7%, n=65) treated with LatB and NZ had detectable Bim1-GFP associated with the collapsed spindle **(D,F).** In contrast, the percentage of LatB and NZ treated *tub4-*Δ*dsyl* cells with detectable Bim1-GFP at SPBs was reduced (37.7%, n=69) **(D,F).** Similarly, the localization of Kar9-GFP in *tub4-*Δ*dsyl* cells treated with LatB and NZ was reduced; 31.3% of *tub4-*Δ*dsyl* cells (n=67) had detectable Kar9-GFP compared to 78% of wild-type cells (n=70; **E,F**).

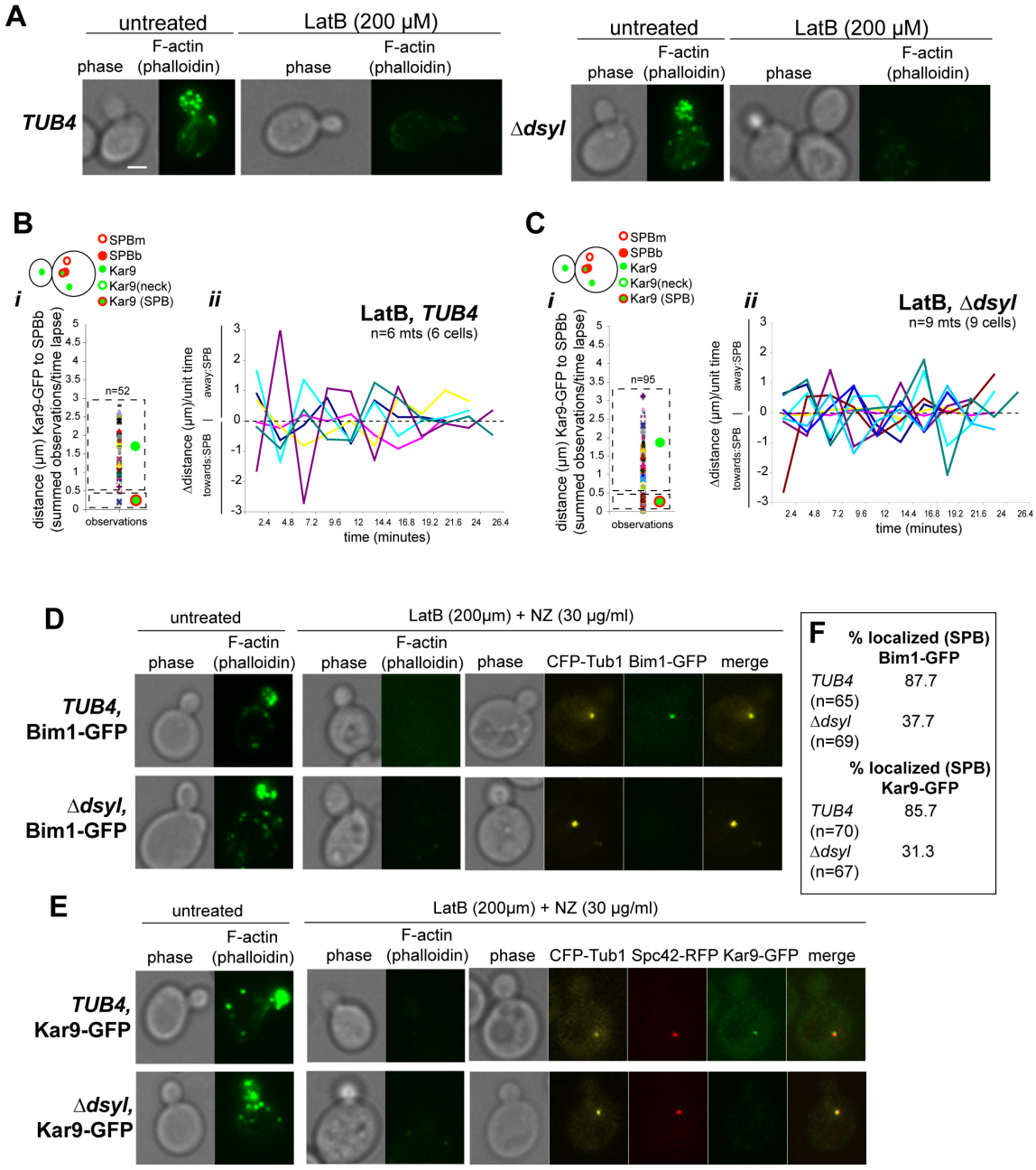
A
untreated
LatB (200 µM)
phase
F-actin (phalloidin)
TUB4
Δdsyl
B
C
SPBm
SPBb
Kar9
Kar9(neck)
Kar9 (SPB)
i
ii
distance (µm) Kar9-GFP to SPBb (summed observations/time lapse)
n=52
n=95
observations
Δdistance (µm)/unit time
away:SPB
towards:SPB
LatB, TUB4
n=6 mts (6 cells)
LatB, Δdsyl
n=9 mts (9 cells)
time (minutes)
D
LatB (200µm) + NZ (30 µg/ml)
CFP-Tub1
Bim1-GFP
merge
TUB4, Bim1-GFP
Δdsyl, Bim1-GFP
E
Spc42-RFP
Kar9-GFP
TUB4, Kar9-GFP
Δdsyl, Kar9-GFP
F
% localized (SPB) Bim1-GFP
TUB4 (n=65) 87.7
Δdsyl (n=69) 37.7
% localized (SPB) Kar9-GFP
TUB4 (n=70) 85.7
Δdsyl (n=67) 31.3

2.4.8 Over-production of Bim1 restores Kar9 function and spindle placement in *tub4-*Δ*dsyl* cells

While Kar9 can localize to astral microtubules in *tub4-*Δ*dsyl* cells, our analysis demonstrates that its localization is not sufficient for function. We hypothesized that the ratio of Bim1 and Kar9 is critical for the assembly of functional Bim1-Kar9 complexes. As such, over-production of Bim1 may restore Kar9-Bim1 interactions and rescue Kar9 function in *tub4-*Δ*dsyl* cells, while overproduction of Kar9 should not. We first assayed for rescue of the Kar9 pathway by determining whether over-production of either protein would restore viability to the *tub4-*Δ*dsyl dhc1*Δ double mutant (see Figure 2.4.2 B,C). *tub4-*Δ*dsyl* cells were transformed with a 2μ vector (pRS423) containing *BIM1* or *KAR9* or 2μ vector, and mated to *dhc1*Δ cells to produce heterozygous diploid strains. Haploid progeny (40 tetrads per condition) were scored for the presence of viable double mutants. We found over-production of Bim1 increased the viability *tub4-*Δ*dsyl dhc1*Δ double mutants (Figure 2.4.8 A). However, over-production of Kar9 did not, nor did the vector control (Figure 2.4.8 A).

We next assessed whether over-production of Bim1 would increase the amount of Bim1 co-purifying with Kar9-ProA in *tub4-*Δ*dsyl* cells. Kar9-ProA was affinity purified from whole cell extracts prepared from wild-type and *tub4-*Δ*dsyl* cells over-producing Bim1 (p*BIM1*) or endogenous Bim1 (pRS423). Bim1 levels increased in *tub4-*Δ*dsyl* cells containing pBIM1, and the amount of Bim1 co-purifying with Kar9-ProA was restored to wild-type levels (Figure 2.4.8 B). As shown before, *tub4-*Δ*dsyl* cells expressing endogenous levels of Bim1 had reduced Bim1 co-purifying with Kar9-ProA (Figure 2.4.8 B).

Figure 2.4.8 Kar9 function is restored by over-production of Bim1

(A) Percentage of viable *tub4-*Δ*dsyl* Δ*dhc1* double mutants recovered in the presence of over-produced Bim1, Kar9 or vector control. Over–production of Bim1 (*pBIM1*) rescued the synthetic lethality observed in *tub4-*Δ*dsyl*Δ*dhc1* double mutants while over-production of Kar9 (*pKAR9*) or expression of the vector control (*pRS423*) did not rescue synthetic lethality. 40 tetrads/mating were scored**. (B)** Bim1 and Kar9 interactions are restored by over-production of Bim1. The level of Bim1 that co-affinity purifies with Kar9 in *tub4-*Δ*dsyl* cells is restored in the presence of over-produced Bim1 relative to cells containing the vector control. **(C)** Astral microtubule guidance is restored by an over-production of Bim1. *tub4-*Δ*dsyl pBIM1* cells have a lower occurrence of microtubule mis-guidance relative to *tub4-*Δ*dsyl pRS423* cells. **(D)** Spindle placement was analyzed in *tub4-*Δ*dsyl pRS423* and *tub4-*Δ*dsyl pBIM1* cells. Over-production of Bim1 (black bars) rescued spindle positioning defects (categories 3 and 4) observed in control cells (grey bars)

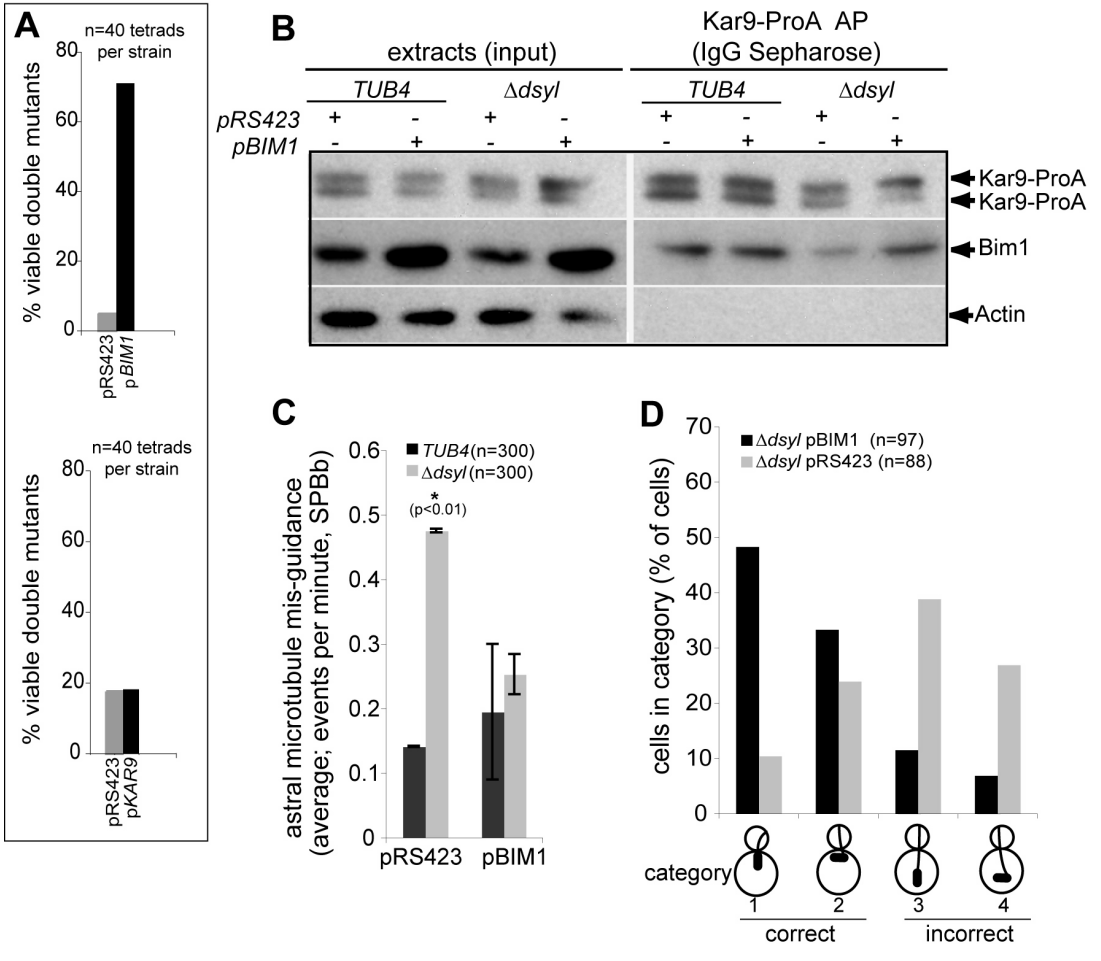
A
n=40 tetrads per strain
% viable double mutants
80
60
40
20
0
pRS423
pBIM1
n=40 tetrads per strain
% viable double mutants
80
60
40
20
0
pRS423
pKAR9
B
extracts (input)
Kar9-ProA AP (IgG Sepharose)
TUB4
Δdsyl
TUB4
Δdsyl
pRS423
pBIM1
Kar9-ProA
Kar9-ProA
Bim1
Actin
C
astral microtubule mis-guidance (average; events per minute, SPBb)
TUB4 (n=300)
Δdsyl (n=300)
*
(p<0.01)
0.6
0.5
0.4
0.3
0.2
0.1
0
pRS423
pBIM1
D
Δdsyl pBIM1 (n=97)
Δdsyl pRS423 (n=88)
cells in category (% of cells)
70
60
50
40
30
20
10
0
category
1
2
3
4
correct
incorrect

We next tested if over-production of Bim1 would rescue the defect in microtubule targeting and spindle placement observed in *tub4-*Δ*dsyl* cells. This analysis revealed over-production of Bim1 does suppress mis-targeting in *tub4-*Δ*dsyl* cells relative to the vector control (Figure 2.4.8 C). Similarly, defects in spindle placement are also rescued in *tub4-*Δ*dsyl* cells over-producing Bim1 relative to the control (Figure 2.4.8 D). Collectively, these analyses suggested that over-production of Bim1 can restore its interaction with Kar9 and their function in microtubule guidance and spindle placement in *tub4-*Δ*dsyl* cells.

Finally, we were curious whether over-production of Bim1 in *tub4-*Δ*dsyl* cells would reduce the cortical dwelling of Kar9-GFP in the bud, and analyzed the distribution and movements of Kar9-GFP in the bud relative to the position of the SPB_b over time in *tub4-*Δ*dsyl pRS423* and *tub4-*Δ*dsyl pBIM1* cells. In *tub4-*Δ*dsyl pRS423* cells, Kar9-GFP movements in the bud did not pull the spindle towards the neck or orient it; at 3 minutes the spindle rotates and becomes mis-oriented and remains mis-oriented and positioned away from the bud neck for the remainder of the time-lapse (Figure 2.4.9 A). In contrast, Kar9-GFP movements were more dynamic and associated with astral microtubules that probed the neck/cortex and retracted back to the SPB_b in *tub4-*Δ*dsyl* cells overproducing Bim1 (Figure 2.4.9 C).

A summary of our analysis of Kar9-GFP movements in representative cells for each strain and condition (*tub4-*Δ*dsyl* pRS423, n=4; *tub4-*Δ*dsyl* p*BIM1*, n=7) are shown in Figure 2.4.9 B and D. In *tub4-*Δ*dsyl pRS423* cells, Kar9-GFP was detected at the cortex and bud neck, but not at the SPB (Figure 2.4.9 B, panel i), and dwelled in these locations without dynamic movement (Figure 2.4.9 B, panel ii). However, over-production of Bim1 in *tub4-*Δ*dsyl* cells restored SPB localization of Kar9-GFP (Figure 2.4.9 D, panel i) and its dynamic movement in the bud (Figure 2.4.9 D, panel ii). Taken together, our analysis suggests that over-production of Bim1 in *tub4-*Δ*dsyl* cells promotes the assembly of functional Bim1-Kar9 complexes.

Figure 2.4.9 Over-production of Bim1 restores Kar9 dynamics in *tub4-*Δ*dsyl* cells

(A) Montage of Kar9-GFP movements in *tub4-*Δ*dsyl pRS423* and *tub4-*Δ*dsyl pBIM1* cells. Over-production of Bim1 rescues the Kar9 associated microtubules dynamics in *tub4-*Δ*dsyl* cells while in the vector control, Kar9-associated microtubules remain non-dynamic (green arrows). **(B, D)** Microtubules/Kar9-GFP foci were tracked during a time course (t<30 min) in *tub4-*Δ*dsyl pRS423* and *tub4-*Δ*dsyl pBIM1* cells. Line graphs depict the length from the microtubule +ends relative to the SPB_b per Δtime (t=2.4 min). Scatter plots display the relative distribution of Kar9-GFP foci relative to the SPB over time. In *tub4-*Δ*dsyl pRS423* cells **(B, panel i),** the Kar9-GFP foci cluster to a region approximately 1.5-3μm in length from the SPB_b indicating the microtubules do not depolymerize back to the SPB_b. Microtubules appeared to be static **(B, panel ii).** In contrast, in *tub4-*Δ*dsyl* cells with over-produced Bim1, the distribution of Kar9-GFP foci relative to the SPB_b **(D, panel i)** and its dynamic movement in the bud **(D, panel ii)** were similar to wild-type.

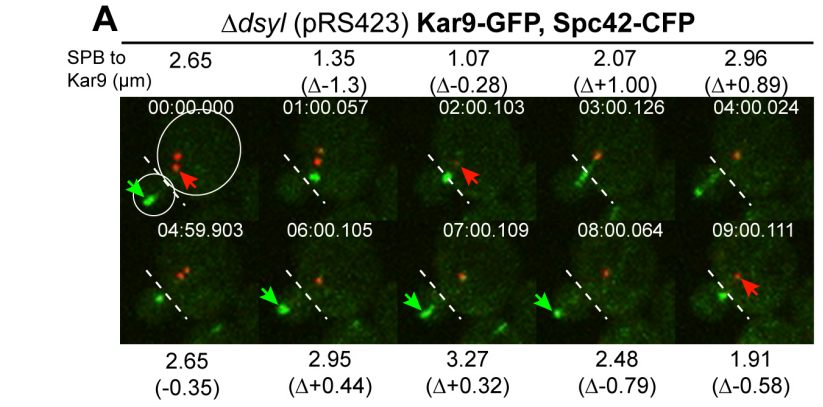
A
Δdsyl (pRS423) Kar9-GFP, Spc42-CFP
SPB to Kar9 (μm)
2.65
1.35 (Δ-1.3)
1.07 (Δ-0.28)
2.07 (Δ+1.00)
2.96 (Δ+0.89)
00:00.000
01:00.057
02:00.103
03:00.126
04:00.024
04:59.903
06:00.105
07:00.109
08:00.064
09:00.111
2.65 (-0.35)
2.95 (Δ+0.44)
3.27 (Δ+0.32)
2.48 (Δ-0.79)
1.91 (Δ-0.58)

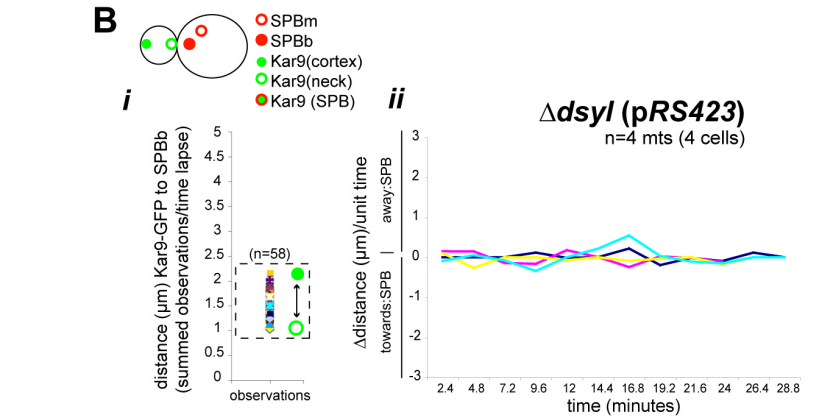
B
SPBm
SPBb
Kar9(cortex)
Kar9(neck)
Kar9 (SPB)
i
distance (μm) Kar9-GFP to SPBb (summed observations/time lapse)
(n=58)
observations
ii
Δdsyl (pRS423)
n=4 mts (4 cells)
Δdistance (μm)/unit time
towards:SPB
away:SPB
time (minutes)

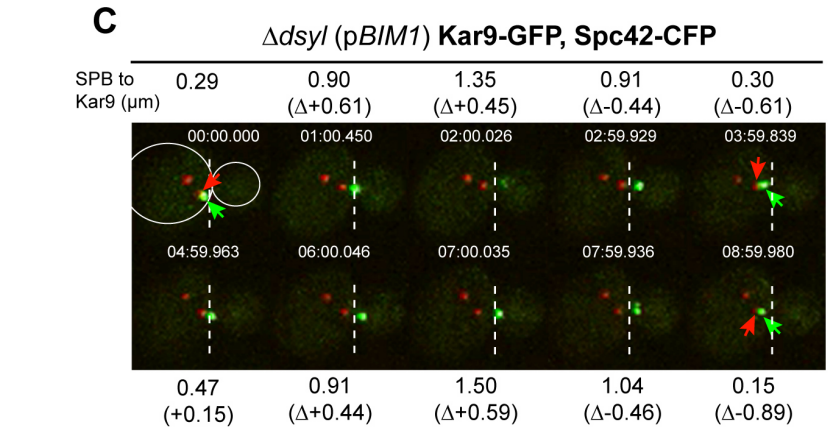
C
Δdsyl (pBIM1) Kar9-GFP, Spc42-CFP
SPB to Kar9 (μm)
0.29
0.90 (Δ+0.61)
1.35 (Δ+0.45)
0.91 (Δ-0.44)
0.30 (Δ-0.61)
00:00.000
01:00.450
02:00.026
02:59.929
03:59.839
04:59.963
06:00.046
07:00.035
07:59.936
08:59.980
0.47 (+0.15)
0.91 (Δ+0.44)
1.50 (Δ+0.59)
1.04 (Δ-0.46)
0.15 (Δ-0.89)

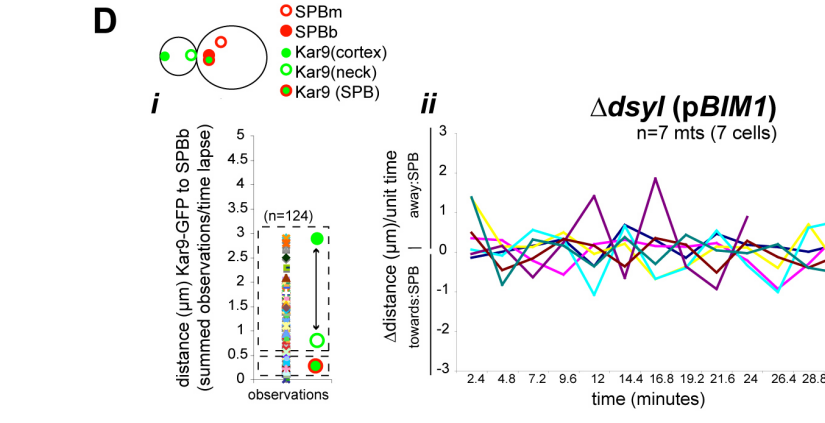
D
SPBm
SPBb
Kar9(cortex)
Kar9(neck)
Kar9 (SPB)
i
distance (μm) Kar9-GFP to SPBb (summed observations/time lapse)
(n=124)
observations
ii
Δdsyl (pBIM1)
n=7 mts (7 cells)
Δdistance (μm)/unit time
towards:SPB
away:SPB
time (minutes)

2.5 Discussion

2.5.1 The roles of Tub4 and SPBs in Kar9-dependant spindle positioning

Numerous studies have demonstrated that the SPBs play a critical role in Kar9-dependent spindle positioning. For instance, many studies have shown that the asymmetric localization of Kar9 to the SPB_{b} ensures its deployment to the astral microtubules adjacent to the bud, which is essential for its function in spindle positioning (Liakopoulos *et al.*, 2003; Maekawa *et al.*, 2003; Maekawa and Schiebel, 2004; Moore *et al.*, 2005). Phospho-inhibiting mutations in residues Ser197 and S496 (*kar9-AA*) that block Kar9 phosphorylation, result in a number of defects including, symmetric localization of Kar9 to both SPBs, inappropriate targeting of astral microtubules associated with both SPBs towards the bud and an increase in the number of cells with the wrong SPB (SPB_{m}) positioned near the bud neck (Liakopoulos *et al.*, 2003). Conversely, loss of Kar9 function (by deletion of Kar9; *kar9*Δ), results in distinct defects including, mis-targeting of microtubules emanating from the SPB_{b} back into the mother cell and failure to orient the spindle near the bud neck (Miller and Rose, 1998; Liakopoulos *et al.*, 2003).

In *tub4-*Δ*dsyl* cells, Kar9 remains associated with microtubules emanating from the SPB_{b}, indicating its asymmetric localization to astral microtubules is preserved. In addition, while *tub4-*Δ*dsyl* cells are less efficient in targeting astral microtubules into the bud, astral microtubules loaded with Kar9 frequently enter the bud but fail to place the spindle at the bud neck. Therefore, the observed defects in spindle placement in *tub4-*Δ*dsyl* cells is not characteristic of a defect in establishing asymmetry, or reminiscent of a complete loss of function *kar9*Δ mutation. Instead, the defects in *tub4-*Δ*dsyl* cells appear to be linked to the ability of Bim1 and Kar9 to assemble into complexes at SPBs and function on microtubule +ends. Our analysis suggests that the SPB, via the c-terminus of Tub4, contributes to the loading and/or

assembly of functional Bim1-Kar9 complexes prior to their deployment to astral microtubules.

2.5.2 Dynamic interactions between Kar9 and the cortex start at the SPB

The cortical dwelling observed in *tub4-Δdsyl* cells suggests that defective +TIP complexes containing Kar9 can tether the +ends of astral microtubules to the cortex or the bud tip, suppress microtubule dynamics and perturb the function of the Kar9 pathway. Our analysis suggests that components of the Bim1-Kar9 complex that regulate its interaction with the cortex are loaded at the SPB, and that this loading is dependent on Tub4. In *tub4-Δdsyl* cells, we observed astral microtubules undergo long pauses and have a slower rate of elongation than astral microtubules in wild-type cells. Significantly, deletion of Kar9 in the *tub4-Δdsyl* mutant increased the elongation rate and decreased the time astral microtubules spent in a paused state. This result strongly suggests that a defective Kar9-complex suppresses the dynamics of astral microtubules in the bud in *tub4-Δdsyl* cells. We also observed a significant increase in the amount of Kar9-GFP associated with the +ends of astral microtubules in the bud. This could be the result of an inappropriately stable interaction with Myo2 and/or cortical actin structures located at the tip of the bud or decreased stability of Kar9 at the $SPB_{\mathbf{b}}$, resulting in its accelerated deployment to microtubule +ends. In either case, our results support that the release of microtubules loaded with Kar9 from the cortex is defective in *tub4-Δdsyl* cells.

We propose that the initial loading of Bim1 and Kar9 at the SPB plays a critical role in assembling a functional +TIP complex, and thus affects how microtubules loaded with Kar9 complexes will subsequently interact with the cortex. It is likely that other proteins that localize to microtubule +ends, or to the bud tip, participate in this process. For example, a kinesin such as Kip3, which travels with Kar9 to the +end and is a +end depolymerase, or the –end-directed motor Kar3, may facilitate the release of Kar9 from Myo2 at the bud tip (Meluh and Rose, 1990; Endow *et al.*, 1994; Miller *et al.*, 1998; Liakopoulos *et al.*, 2003;

Gupta *et al.*, 2006). Alternately, a negative regulator of the Kar9-Myo2 interaction may travel with Kar9 to the cortex in an inactive state, and be activated when the Kar9-Myo2 complex reaches polarity proteins located in the tip of the bud. It is also possible that Cdc28/cyclin complexes, which colocalize with Kar9 and Bim1 on microtubule +ends, differentially phosphorylates these +TIPs and/or cortical targets at various cellular localizations and that this is dependent on initial events at SPBs. All these possibilities are not mutually exclusive and could act in combination to coordinate de-polymerization of the +end with release of Kar9 from Myo2 at the bud tip.

2.5.3 Bim1-Kar9 interactions at the cortex

Recent studies indicate that the stoichiometry of APC and EB1, +TIP proteins which share homology with Kar9 and Bim1 respectively, has functional consequences on microtubule dynamics and organization (Nakamura *et al.*, 2001; Green *et al.*, 2005). Additionally, previous studies suggest that frequency of pauses increases in cells lacking Bim1, resulting in shorter astral microtubules (Tirnauer *et al.*, 1999). It is therefore reasonable to conclude that a decreased ratio of Bim1 and Kar9 at astral microtubule +ends would similarly alter microtubules dynamics in yeast. While the time astral microtubule spent paused is similarly increased in *tub4-*Δ*dsyl* cells, long astral microtubules are observed rather than short microtubules. We suggest that Kar9, which does not associate with microtubules in the absence of Bim1, is responsible for this difference; Bim1 levels are reduced but Kar9 remains associated with the microtubule, with Myo2, and with cortical actin. This is consistent with a previous study that suggests Kar9, via polarity proteins such as Bud6, may promote microtubule stabilization within the bud (Huisman *et al.*, 2004). We speculate that the decreased Bim1-GFP signal at microtubule +ends results from the combination of a failure of Bim1 to be properly incorporated into complexes initially at SPBs and its preferential disassociation from Kar9 when the complex dwells at the cortex.

2.5.4 Tub4 as a scaffold: a model for post-nucleation function in microtubule organization

The defects in Bim1 and Kar9 SPB localization observed in *tub4-Δdsyl* cells correlates with perturbation of the function of the Kar9 pathway, suggesting that the initial localization of +TIP proteins to SPBs is important for both establishing asymmetry and for assembling a functional Bim1-Kar9 complex. We propose that Tub4, via its carboxyl terminus, may influence the function of proteins involved in the loading and/or deployment of Bim1 and Kar9 at SPBs. Tub4 does not appear to directly interact with Bim1 or Kar9 based on co-purification experiments (our un-published data), and the incomplete penetrance of the defect in SPB loading further suggests that this aspect of Tub4 function is mediated through its interaction with an as yet unidentified effector protein or complex. However, Bim1's ability to load at the SPB is likely to be important for complex formation. Over-production of Bim1 in *tub4-dsyl* cells may stabilize its interaction with Kar9 at SPBs, and allow a functional Kar9 complex to assemble prior to its deployment to the microtubule. However, we cannot exclude the possibility that over-production of Bim1 also promotes its association with Kar9 at +ends, and thereby restores normal interactions between the +TIP complex and the cortex of the bud.

Our analysis supports a novel post-nucleation role for Tub4 in influencing the behavior of astral microtubules through +TIP proteins. The affect of the *tub4-Δdsyl* mutation on microtubule dynamics is rescued by deletion of Kar9, strongly suggesting that Tub4 influences microtubule dynamics through +TIPs instead of altering the structure of the microtubule lattice as previously proposed (Usui and Schiebel, 2001). An exciting possibility is that the highly accessible c-terminus of γ-tubulin (Aldaz *et al.*, 2005) acts as a scaffold at the interface between the SPB and the minus ends of microtubules. This possible role for Tub4 may spark a renewed interest in previous studies implicating γ-tubulin in nucleation-independent aspects of microtubule organization (Masuda and Shibata, 1996; Paluh *et al.*, 2000; Vogel and Snyder, 2000; Vogel *et al.*, 2001).

2.6 Acknowledgements

We thank Dr. Howard Bussey, Dr. Guillaume Lesage (CIAN, McGill University), Dr. Craig Mandato and Dr. Monique Zetka for critical reading of the manuscript. We thank Robin Battye, Jelena Jevtic, and John Arbuckle of Quorum Technologies for ongoing support and development of the WaveFX imaging system. JV is supported by a New Investigator Award from the Canadian Institutes of Health Research (MSH 69117). RM is supported by a grant from the National Science Foundation (MCB 0414768). This research was supported by an operating grant from the Canadian Institutes of Health Research (MOP-64404) and infrastructure grants from the Canada Foundation for Innovation to JV (CFI 7395) and to the Developmental Biology Research Initiative of McGill University (CFI 8298).

2.7 The role of Tub4 in coordinating +TIP function with regulation at SPBs

As described, Tub4 has a well-established role in microtubule nucleation and a less understood role in microtubule organization. The results presented in Chapter 2 reveal a novel contribution of Tub4 in coordinating the assembly of +TIP complexes prior to their deployment to microtubule +ends. Furthermore, the assembly of +TIP complexes at SPBs appears to be important for their function during spindle placement.

Following the findings presented in Chapter 2, we were curious in mechanistically understanding how Tub4 influences the formation and function of +TIP complexes at SPBs. Since we were unsuccessful in detecting interactions between Tub4 and the +TIPs Bim1 and Kar9, we suspected that Tub4 influences their assembly and function by affecting their regulation. Specifically, we suspected that at SPBs Tub4 affects the regulation of Bim1 and Kar9 by Cdc28/cyclin complexes.

In the following chapter, I present novel findings revealing that Kar9 function is disrupted in the *tub4-*Δ*dsyl* mutant due to a perturbation of Bim1 function in spindle placement. Furthermore, I show that Bim1 is phosphorylated during the cell cycle and that this phosphorylation is dependent on Tub4, Cdc28 and the B-type cyclins. Collectively, this data suggests that Tub4 promotes the proper assembly of Bim1-Kar9 complexes by influencing their regulation at spindle poles.

Chapter 3: Tub4 Is Required For The Proper Regulation Of Bim1 At SPBs Via Cdc28/Cyclin Complexes

3.1 Introduction

During asymmetric division, microtubule plus end interacting proteins (+TIPs) regulate the dynamics and organization of astral microtubule plus ends (+ends) during spindle placement in various cell types (Pearson and Bloom, 2004). In budding yeast, the APC-like protein Kar9 and the EB1 ortholog Bim1 are +TIPs that facilitate pre-anaphase spindle placement to the bud neck, prior to the onset of mitosis (Miller and Rose, 1998; Tirnauer *et al.*, 1999; Lee *et al.*, 2000; Kusch *et al.*, 2002; Liakopoulos *et al.*, 2003; Maekawa *et al.*, 2003). Intriguingly, Bim1 and Kar9 also localize to microtubule organizing centres (MTOCs), which are spindle pole bodies (SPBs) in yeast, independently of detectable microtubules (Liakopoulos *et al.*, 2003; Cuschieri *et al.*, 2006). While much is known regarding the function of +TIPs on microtubule +ends, the functional significance for their localization to SPBs has remained elusive for some time.

Currently it is established that Bim1 and Kar9 localize to SPBs in order to promote Kar9 phosphorylation by the Cdk1 ortholog, Cdc28 and the B-type cyclins. Phosphorylation of Kar9 at SPBs is critical for Kar9 asymmetry to the "old" SPB proximal to the bud (SPB_b), which ensures that only this pole and its associated microtubules are targeted into the bud during spindle placement (Liakopoulos *et al.*, 2003; Maekawa *et al.*, 2003; Maekawa and Schiebel, 2004; Moore *et al.*, 2005; Moore and Miller, 2007). Recently we identified an additional significance for the SPB localization of Bim1 and Kar9. Specifically, we demonstrated that the localization of these +TIPs to SPBs is important for their proper complex formation and function on microtubule +ends (Cuschieri *et al.*, 2006). As was described in Chapter 2, we identified that these events are dependent upon the conserved MTOC component, γ-tubulin or Tub4 in yeast (Cuschieri *et al.*, 2006).

γ-tubulin/Tub4 has a well established role in promoting microtubule nucleation, yet recent studies are revealing additional post-nucleation functions of γ-tubulin/Tub4 in the control of microtubule organization and dynamics (Cuschieri *et al.*, 2007). Specifically, we reported that cells harboring a Tub4 carboxyl deletion (*tub4-Δdsyl;*(Vogel and Snyder, 2000)) have perturbed pre-anaphase spindle placement due to non-functional Kar9 complexes on their astral microtubule +ends (Cuschieri *et al.*, 2006). These complexes fail to localize to the SPB_b, have reduced levels of Bim1 and do not promote dynamic interactions with the bud cortex. This suggested that the function of +TIPs on microtubule +ends is coordinated with events that occur at SPBs in a Tub4 dependent manner. What still remains to be determined is how Tub4 mechanistically influences these events at the SPB_b, why Kar9 is non-functional in *tub4-Δdsyl* cells and whether the function of Bim1 is affected by the *tub4-Δdsyl* mutation.

Chapter 3, discusses the results and progress I have made in answering some of these questions since our characterization of the *tub4-Δdsyl* mutant. Furthermore, some points of discussion are introduced regarding my results that will be elaborated on further in Chapter 4. In summary, we have evidence suggesting that the inability of Kar9 to promote proper astral microtubule dynamics and spindle placement in *tub4-Δdsyl* cells, is a consequence of disrupted Bim1 function. Additionally, our data suggests that Bim1 is differentially regulated throughout the cell cycle in a manner that is dependent on Tub4, Cdc28 and the early B-type cyclins. Our work proposes that Bim1 phosphorylation is important for its proper localization and function on microtubule +ends. Finally, we speculate that Tub4 promotes Bim1 phosphorylation at SPBs by scaffolding Cdc28/cyclin complexes to these sites.

3.2 Results and discussion

3.2.1 Bim1 function is perturbed by the *tub4-*Δ*dsyl* mutation

In small budded wild-type cells, Bim1 preferentially localizes to SPBs and the +ends of growing and shrinking astral and spindle microtubules (Tirnauer *et al.*, 1999; Wolyniak *et al.*, 2006). On astral microtubule +ends, Bim1 and Kar9 cooperatively promote dynamic interactions with the bud neck and cortex to achieve proper spindle placement (Tirnauer *et al.*, 1999; Adames and Cooper, 2000; Wolyniak *et al.*, 2006). Conversely in *tub4-*Δ*dsyl* small budded cells, astral microtubule dynamics are decreased due to the presence of non-functional Kar9 complexes on their +ends (Cuschieri *et al.*, 2006). These complexes have reduced levels of Bim1 and rarely localize to the $SPB_{\mathbf{b}}$. It is known that Bim1 is required for Kar9 localization to the $SPB_{\mathbf{b}}$ (Liakopoulos *et al.*, 2003). As such, since Bim1 is required for both microtubule dynamics and Kar9 SPB localization, we speculated that spindle positioning defects in *tub4-*Δ*dsyl* cells result mainly from a perturbation of Bim1 function. Consistent with this hypothesis, we previously demonstrated that over-production of Bim1 protein rescues the lethality of *tub4-*Δ*dsyl dhc1*Δ double mutants, suggesting that in these cells the function of the Kar9 pathway is restored (Cuschieri *et al.*, 2006). We also demonstrated that over-produced Bim1 restores astral microtubule dynamics and spindle placement in *tub4-*Δ*dsyl* cells (Cuschieri *et al.*, 2006).

While this evidence strongly supports that Bim1 function in spindle placement is perturbed by the *tub4-*Δ*dsyl* mutation, both Bim1 and Tub4 have complicated genetic interaction profiles that indicate these proteins are also involved in regulating mitotic spindle function (Tong *et al.*, 2001; Vogel *et al.*, 2001; Gardner *et al.*, 2008)(personal communication with J.Vogel and T. Nguyen). Therefore, over-production of Bim1 may not be specifically restoring Kar9 function but rather be causing a general enhancement of microtubule dynamics in *tub4-*Δ*dsyl* cells. To discriminate between these possibilities we took a genetic approach and tested if over-produced Bim1 rescues the lethality

of the *tub4-*Δ*dsyl* mutation in combination with mutations that disrupt the dynein pathway (*kip2*Δ*, arp1*Δ) or spindle microtubule function (*mad2*Δ*, cin8*Δ*, swe1*Δ*, cik1*Δ). The mutations chosen for this analysis were previously found to be lethal in combination with the *tub4-*Δ*dsyl* mutation (our unpublished data).

We expected that if over-produced Bim1 specifically restores Kar9 function, then it would only rescue lethality of the *tub4-*Δ*dsyl* mutation with mutations that disrupt the dynein pathway. For this analysis, *tub4-*Δ*dsyl* cells with a 2μ BIM1 over-expression vector (pLC1 or pBIM1; (Cuschieri *et al.*, 2006)) or an empty vector (pRS423; (Sikorski and Hieter, 1989)), were mated to the various mutants and haploid progeny (40 tetrads/condition) were scored for the presence of viable double mutants.

We found that over-produced Bim1 specifically rescued lethality between the *tub4-*Δ*dsyl* mutation and mutations that perturb the dynein pathway but not spindle function (Figure 3.2.1 A). 65.7% of *tub4-*Δ*dsyl* Δ*kip2* pBIM1 double mutants were viable, relative to only 17.7% in crosses containing the control vector (Figure 3.2.1 B). Likewise, 51.4% of *tub4-*Δ*dsyl arp1*Δ pBIM1 double mutants were viable relative to 17.1% of double mutant spores containing the control vector (Figure 3.2.1 B). In contrast, the presence of over produced Bim1 protein (pBIM1) had no rescuing affect on the lethality of the *tub4-*Δ*dsyl* mutation combined with mutations that affect spindle function (Figure 3.2.1 A). Collectively, these results are consistent with the hypothesis that spindle positioning defects in *tub4-*Δ*dsyl* cells result from a loss of Bim1 function that is specific to its role in Kar9 dependent spindle positioning.

In higher eukaryotes, an interaction between EB1 and the carboxyl terminus of APC (C-APC) is important for their cooperative function in regulating microtubule dynamics (Nakamura *et al.*, 2001; Green *et al.*, 2005). Moreover, yeast Bim1 protein can effectively substitute for human EB1 in coordinating microtubule dynamics, but only in the presence of the C-APC (Nakamura *et al.*, 2001). This suggests that a similar functional dependency exists for Bim1 and Kar9 in budding yeast. Consistent with this, synergistic relationships in the coordination of microtubule dynamics have been previously described for Bim1

and the +TIP, Stu2 (Wolyniak *et al.*, 2006). Over-production of Bim1 may be restoring interactions with Kar9 that are disrupted by the *tub4-*Δ*dsyl* mutation and therefore restoring an integral functional synergy with Kar9 to promote astral microtubule dynamics in these cells.

Figure 3.2.1 Bim1 function is perturbed in *tub4-*Δ*dsyl* cells

(A) Over-produced Bim1 rescues synthetic lethality between the *tub4-*Δ*dsyl* mutation and mutations within the dynein pathway, but not mutations affecting spindle function. *tub4-*Δ*dsyl* cells containing pBIM1 or the control vector pRS423 were mated to a series of query mutations that affected dynein function or spindle microtubule function. Spores (40 tetrads per cross) were scored for the presence of viable double mutants. Plus indicates synthetic viable interactions, minus indicates synthetic dead/sick**. (B)** Graph of synthetic rescue observed in *tub4-*Δ*dsyl arp1*Δ and *tub4-*Δ*dsyl kip2*Δ double mutants in the presence or absence of over-produced Bim1. 51.4% of *tub4-*Δ*dsyl arp1* double mutants were viable in the presence of over-produced Bim1 relative to only 17.1% of those containing pRS423. Likewise 65.7% of *tub4-*Δ*dsyl kip2*Δ double mutants were viable in the presence of over-produced Bim1 relative to only 17.7% of those containing pRS423. **(C)** Bim1 migrates as multiple isoforms. Bim1 protein from wild-type total cell extracts was assessed using 2D SDS-PAGE and found to migrate as multiple acidic isoforms, consistent with Bim1 being a phospho-protein. Bim1 antibody (R.Miller) was used to detect Bim1. **(D)** Bim1 is a phospho-protein. Bim1 protein from wild-type total cell extracts was assessed using 2D SDS-PAGE following treatment with or without λ-PPase in the presence/absence of inhibitors. Isoforms were sensitive to λ-PPase indicating that Bim1 is a phospho-protein.

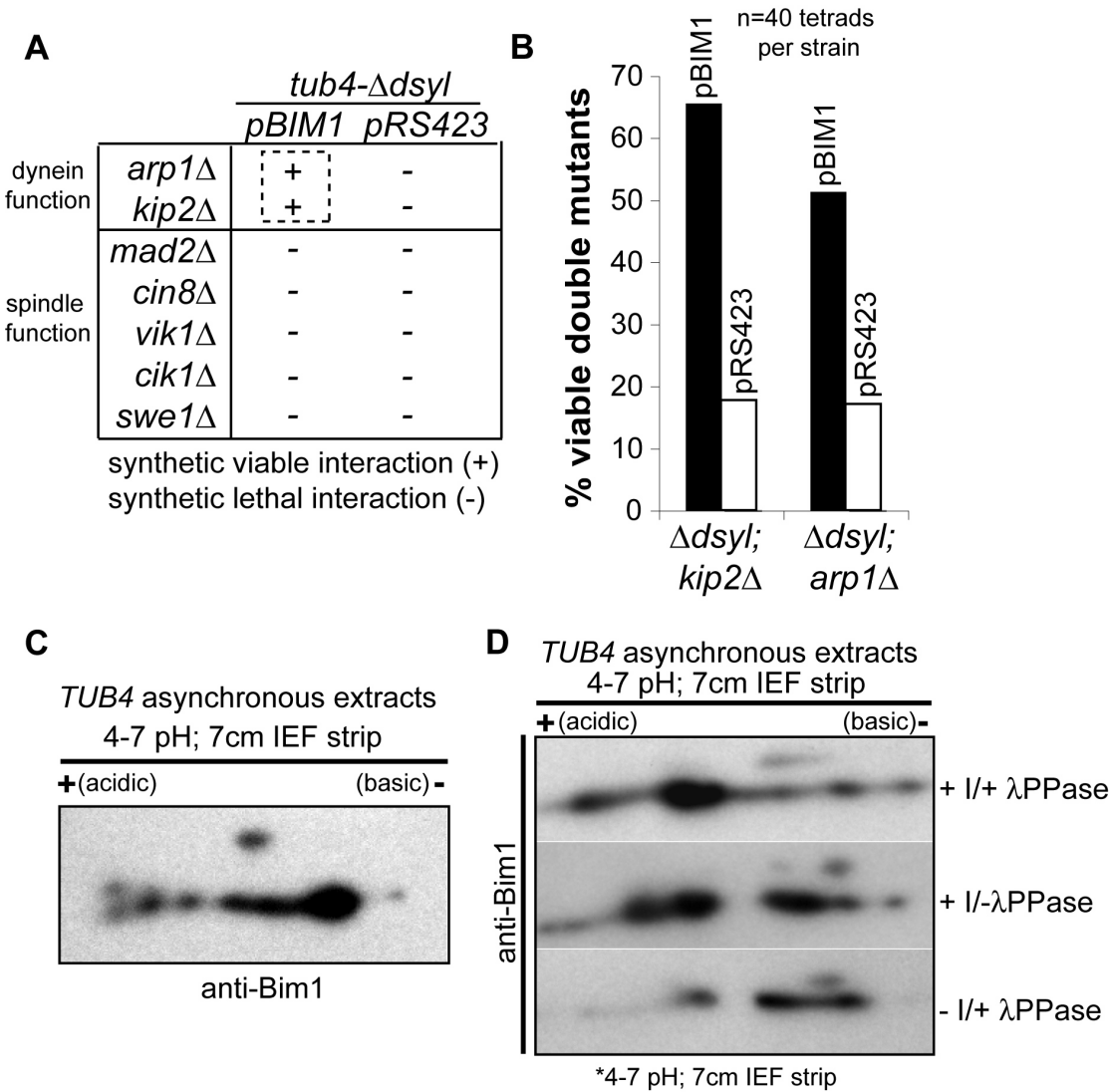
A
tub4-Δdsyl
pBIM1 pRS423
dynein function
arp1Δ + -
kip2Δ + -
spindle function
mad2Δ - -
cin8Δ - -
vik1Δ - -
cik1Δ - -
swe1Δ - -
synthetic viable interaction (+)
synthetic lethal interaction (-)
B
n=40 tetrads per strain
% viable double mutants
70
60
50
40
30
20
10
0
pBIM1
pRS423
pBIM1
pRS423
Δdsyl; kip2Δ
Δdsyl; arp1Δ
C
TUB4 asynchronous extracts
4-7 pH; 7cm IEF strip
+(acidic) (basic)-
anti-Bim1
D
TUB4 asynchronous extracts
4-7 pH; 7cm IEF strip
+(acidic) (basic)-
anti-Bim1
+ I/+ λPPase
+ I/-λPPase
- I/+ λPPase
*4-7 pH; 7cm IEF strip

3.2.2 Bim1 is post-translationally modified by phosphorylation

Our data is consistent with a loss of Bim1 function in *tub4-Δdsyl* cells, however it remains unclear how this occurs. It is likely that the loss of Bim1 function is attributed solely to its reduced localization at SPBs and microtubule +ends in *tub4-Δdsyl* cells. For example, in fission yeast γ-tubulin complex proteins have been shown to affect microtubule dynamics by altering the localization of +TIPs (Zimmerman and Chang, 2005). Yet irrespective of this, we are interested in understanding how Tub4 influences the formation of Bim1-Kar9 complexes at SPBs and why the localization of Bim1 in these complexes is reduced by the *tub4-Δdsyl* mutation (Liakopoulos *et al.*, 2003; Maekawa *et al.*, 2003; Cuschieri *et al.*, 2006). As was discussed in Chapter 2, we hypothesize that the Tub4 carboxyl terminus acts as a SPB scaffold that enables the local accumulation and assembly of +TIPs into complexes. Several lines of evidence support this hypothesis, which will be discussed in depth in Chapter 4.

One caveat to our hypothesis is that Tub4 does not interact with Bim1 and Kar9 based on repeated co-IP assays for interaction (unpublished data). Therefore, we asked whether Tub4 promotes the assembly of +TIPs by influencing +TIP regulation at SPBs. For instance, Tub4 may scaffold regulatory complexes in order to facilitate regulation of +TIPs at SPBs and promote their assembly into complexes. In support of this, localization of Cdc28 to SPBs is independent of either Bim1 or Kar9, suggesting that a SPB component like Tub4 may scaffold this regulator (Liakopoulos *et al.*, 2003; Maekawa *et al.*, 2003; Maekawa and Schiebel, 2004). Additionally, phosphorylation of Kar9 mediates binding to Bim1 at SPBs as well as its association with the +TIP Stu2 at SPBs, thereby demonstrating a strong involvement for regulation in +TIP complex assembly at this locaction (Trzepacz *et al.*, 1997; Liakopoulos *et al.*, 2003; Honnappa *et al.*, 2005; Moore and Miller, 2007). While the *tub4-Δdsyl* mutation perturbs the SPB localization of Bim1 and Kar9 it does not disrupt Kar9 asymmetric localization to MTs associated with the SPB_b (Cuschieri *et al.*, 2006). Furthermore in *tub4-Δdsyl* cells, our previous analysis of Kar9 protein

revealed that phosphorylation still occurs (Cuschieri *et al.*, 2006). This indicates that the affect of Tub4 on Bim1 localization and function is likely independent of Kar9 phosphorylation events pertaining to its asymmetric localization. For these reasons, I did not pursue assessing Kar9 phosphorylation.

Intriguingly, little is known whether Bim1 is phosphorylated at SPBs and if this has any affect on its localization and/or function. Since Bim1 localization and function appear to be dependent on Tub4 during S-phase, we were interesting in determining whether Tub4 influences these events through a phosphorylation dependent mechanism. We began investigating this by first determining whether Bim1 is post-translationally modified in wild-type cells using 2-dimensional SDS polyacrylamide gel electrophoresis (2D SDS-PAGE). We chose this electrophoresis method since Bim1 migrates as a singlet on 1D SDS-PAGE. For this analysis, proteins were extracted from asynchronous wild-type cells and separated based on charge and size. Standard Western blotting techniques were used and a Bim1 antibody was used for detection of Bim1 isoforms (Moore *et al.*, 2005). In wild-type extracts we found Bim1 migrates as multiple isoforms, supporting that Bim1 is post-translationally modified (Figure 3.2.1 C). In order to determine whether these Bim1 isoforms represent phosphorylation events, we treated the asynchronous cell extracts with λ-phosphatase (λ-PPase) in the presence or absence of PPase inhibitors and assessed these samples using 2D-PAGE. In agreement with Bim1 being a phosphoprotein, Bim1 isoforms were sensitive to λ-PPase treatment and an enrichment of the basic Bim1 isoforms was observed (Figure 3.2.1 D). Collectively our data suggests that Bim1 is post-translationally regulated in wild-type cells via phosphorylation.

Kar9 is maximally phosphorylated in S phase of the cell cycle during early spindle placement (Maekawa *et al.*, 2003). We were curious whether Bim1 phosphorylation is similarly cell cycle regulated. To test this, wild-type cells expressing Kar9-GFP and Spc42-CFP (SPB component) were synchronized using the yeast mating phermone alpha-factor (α-factor). This enabled us to assess Bim1 phosphorylation in protein extracts obtained from cells at a uniform

cell cycle phase and attribute specific isoforms with cell cycle progression. Once cells uniformly entered the cell cycle, samples were taken at 20 minute intervals (for a total of 60 minutes) and extracted for analysis via 2D SDS-PAGE. In addition, the localization of Kar9-GFP relative to the SPBs (Spc42-CFP) was microscopically assessed for each time-point to ensure that Kar9 asymmetry on the SPB_b and spindle placement were not altered by the synchronization process. The results of this analysis indicated that Bim1 is differentially phosphorylated throughout the cell cycle with phosphorylation being maximal during the S/G2 transition when early spindle placement occurs (time=60min; Figure 3.2.2 A). Thus, like Kar9, Bim1 phosphorylation changes throughout the cell cycle.

If the Tub4 carboxyl terminus influences Bim1 localization and function by affecting its regulation, then we expected that Bim1 phosphorylation would be altered as a result of the *tub4-*Δ*dsyl* mutation. To test this possibility, we assessed whether Bim1 phosphorylation during the cell cycle was altered by the *tub4-*Δ*dsyl* mutation using the same experimental design described for wild-type cells. In agreement with our prediction, we found that Bim1 phosphorylation is altered by the *tub4-*Δ*dsyl* mutation (Figure 3.2.2 B). One interesting observation is that the *tub4-*Δ*dsyl* mutation appears to primarily alter Bim1 phosphorylation at 60 minutes, when Bim1 phosphorylation is maximal (Figure 3.2.2 B). The significance of this result is that at this time-point, spindle positioning is defective in *tub4-*Δ*dsyl* cells due to Kar9-dependent dwelling of astral microtubules with the bud cortex, as can be seen in the accompanying fluorescent image (Figure 3.2.2B, see fluorescence image). It is tempting to speculate that the synchrony of these events in *tub4-*Δ*dsyl* cells represents a functional link between Bim1 phosphorylation and spindle placement. However, at this point we can only conclusively state that Bim1 is differentially phosphorylated throughout the cell cycle and that phosphorylation is altered by the *tub4-*Δ*dsyl* mutation during early spindle placement. These findings are consistent with a putative role for Tub4 in Bim1 regulation.

Figure 3.2.2 Bim1 is phosphorylated in a Tub4 dependent manner

(A & B) Wild-type and *tub4-*Δ*dsyl* cells were synchronized in the cell cycle using α-factor. Every 20 minutes, a sample was taken from each strain, extracted for protein and analyzed using 2D SDS-PAGE. A sample was also taken at each time-point for microscopic analysis (DIC and fluorescence; left of gel images). At 60 minutes, Bim1 phospho-isoforms are lost in the *tub4-*Δ*dsyl* extract (black arrows) relative to the corresponding time-point in the wild-type extract (black arrows). This time-point corresponds to when spindle positioning defects caused by Kar9-GFP (green foci) dwelling at the cortex (see accompanying microscopic image, left) are obvious in *tub4-*Δ*dsyl* cells. Cartoon representations (right of gel images) indicate the position of Kar9-GFP and the SPBs (Spc42-CFP) in the microscopic images. Bim1 isoforms are detected using a Bim1 antibody.

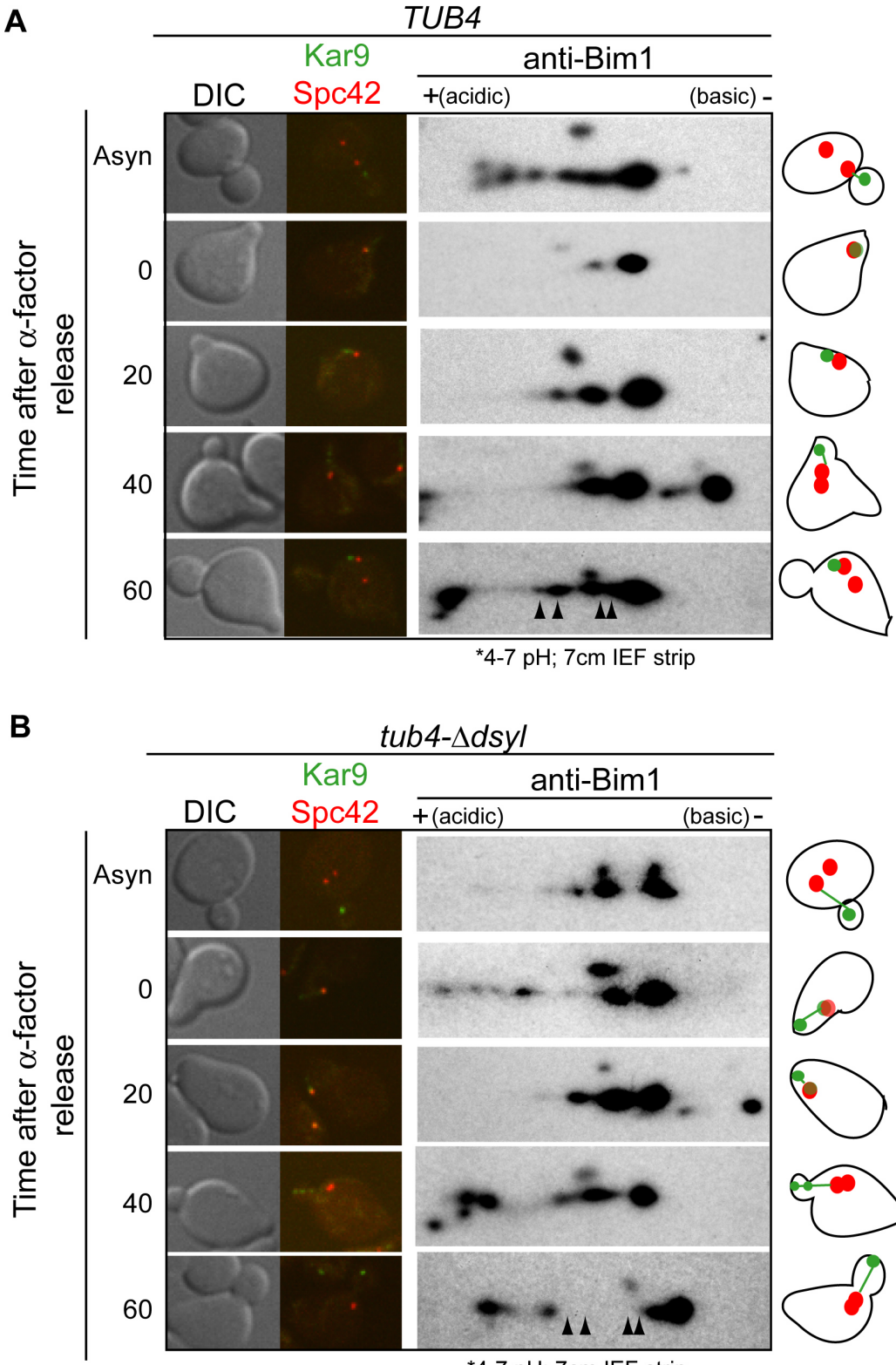
A
TUB4
Kar9
Spc42
DIC
anti-Bim1
+(acidic)
(basic) -
Asyn
0
20
40
60
Time after α-factor release
*4-7 pH; 7cm IEF strip
B
tub4-Δdsyl
Kar9
Spc42
DIC
anti-Bim1
+(acidic)
(basic) -
Asyn
0
20
40
60
Time after α-factor release
*4-7 pH; 7cm IEF strip

3.2.3 Examining the role of Cdc28 in Bim1 phosphorylation

Our findings are consistent with a function for Tub4 in promoting Bim1 regulation. To mechanistically understand how this occurs, we decided to investigate the kinase responsible for Bim1 phosphorylation, with the anticipation that this information will provide a means to understand how Tub4 promotes phosporylation at the SPB. One obvious candidate that may phosphorylate Bim1 is Cdc28. Several lines of evidence are in agreement with this. First, in wild-type cells Cdc28 co-localizes with Bim1 to SPBs and associates with microtubule +ends in complex with both Bim1 and Kar9 (Maekawa *et al.*, 2003). Additionally, Cdc28 phosphorylates Kar9 and this is known to affect its interaction with Bim1 (Liakopoulos *et al.*, 2003; Maekawa *et al.*, 2003; Maekawa and Schiebel, 2004; Moore *et al.*, 2005; Moore and Miller, 2007). Cdc28 has a reported 2-hybrid interaction with Bim1 (Maekawa *et al.*, 2003) and finally, analysis of the Bim1 amino acid sequence reveals two evolutionarily conserved Cdc28 consensus sites at serine 147 and serine 165. For these reasons, I pursued testing whether Cdc28 phosphorylates Bim1.

To test our hypothesis, we first examined if Bim1 and Cdc28 physically interact *in vivo* by co-immunoprecipitation analyses in wild-type and *tub4-*Δ*dsyl* cells. A detected interaction between these two proteins would strengthen the hypothesis that Bim1 is a substrate of Cdc28. Therefore, wild-type and mutant cells expressing Bim1-3XFLAG and Cdc28-TAP were extracted for protein and Cdc28 was precipitated using a polyclonal TAP antibody (Openbiosystems, Huntsville AL). Bim1 was detected on Western blots using a monoclonal FLAG antibody (Sigma). An untagged wild-type strain and wild-type strains containing either a Cdc28-TAP or Bim1-3XFLAG alone were used as controls. Our results reveal that Bim1 and Cdc28 physically interact in wild-type cells (Figure 3.2.3 A). Conversely, in *tub4-*Δ*dsyl* cells we could not detect an interaction between Bim1 and Cdc28. This reveals that interactions between Cdc28 and Bim1 are either reduced or lost due to the *tub4-*Δ*dsyl* mutation. Thus, Bim1 interacts with Cdc28 in a manner that is dependent on the Tub4 DSYL residues.

Figure 3.2.3 Cdc28 is a candidate kinase for Bim1 phosphorylation

(A) Interactions between Cdc28-TAP and Bim1-3XFLAG were assessed in wild-type and *tub4-*Δ*dsyl* protein extracts. Cdc28-TAP was purified using an anti-TAP antibody and the detection of Bim1-3XFLAG was detected on Western blots using an anti-FLAG antibody. The amount of Bim1-3XFLAG purifying in extracts obtained from the *tub4-*Δ*dsyl* strain was dramatically reduced relative to the wild-type condition, suggesting that interactions between Cdc28 and Bim1 are dependent on Tub4. **(B)** Analysis of Bim1 phosphorylation in the *cdc28-as1* allele. *cdc28-as1* cells expressing Bim1-3XFLAG were extracted for protein following incubation with the chemical inhibitor 1NM-PP1 or DMSO as a control for either 15 or 30 minutes. Extracts were then assessed using 2D SDS-PAGE. Bim1-3XFLAG phospho-isoforms were lost following treatment with 1NM-PP1 for 30 minutes, implicating Cdc28 as a potential kinase for Bim1 phosphorylation.

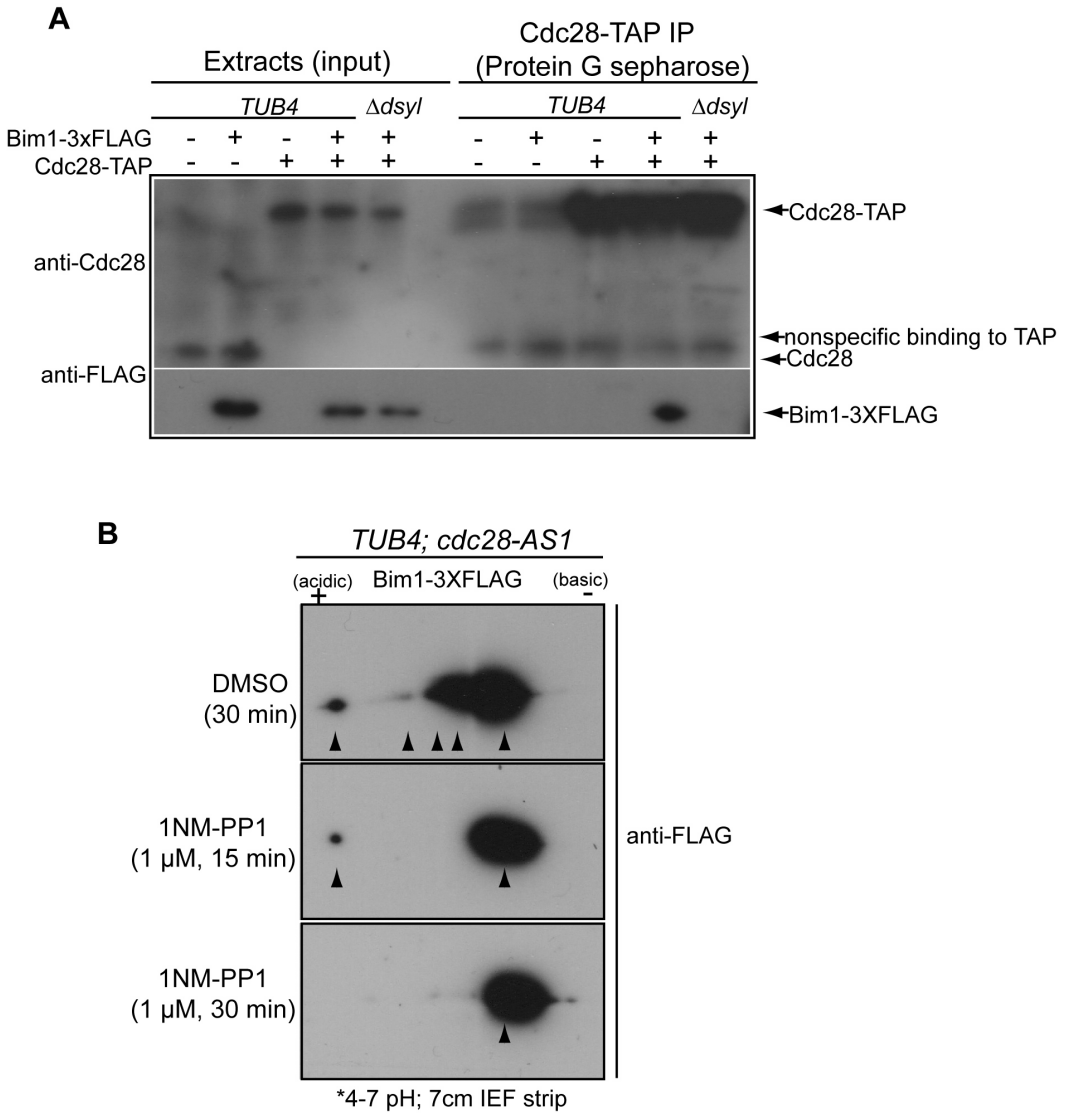
A
Extracts (input)
Cdc28-TAP IP
(Protein G sepharose)
TUB4
Δdsyl
TUB4
Δdsyl
Bim1-3xFLAG - + - + + - + - + +
Cdc28-TAP - - + + + - - + + +
anti-Cdc28
anti-FLAG
Cdc28-TAP
nonspecific binding to TAP
Cdc28
Bim1-3XFLAG
B
TUB4; cdc28-AS1
(acidic) Bim1-3XFLAG (basic)
+
-
DMSO
(30 min)
1NM-PP1
(1 μM, 15 min)
1NM-PP1
(1 μM, 30 min)
anti-FLAG
*4-7 pH; 7cm IEF strip

The interaction between Bim1 and Cdc28 is in agreement with our hypothesis of Cdc28 being a potential kinase responsible for phosphorylating Bim1. However, we wanted to more directly assess whether inhibiting Cdc28 activity perturbs Bim1 phosphorylation. We decided to examine Bim1 phosphorylation in the Cdc28 chemically sensitive allele, *cdc28-as1,* which contains a mutation within the ATP binding pocket of Cdc28 that confers sensitivity to the small molecule chemical inhibitor 1NM-PP1 (Bishop *et al.*, 2000). In the presence of 1NM-PP1, Cdc28 kinase activity in the *cdc28-as1* background is quickly and conditionally abolished (Bishop *et al.*, 2000). This is a useful chemical genetics tool as it enables us to rapidly inhibit Cdc28 kinase activity, which is an important consideration as Cdc28 regulates a number of different substrates that are important for proper cell cycle progression. Therefore, *cdc28-as1* cells expressing Bim1-3XFLAG were incubated in the presence of DMSO or 1 μM 1NM-PP1 inhibitor for either 15 or 30 minutes at room temperature and subsequently extracted for 2D SDS-PAGE analysis.

Our results revealed that following 30 minutes of incubation with 1 μM 1NM-PP1 inhibitor, all the detectable Bim1-3XFLAG acidic isoforms were lost relative to the DMSO control (Figure 3.2.3 B). Furthermore, we observed an overall shift of Bim1-3XFLAG protein towards the basic end of the gel (Figure 3.2.3 B). Conversely, incubation of the extract after 15 minutes with the 1 μM 1NM-PP1 inhibitor resulted in a similar isoform pattern to that of the DMSO control condition (Figure 3.2.3 B). Notably, the overall Bim1 phospho-isoform pattern in all conditions varied from our previous analyses, which we attribute to the Bim1 antibody having a higher sensitivity for less abundant isoforms relative to the FLAG antibody. Unfortunately, this cannot be avoided, as we no longer have access to the Bim1 antibody (prepared by Rita Miller) used in our previous experiments.

At this point, we cannot eliminate the possibility that the alteration of Bim1 isoforms in the *tub4-*Δ*dsyl* background results from the perturbation of a different kinase that phosphorylates Bim1, which in turn, is regulated by Cdc28. To address this issue, an *in vitro* kinase assay to test whether Cdc28 directly

phosphorylates Bim1 is required. While this has not been presently done, we have begun making the strains necessary for this experiment (in collaboration with D.Chen). Therefore, at this point we can conclude that perturbation of Cdc28 activity results in an alteration of Bim1 phosphorylation, which is consistent with Cdc28 being a potential kinase responsible for Bim1 phosphorylation.

3.2.4 Investigating the role of Tub4 in Bim1 phosphorylation

Taken together, our data reveals that the *tub4-*Δ*dsyl* mutation and the *cdc28-as1* mutation have similar effects on Bim1 phosphorylation, in that both mutations appear to abolish Bim1 phospho-isoforms. It is tempting to speculate that this similarity reflects a link between Tub4 and potential Cdc28 dependent phosphorylation of Bim1. While this requires further experimentation to be validated, this hypothesis is consistent with Bim1/Cdc28 interactions being dependent on Tub4 (Figure 3.2.3 A). Since Tub4 and Bim1 do not physically associate, we suspected that Tub4 might interact with Cdc28 and thus indirectly influence Bim1. As already stated, Cdc28 localization to SPBs is independent of Bim1 and Kar9, indicating that other SPB associated proteins, such as Tub4, may facilitate its localization to these organelles (Maekawa *et al.*, 2003). We were also curious whether the Tub4 carboxyl terminus plays a role in modulating Cdc28 localization to the SPB and phosphorylation of its targets at this location; for example decreased interactions between Cdc28 and Bim1 might result from a perturbed localization of Cdc28 to SPBs in *tub4-*Δ*dsyl* cells.

We began testing these possibilities by first determining whether Cdc28 and Tub4 co-purify in wild-type and *tub4-*Δ*dsyl* cells. Additionally, we also tested whether potential interactions were maintained in the absence of Kar9 (*kar9*Δ) or Bim1 (*bim1*Δ). Cells expressing Cdc28-TAP were extracted for protein and Cdc28 was immuno-precipitated using a polyclonal TAP antibody (Openbiosystems, Huntsville AL). For detection of Tub4 on Western blots, a polyclonal Tub4 antibody was used (Santa Cruz).

Figure 3.2.4 Analysis of Cdc28/Tub4 interactions and co-localization

(A) Co-immunoprecipitation analysis of Tub4 and Cdc28. Wild-type, *kar9*Δ, *bim1*Δ and *tub4-*Δ*dsyl* cells expressing Cdc28-TAP were extracted for protein. Cdc28-TAP was purified from extracts and assessed for the detection of Tub4. Interactions between Cdc28-TAP and Tub4 were detected in all backgrounds including extracts obtained from *tub4-*Δ*dsyl* cells, suggesting that interactions between Tub4 and Cdc28 are independent of the DSYL residues. **(B)** Analysis of Cdc28-GFP localization in wild-type cells expressing Spc42-CFP revealed that Cdc28-GFP localizes to SPBs, kinetochores (asterisk), astral microtubule +ends (green arrows), the bud neck and the bud tip (white arrows). **(C)** Analysis of Cdc28-GFP localization described in B in the presence of NZ (30µg) revealed that the maintained localization of Cdc28-GFP to kinetochores, SPBs, bud tip and bud neck are independent of microtubules. Green arrows point to collapsed SPBs **(D)** Analysis of Cdc28-GFP localization in *tub4-*Δ*dsyl* cells expressing Spc42-CFP revealed that Cdc28-GFP localizes to SPBs, kinetochores (asterisk) and astral microtubule +ends (green arrows) but not the bud neck and the bud tip. **(E)** The maintained localization of Cdc28-GFP to SPBs and kinetochors in *tub4-*Δ*dsyl* cells is independent of microtubules. **(F)** Quantification of Cdc28-GFP in wild-type and *tub4-*Δ*dsyl* cells as shown in **B** and **D**.

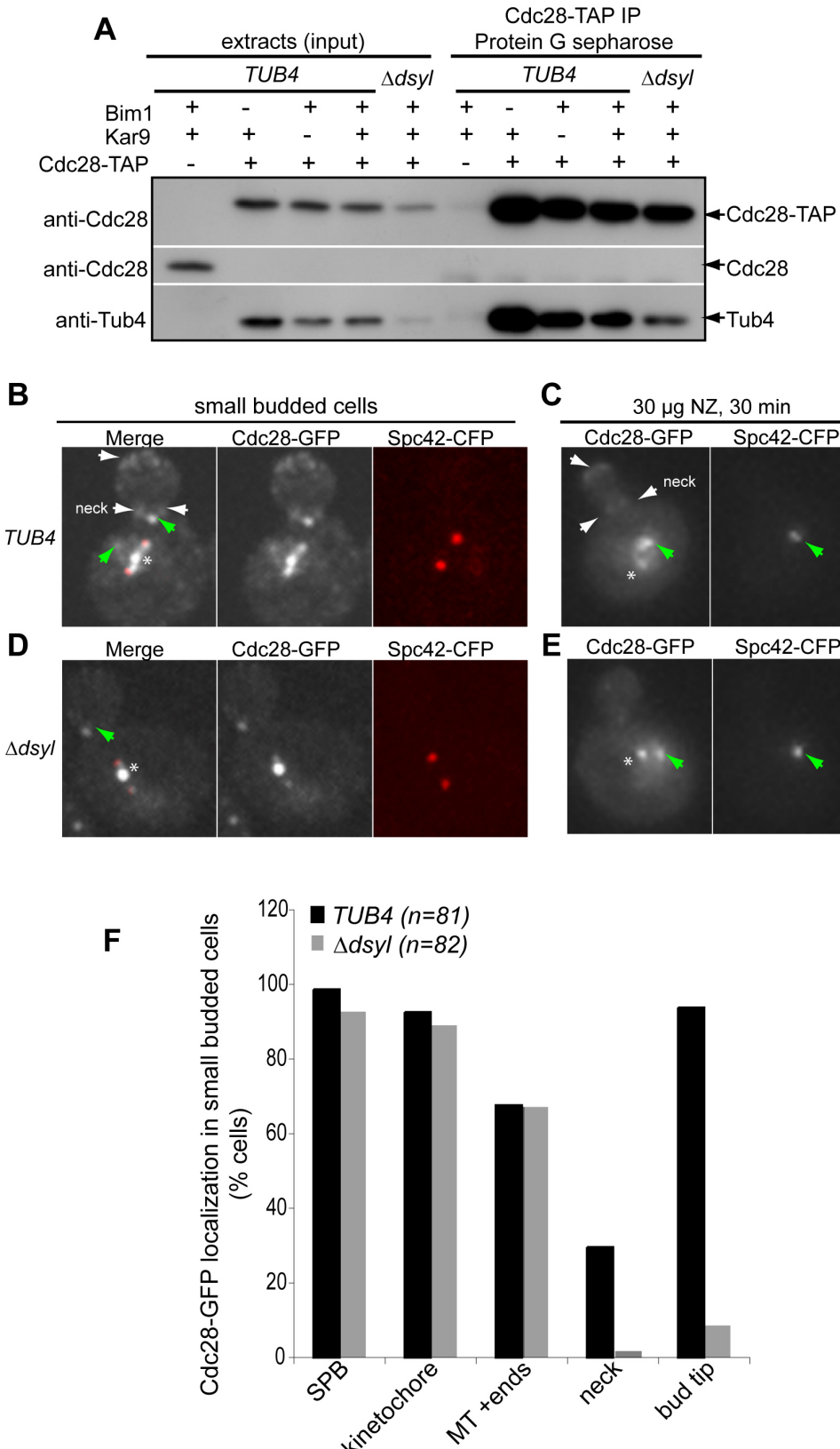
A
extracts (input)
Cdc28-TAP IP
Protein G sepharose
TUB4
Δdsyl
TUB4
Δdsyl
Bim1 + - + + + + - + + +
Kar9 + + - + + + + - + +
Cdc28-TAP - + + + + - + + + +
anti-Cdc28
anti-Cdc28
anti-Tub4
Cdc28-TAP
Cdc28
Tub4
B
small budded cells
Merge
Cdc28-GFP
Spc42-CFP
TUB4
neck
C
30 µg NZ, 30 min
Cdc28-GFP
Spc42-CFP
neck
D
Merge
Cdc28-GFP
Spc42-CFP
Δdsyl
E
Cdc28-GFP
Spc42-CFP
F
TUB4 (n=81)
Δdsyl (n=82)
Cdc28-GFP localization in small budded cells (% cells)
120
100
80
60
40
20
0
SPB
Kinetochore
MT +ends
neck
bud tip

We found that Tub4 and Cdc28-TAP interact in wild-type, *kar9*Δ and *bim1*Δ cells (Figure 3.2.4 A). Interestingly, this interaction was also maintained in *tub4*-Δ*dsyl* cells, suggesting that the Tub4 DSYL residues are dispensable for interactions with Cdc28 (Figure 3.2.4 A). Importantly we found that the levels of Cdc28 protein detected in *tub4*-Δ*dsyl* extracts has been inconsistent and therefore we wish to revisit this experiment and determine Cdc28 levels relative to a loading control.

While this result suggests that Tub4 and Cdc28 interact in a manner that is independent of the DSYL residues, we wanted to determine whether this reflected events at SPBs, since co-IPs represent protein-protein interactions in whole cell extracts. Thus, we chose to microscopically examine Cdc28 localization in small budded wild-type and *tub4*-Δ*dsyl* cells to determine if its localization was altered by the *tub4*-Δ*dsyl* mutation. Live-cell fluorescent microscopy was performed in wild-type and *tub4*-Δ*dsyl* small budded cells expressing Cdc28-GFP and the SPB marker, Spc42-CFP. As was previously described, in wild-type cells Cdc28-GFP localized to a number of cellular locations including, SPBs, microtubule +ends and the bud neck (Figure 3.2.4 B) (Maekawa *et al.*, 2003). To our surprise, Cdc28-GFP foci also seemed to localize to kinetochores and the bud tip, which are novel localizations for this kinase (Figure 3.2.4 B).

To ensure that these detected Cdc28-GFP foci were not the +ends of astral microtubules or spindle microtubules being misinterpreted for the bud tip and kinetochores respectively, we treated cells with nocodazole (NZ) for 30 minutes. These foci, as well as those corresponding to the bud neck and SPBs remained, while only Cdc28-GFP on microtubule +ends was abolished (Figure 3.2.4 C). Thus, Cdc28-GFP localizes to SPBs, microtubule +ends, kinetochores and the bud neck and tip in small budded wild-type cells.

We next assessed Cdc28-GFP localization in *tub4*-Δ*dsyl* cells. Similar to wild-type cells, Cdc28-GFP localized to SPBs, microtubule +ends and kinetochores in *tub4*-Δ*dsyl* cells (Figure 3.2.4 D). These Cdc28-GFP foci, with the exception of those associated with microtubule +ends, also remained in the

absence of detectable microtubules when treated with NZ (Figure 3.2.4 E). Interestingly, Cdc28-GFP localization at the bud neck and bud tip was heavily reduced in small budded *tub4-*Δ*dsyl* cells (Figure 3.2.4 D). Only 2.4% of small budded *tub4-*Δ*dsyl* cells (n=82) had obvious Cdc28-GFP localization to the bud neck compared to 29.6% of wild-type cells (n=81) (Figure 3.2.4 F). Strikingly, only 8.5% of small budded *tub4-*Δ*dsyl* cells (n=82) had detectable Cdc28-GFP localization to the bud tip relative to 93.8% of wild-type cells (n=81) (Figure 3.2.4 F). These microscopy results suggest that the DSYL residues are not required for Cdc28 SPB localization. Therefore, the failure of Bim1 and Cdc28 to interact in *tub4-*Δ*dsyl* cells may not result from a failure of Cdc28 to localize to SPBs. Thus, the question remains why Bim1 phosphorylation, SPB/+end localization and interactions with Cdc28 are reduced in *tub4-*Δ*dsyl* cells.

One possibility is that the loss of Bim1 localization to the SPB in *tub4-*Δ*dsyl* cells is independent of its phosphorylation status and the failure of Cdc28 to interact with Bim1 (and possibly phosphorylate Bim1) is due to low preexisting levels of Bim1 already at SPBs in this mutant. However, we feel this is unlikely given that phosphorylation of other +TIPs is very important for modulating their cellular localization (Rickard and Kreis, 1991; Vaughan *et al.*, 2002; Liakopoulos *et al.*, 2003; Maekawa *et al.*, 2003; Moore *et al.*, 2005). Alternatively, it is possible that Tub4 affects the dynamics of Cdc28/Bim1 associations at SPBs and potentially other cellular locations, which are not obvious by our current microscopy methods. For example, the altered localization of Cdc28 to various cellular locations may reflect altered dynamics or off-loading from the SPB. Therefore, though Cdc28 is observed at SPBs its interaction with Bim1 may be defective. Using fluorescence recovery after photobleaching (FRAP) on Cdc28-GFP foci in wild-type and mutant cells would provide insight to this. Another possibility is that the *tub4-*Δ*dsyl* mutation disrupts the ability of another unknown effector protein that facilitates interactions between Cdc28 and Bim1. Consistent with this, phosphorylation of Kar9 at the SPB_b via Cdc28/Clb5 is known to depend on the +TIP Bik1 (Moore *et al.*, 2005). Finally, it is also possible that Tub4 influences the localization of an associated

Cdc28 cyclin necessary to confer Cdc28 binding and regulation of +TIPs like Bim1 at SPBs. Though many of these possibilities are not mutually exclusive, we have preliminary evidence supporting this latter hypothesis.

3.2.5 Investigating the role of early B-type cyclins in Bim1 phosphorylation

Cdc28 activity and substrate specificity are modulated by its associated cyclins (Loog and Morgan, 2005). The S-phase cyclin Clb5 and the S/G2 cyclin Clb4 are implicated in Kar9 phosphorylation and multiple aspects of Kar9 function (Liakopoulos *et al.*, 2003; Maekawa *et al.*, 2003; Maekawa and Schiebel, 2004; Moore *et al.*, 2005; Moore and Miller, 2007). If Cdc28 phosphorylates Bim1, it is likely that these would be the potential cyclins involved, given that their expression coincides with maximal Bim1 phosphorylation.

One intriguing result that makes Clb4 relevant to our research, is that we and others have observed that cells depleted of Clb4 (*clb4*Δ) exhibit astral microtubule +end dwelling in the bud tip (Maekawa and Schiebel, 2004), reminiscent to what is observed in *tub4-*Δ*dsyl* cells (Figure 3.2.5 A). Interestingly these prolonged interactions in *clb4*Δ mutant cells are also dependent on Myo2 and actin (Maekawa and Schiebel, 2004). It is thought that in addition to Kar9, Clb4 phosphorylates proteins at the cortex to regulate microtubule associations at this site (Maekawa and Schiebel, 2004; Moore and Miller, 2007). Therefore, we speculate that a failure of Clb4 to be properly scaffolded at the SPB in *tub4-*Δ*dsyl* cells perturbs necessary regulatory events at SPBs (possibly Bim1 phosphorylation) that are integral to the formation of functional +TIP complexes. Since Clb4 transport to the cortex is dependent upon Kar9 and astral microtubule +ends, the formation of defective complexes that reach the cortex would likely cause astral microtubule dwelling in *tub4-*Δ*dsyl* cells similar to a *clb4*Δ mutant.

To begin testing this, we microscopically assessed Clb4 localization in small budded wild-type and *tub4-*Δ*dsyl* cells expressing Clb4-VFP and Spc42-

CFP. Our analysis revealed that in wild-type cells, Clb4-VFP foci localize to SPB_b and to astral microtubule +ends that emanate from this pole (Figure 3.2.5 B) while in *tub4-*Δ*dsyl* cells, Clb4-VFP preferentially localizes to microtubule +ends and is rarely observed at the SPB_b (Figure 3.2.5 B). This supports our hypothesis that the *tub4-*Δ*dsyl* mutation prevents Clb4 localization at the SPB_b, which is consistent with the hypothesis that Tub4 scaffolds cyclins involved in +TIP complex assembly and function.

We also have evidence that suggests Tub4 modulates the regulation of +TIPs at SPBs via Cdc28/Clb5 complexes. It has previously been demonstrated that different Cdc28/cyclin complexes use specific mechanisms for substrate targeting (Loog and Morgan, 2005). Specifically, Cdc28/Clb5 complexes target substrates using a bipartite recognition sequence that includes the Cdc28 consensus sequence and a cyclin (Cy or RXL) binding motif (Cross *et al.*, 1999; Takeda *et al.*, 2001; Loog and Morgan, 2005). Tub4 contains an evolutionarily conserved cyclin binding domain (Figure 3.2.5C), suggesting that it may itself be a direct target of Cdc28/Clb5, which is consistent with a previous study that demonstrates Tub4 is a phospho-protein (Vogel *et al.*, 2001). In addition to this, interactions between Tub4 and Clb5 at SPBs may also be important to bring this cyclin in proximity to possible +TIP substrates like Bim1 or Kar9 (discussed further in Chapter 4).

In addition, we previously assessed the phosphorylation pattern of Bim1 using 2D SDS-PAGE in extracts obtained from cells depleted of Clb5 (*clb5*Δ). This was compared to Bim1 isoform profiles in wild-type and *tub4-*Δ*dsyl* cells and interestingly we found that Bim1 phospho-isoforms were perturbed by the *clb5*Δ mutation similar to that in *tub4-*Δ*dsyl* cells (Figure 3.2.5D). Therefore, it is possible that Tub4 recruits Clb5 for phosphorylation events that are independent of its role in phosphorylating Kar9 at Ser496. We speculate that while Cdc28/Clb5 modulates Kar9 phosphorylation it is also phosphorylating other targets like Bim1 in order to promote +TIP complex assembly.

Figure 3.2.5 Investigating the role of early B-type cyclins in Bim1 phosphorylation

(A) Montage of astral microtubule behaviour in *clb4*Δ cells expressing GFP-Tub1. In *clb4*Δ cells astral microtubule +ends dwell at the bud cortex, which is reminiscent of the defect in *tub4*-Δ*dsyl* cells. White arrowhead denotes tip of the microtubule in each frame. Dashed circles outline the mother and bud in the first frame. Each time-point represents 3 second intervals. **(B)** Microscopic analysis of Clb4-VFP in wild-type and *tub4*-Δ*dsyl* cells. In wild-type cells, Clb4-VFP localizes to the SPB_b (white arrow), while in *tub4*-Δ*dsyl* cells Clb4-VFP exhibits a preferential localization to the astral microtubule +end. **(C)** Primary amino acid sequence alignment of γ-tubulin in various eukaryotic systems reveals an evolutionarily conserved cyclin binding (RXL or *Cy;* green box). **(D)** Comparison of Bim1 phosphorylation in wild-type, *tub4*-Δ*dsyl* and *clb5*Δ cells reveals that Bim1 phospho-isoforms are similarly reduced in *clb5*Δ and *tub4*-Δ*dsyl* cells.

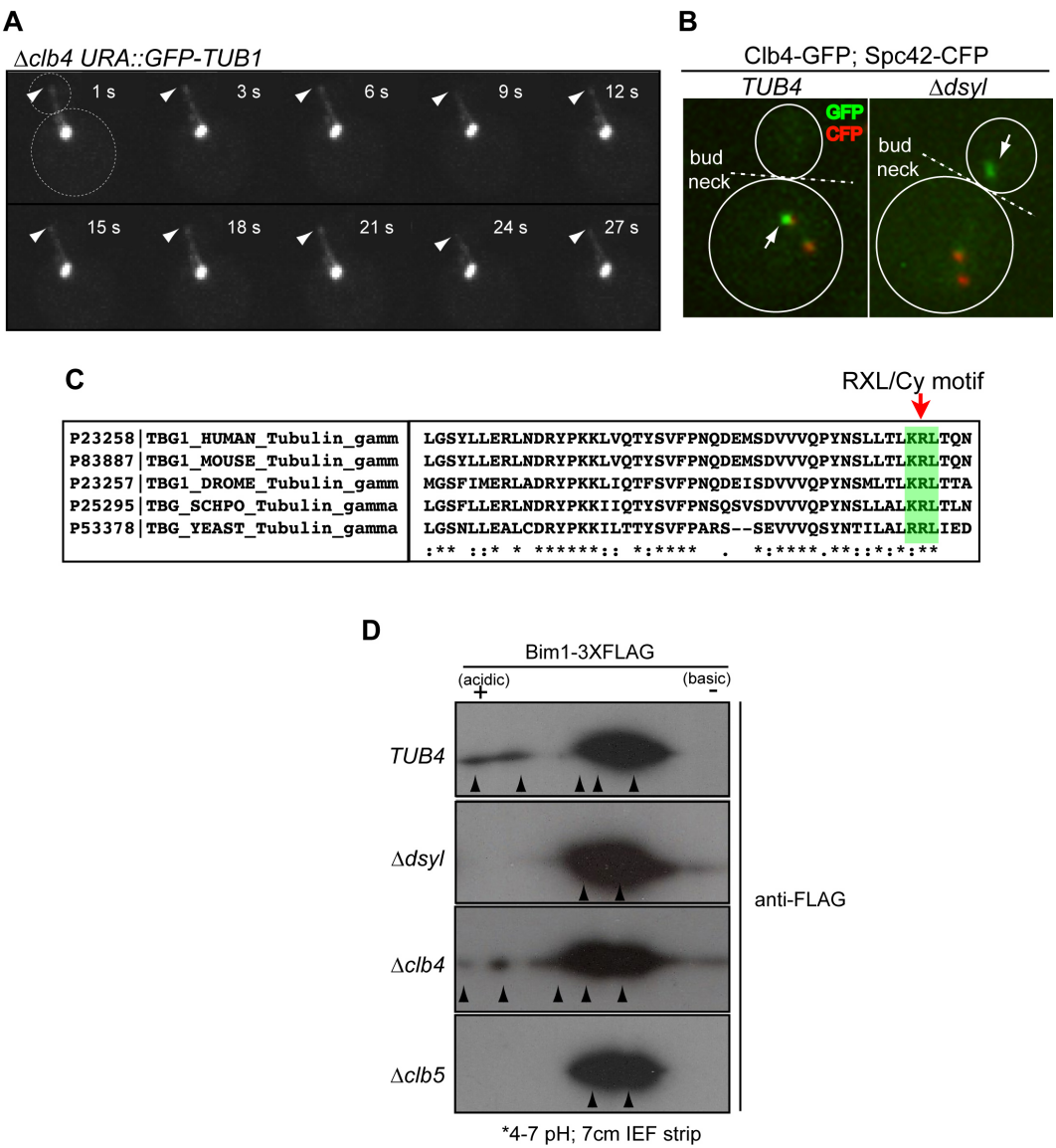
A
Δclb4 URA::GFP-TUB1
1 s
3 s
6 s
9 s
12 s
15 s
18 s
21 s
24 s
27 s
B
Clb4-GFP; Spc42-CFP
TUB4
Δdsyl
GFP
CFP
bud neck
bud neck
C
RXL/Cy motif
P23258|TBG1_HUMAN_Tubulin_gamm LGSYLLERLNDRYPKKLVQTYSVFPNQDEMSDVVVQPYNSLLTLKRLTQN
P83887|TBG1_MOUSE_Tubulin_gamm LGSYLLERLNDRYPKKLVQTYSVFPNQDEMSDVVVQPYNSLLTLKRLTQN
P23257|TBG1_DROME_Tubulin_gamm MGSFIMERLADRYPKKLIQTFSVFPNQDEISDVVVQPYNSMLTLKRLTTA
P25295|TBG_SCHPO_Tubulin_gamma LGSFLLERLNDRYPKKIIQTYSVFPNSQSVSDVVVQPYNSLLALKRLTLN
P53378|TBG_YEAST_Tubulin_gamma LGSNLLEALCDRYPKKILTTYSVFPARS--SEVVVQSYNTILALRRLIED
:** ::* * ******:: *:**** . *:****.**::*:*:**
D
Bim1-3XFLAG
(acidic)
(basic)
+
-
TUB4
Δdsyl
Δclb4
Δclb5
anti-FLAG
*4-7 pH; 7cm IEF strip

Collectively, our preliminary data is in agreement with Tub4 scaffolding cyclins at the SPB in order to promote proper regulation of +TIPs via Cdc28 (discussed in Chapter 4). Therefore, we wish to test if Tub4 interacts with either Clb4 or Clb5 or is required for the binding of either cyclin to Cdc28. We will test these possibilities using co-immunoprecipitation in wild-type and *tub4-*Δ*dsyl* backgrounds. We predict that interactions between Tub4 and Clb4 or Clb5 will be perturbed in the *tub4-*Δ*dsyl* background. Furthermore, we expect that the results of these experiments will correlate to the cyclin primarily involved in Bim1 phosphorylation. Presently we have made a wild-type strain expressing Cdc28-TAP and Clb4-3XFLAG. We have encountered difficulty in creating the *tub4-*Δ*dsyl* reciprocal strain since the *TUB4* and *CLB4* genes are linked on chromosome 12. We are currently trying to introduce the *CLB4-3XFLAG* DNA into the *tub4-*Δ*dsyl* background using homologous recombination which is amenable in budding yeast. Unfortunately, we also have experienced technical issues in creating the Clb5-3XFLAG protein fusion in both wild-type and *tub4-*Δ*dsyl* cells. We are trying different transformation techniques in order to favour homologous recombination and integration of our *CLB5-3XFLAG* product at the endogenous *CLB5* 3' locus.

3.3 Conclusion

In summary, our results suggest that the loss of Kar9 function in *tub4-*Δ*dsyl* cells is attributed to a loss of Bim1 function. Over-production of Bim1 protein rescues a number of the defects caused by the *tub4-*Δ*dsyl* mutation, yet only with respect to spindle placement. While Tub4 does not interact with either Bim1 or Kar9 it does appear to be important for proper Bim1 phosphorylation and interaction with Cdc28. Our results implicate Cdc28 as a potential kinase responsible for Bim1 phosphorylation and also implicate a role for the DSYL residues in this process. Our preliminary results also reveal a putative role for Tub4 as a SPB scaffold for cyclins. Future work directed towards understanding the mechanism of +TIP regulation at the SPB while likely elucidate mechanisms

for Tub4, Cdc28 and the cyclins in coordinating microtubule +end behaviour with regulation at spindle poles.

3.4 Materials and methods

3.4.1 Strain construction

All strains used in this study (Table 3.4.1) were created using PCR-based transformation, standard non-integrative plasmid transformation and mating procedures (Christianson *et al.*, 1992; Longtine *et al.*, 1998). Media (rich media; yeast extract, peptone, adenine sulfate, dextrose (YPAD) and synthetic complete, SC) and general yeast methods are described (Guthrie, 1991).

3.4.2 Synthetic lethality analysis of *tub4-*Δ*dsyl* cells containing over-produced Bim1

To test if over-production of Bim1 protein could rescue synthetic lethal interactions between the *tub4-*Δ*dsyl* mutation and various array mutations (*gene*Δ*::KanMX*); *tub4-*Δ*dsyl pBIM1* and *tub4-*Δ*dsyl pRS423* cells were grown in –HIS liquid media (SC media containing adenine sulfate, tryptophan, uracil and leucine) to maintain selection for cells carrying either vector, mated to array mutants and scored for viability. Matings were plated on –HIS agar plates and streaked on similar plates for the isolation of single colonies. Single colonies where then sporulated in low nitrogen liquid medium and meiotic products (tetrads) obtained (Guthrie, 1991). Tetrads were dissected on a Nikon E400 micromanipulator. For each analysis, meiotic products of 40 tetrads (spores) were grown on rich medium (YPAD) at 25˚C. The segregation of *tub4-*Δ*dsyl* mutation was confirmed by suppression of growth on rich medium at 37˚C as previously described (Vogel *et al.*, 2001). The segregation of array mutations was confirmed on YPAD containing G418 drug selection. Segregation of *pBIM1* or *pRS423* was confirmed by growth on –HIS agar plates.

TABLE 3.4.I. Yeast strains and plasmids used in Chapter 3

Strain	Genotype†	Source
YJV153	*MAT**a** TUB4::TRP1, URA3::GFP::TUB1*	(Vogel *et al.*, 2001)
YJV157	*MAT**a** tub4-Δdsyl::TRP1, URA3::TUB1::GFP*	This study
YJV149	*MAT**a** TUB4:TRP1*	(Vogel *et al.*, 2001)
YJV126	*MAT**a** tub4-Y445D::TRP1*	(Vogel *et al.*, 2001)
YLC11	*MAT**a** tub4-Δdsyl::TRP1*	This study
YJV148	*MATa TUB4::TRP1*	(Vogel *et al.*, 2001)
YLC15	*MATa tub4-Δdsyl::TRP1*	This study
Y00147	*MAT**a** bim1::kan*MX6, *TRP1*, *leu2-3,112*	(Brachmann *et al.*, 1998)
Y01023	*MAT**a** kar9::kan*MX6 *TRP1*, *leu2-3,112*	(Brachmann *et al.*, 1998)
Y01039	*MAT**a** vik1::kan*MX6 *TRP1*, *leu2-3,112*	(Brachmann *et al.*, 1998)
Y01957	*MAT**a** arp1::kanMX6 TRP1*, *leu2-3,112*	(Brachmann *et al.*, 1998)
Y00784	*MAT**a** cik1::kanMX6 TRP1*, *leu2-3,112*	(Brachmann *et al.*, 1998)
Y00147	*MAT**a** cin8::kanMX6 TRP1*, *leu2-3,112*	(Brachmann *et al.*, 1998)
Y02097	*MAT**a** kip2::kanMX6 TRP1*, *leu2-3,112*	(Brachmann *et al.*, 1998)
Y01392	*MAT**a** mad2::kanMX6 TRP1*, *leu2-3,112*	(Brachmann *et al.*, 1998)
Y01238	*MAT**a** swe1::kanMX6 TRP1*, *leu2-3,112*	(Brachmann *et al.*, 1998)
YLC130	*MAT**a** tub4-Δdsyl::TRP, URA3::GFP::TUB1,* pRS423	(Cuschieri *et al.*, 2006)
YLC135	*MAT**a** tub4-Δdsyl::TRP, URA3::GFP::TUB1,* pBIM1(pLC1)	(Cuschieri *et al.*, 2006)
SCO119	*MAT**a** CDC28::TAP::URA3*	(Huh *et al.*, 2003)
YLC233	*MAT**a** TUB4::TRP1, CDC28::TAP::URA3*	This study
YLC235	*MAT**a** tub4-Δdsyl::TRP1, CDC28::TAP::URA3*	This study
YLC345	*MAT**a** BIM1-3XFLAG*	This study
YLC188	*MAT**a** TUB4::TRP1, CLB4::VFP::HIS3, SPC42::CFP::KANMX6*	This study
YLC191	*MAT**a** tub4-Δdsyl::TRP1, CLB4::VFP::HIS3, SPC42::CFP::KANMX6*	This study
YLC159	*MAT**a** TUB4::TRP1, KAR9::GFP::TRP1, SPC42::CFP::KANMX6*	(Cuschieri *et al.*, 2006)
YLC487	*MAT**a** tub4-Δdsyl::TRP1, KAR9::GFP::TRP1, SPC42::CFP::KANMX6,*	This study
YLC368	*MAT**a** TUB4::TRP1, CDC28::TAP::URA3, BIM1::3XFLAG::KANMX6*	This study
YLC443	*MAT**a** tub4-Δdsyl::TRP1, CDC28::TAP::URA3, BIM1::3XFLAG::KANMX6*	This study
F80G	*MAT**a**, cdc28-as1*	(Bishop *et al.*, 2000)
YLC525	*MAT**a**, cdc28-as1 BIM1-3XFLAG::KAN*	This study
Y95700	*MAT**a**, CDC28::GFP::HIS3*	(Huh *et al.*, 2003)
YLC516	*MAT**a** CDC28::GFP::HIS3 SPC42::CFP::KANMX6*	This study
YLC520	*MAT**a** tub4-Δdsyl::TRP, CDC28::GFP::HIS3, SPC42::CFP::KANMX6*	This study

Plasmid	Description	Source
pRS423	pCEN; HIS3 2μ	Christianson and Heiter,1992
pLC1	*BIM1* ORF + 600 bp of 5' UTR and 200 bp of 3'UTR inserted in pRS423 at ClaI and SacI sites	(Cuschieri *et al.*, 2006)

†All strains are S288C (*his3-Δ200, lys2-801, ura3-52, trp1-Δ1, ade2-101)*

3.4.3 Preparation of cell extracts for 2-Dimensional SDS-PAGE

All steps were performed at 4˚C unless indicated. 5 ml cultures were grown overnight in YPAD media at 25˚C. Cells were pelleted at 5000xg for 5 minutes, washed in 500 ul of PGSK buffer (50 mM $Na_2HPO_4 \cdot 2H_2O$, 4 mM $NaH_2PO_4 \cdot H_2O$, 50 mM NaCl, 5 mM KCl, and 60 mM glucose and 4% CHAPs containing, PIC, 25 mM NaF, 20 mM BGP, 25 mM DTT, 10 mM O-vandate, PMSF). Whole cell extracts were diluted in PGSK buffer in a volume equal to the volume of the pellet. Glass beads were added to a final volume equal to the volume of the resuspended pellet. Extracts were vortexed 20 minutes, spun for 85000xg for 10 minutes and then precipitated overnight with 9 volumes of ice-cold Acetone at -80˚C. Precipitates were spun at 10000xg for 10 minutes. Supernatants were sucked out and pellets air-dried for 10 minutes at room temperature. Dried pellets were then resuspended in 50-100 ul of rehydration buffer (100 mM Tris pH 8, 6M Urea, 30% v/v Glycerol, 2% w/v SDS) and assayed for protein concentration. For synchronization of cells with α-factor, 30 ml overnight cells were diluted to an OD^{600} of 0.4-05, pelleted at 5000xg for 1 minute and resuspended into 30 ml of fresh YPAD media containing 5 µg/ml of α-factor. Cells were allowed to grow for one cell cycle (approximately 90 minutes) and then an additional 5 µg/ml of α-factor was added directly to the cell cultures. Cells grew for 1 hr, were then pelleted at 5000xg for 5 minutes and then released from the arrest by being resuspended into 30 ml of fresh YPAD. 5 ml aliquots (minus 0.5 ml for microscopic analysis) were taken every 20 minutes following release, pelleted at 5000xg for 5 minutes and snap frozen. Each aliquot was then extracted as described above.

3.4.4 2-Dimensional SDS PAGE of Bim1

40 µg/strip of protein in rehydration buffer was used for the detection of Bim1 isoforms. For each protein sample, 1.25 ul of ampholytes (range 3-10 Biorad Hercules CA) and rehydration buffer (containing 0.002% w/v

Bromophenol Blue) were added to a final volume of 125 ul. Samples were then absorbed overnight in 7 cm 4-7 pH linear strips (Biorad, Hercules CA) using active rehydration methods. Samples were then focused at 50 mA/gel for a total of 10000 volthours.

3.4.5 Electrophoresis and immunoblotting

SDS-polyacrylamide gel electrophoresis and immunoblotting was performed as previously described (Vogel *et al.*, 2001). Anti-TAP (Open Biosystems Huntsville IL) was used at 1:7000 in TBS-0.20% tween-20 (TBS-T). A polyclonal anti-Bim1 antibody was used at 1:4000. Monoclonal anti-FLAG (Sigma) was used at 1:20000 in TBS-T. Polyclonal anti-Cdc28 and anti-Tub4 antibodies (Santa-Cruz) were used at 1:4000 in TBS-T. Anti-rabbit (anti-TAP and anti-Bim1), anti-mouse (anti-FLAG) or anti-Goat (anti-Cdc28 and anti-Tub4) HRP-conjugated secondary antibodies were used at 1:10,000, 1:20000 and 1:7000 in TBS/T-20 respectively (Amersham Arlington Heights IL; Santa Cruz). Protein/antibody complexes were detected using ECL (Amersham Arlington Heights IL).

3.4.6 λ-Phosphatase treatment

All steps were performed at 4˚C unless indicated. 5ml cultures were grown overnight in YPAD media at 25˚C. Cells were pelleted at 5000xg for 5 minutes, washed in 500 µl of PGSK buffer containing only PIC, 20 mM BGP and 25 mM DTT. Whole cell extracts were diluted in PGSK buffer in a volume equal to the volume of the pellet. Glass beads were added to a final volume equal to the volume of the resuspended pellet. Extracts were vortexed 20 minutes, spun for 85000xg for 10 minutes. Approximately 100 µl of cleared extracts were recovered and adjusted for protein concentration. 40 µg of cleared extracts were incubated at 37˚C for 15 minutes with PPase buffer, PIC and in the presence or absence of PPase inhibitors (10 mM o-vandate, 25 mM NaF and 20 mM BGP).

To the extract without PPase inhibitors and to one extract containing PPase inhibitors, 20 units of λPPase was added. All extracts were incubated at 37˚C for an additional 30 minutes. 9 volumes of ice-cold Acetone was added to extracts and extracts left to precipitate over-night at -80˚C. Cells were then prepared for 2D-SDS PAGE analysis as previously described.

3.4.7 Co-Immunoprecipitation

All steps were performed at 4˚C unless indicated otherwise. Whole cell extracts were prepared as previously described (Vogel *et al.*, 2001). Extracts were clarified by centrifugation for 10 minutes at 10000xg. For IPs, 900 μl of 1x IP buffer (lysis buffer + 0.1% NP-40) was added to clarified extracts. An aliquot of undiluted extract (input) was diluted 1:1 with 2x sample buffer (SB) for analysis. For co-immunoprecipitation, 5μg of antibody (anti-TAP; Open Biosystems Huntsville AL) was added to diluted extracts, which rotated over night. Diluted extracts were incubated with pre-equilibrated IgG sepharose (25μl; 50% slurry) for 4 hours. Beads were washed 6 times with IP buffer, pelleted at 2000 xg for 1 minute and the supernatant aspirated. Bound proteins were recovered from the beads by incubating in 40 μl of 2x SB for 7 minutes at 90˚C.

3.4.8 Fluorescent microscopy methods

Microscopy methods used for Cdc28-GFP and Clb4-GFP localizations were performed as described in Chapter 2 (Cuschieri *et al.*, 2006). A modification from this previously described was that optical sections (0.5 μm) were acquired from the top of the focal plane to the bottom of the focal plane continuously for 1 time-point using Volocity 3DM (Improvision, UK).

3.5 Acknowledgments

We would like to thank Dr. Elke Kuster-Schöck for assistance with the 2D SDS-PAGE experiments of Bim1 phosphorylation. We also thank Dr. Rita Miller for use of the Bim1 antibody in a number of the experiments described. Finally, we thank all members of the Vogel lab for fruitful scientific discussions and critiquing of this work.

Chapter 4: Discussion

4.1 The role of Bim1 phosphorylation

As presented in Chapter 3, we have used 2D SDS-PAGE in combination with λ-PPase treatments (Figure 3.2.1) and revealed that Bim1 is differentially regulated throughout the cell cycle by phosphorylation. This is the first time that Bim1 has been identified as a phospho-protein. We believe that Bim1 phosphorylation has been under investigated to date since it migrates largely as a very strong single band on 1D SDS-PAGE and does not allow for easy detection of multiple isoforms (Figure 2.4.4). Post-translational modification of Bim1 is not surprising, given the complex genetic interaction network of Bim1 and its function in multiple essential cellular processes (Tong *et al.*, 2001).

We speculate that Bim1 phosphorylation is intimately tied to its localization during spindle placement. Specifically, we predict that phosphorylation of Bim1 promotes its residency at the SPB and incorporation into +TIP complexes with Kar9. In higher eukaryotes, phosphorylation of the +TIPs CLIP-170 and $p150^{glued}$ decreases their ability to bind to microtubules, revealing that phosphorylation is an effective means of governing +TIP localization (Rickard and Kreis, 1991; Choi *et al.*, 2002; Vaughan *et al.*, 2002). Therefore, Bim1 phosphorylation may decrease its affinity for microtubules and promote its binding and accumulation to the SPB for its assembly into +TIP complexes, prior to deployment on microtubule +ends. Microtubule binding assays in the presence of constitutively phosphorylated versus unphosphorylated Bim1 would shed light on this issue. However, our finding that Bim1 is maximally phosphorylated during S/G2 is consistent with our prediction that phosphorylation is important for its role during spindle placement.

Our results suggest that many of the defects observed in *tub4-Δdsyl* cells, are all a result of perturbed Bim1 function and aberrant localization, which we attribute to decreased Bim1 phosphorylation in this background. Loss of Bim1 phosphorylation in *tub4-Δdsyl* cells likely prevents its assembly into +TIP

complexes at the SPB. Over-production of Bim1 protein compensates for this by enabling excess Bim1 to become incorporated into Kar9 complexes at SPBs, and restore astral microtubule dynamics in an otherwise mutant background. In agreement with this, we demonstrated that over-production of Bim1 protein in *tub4-*Δ*dsyl* cells restored interactions between Bim1 and Kar9 in co-affinity purifications (Figure 2.4.8) (Cuschieri *et al.*, 2006).

If phosphorylation affects Bim1 localization to SPBs and assembly into +TIP complexes, then presumably phosphorylation somehow modifies the interaction between Bim1 and Kar9 or their assembly into complexes at the SPB. In higher eukaryotes as well as yeast, phosphorylation of APC/Kar9 by Cdk1/Cdc28 was shown to decrease its binding affinity for EB1/Bim1 by preventing the stabilization of transient interactions between the two +TIPs (Trzepacz *et al.*, 1997; Liakopoulos *et al.*, 2003; Honnappa *et al.*, 2005). Kar9 phosphorylation at Ser197 is also thought to decrease its binding to the $SPB_{\mathbf{b}}$ by attenuating its interaction with the +TIP, Stu2 (Moore and Miller, 2007). As such, it is reasonable to posit that Bim1 phosphorylation may similarly influence its binding properties with Kar9. However, unlike Kar9 phosphorylation, our results suggest that Bim1 phosphorylation may promote the binding between Bim1 and Kar9 at the $SPB_{\mathbf{b}}$ to enable their interactions on microtubule +ends.

Mechanistically, Bim1 phosphorylation may promote interactions with Kar9, as well as their residency at the $SPB_{\mathbf{b}}$, by reducing phosphorylation of Kar9 at Ser197. Though phosphorylation of this residue appears to also be important to coordinate Kar9 asymmetry along with phosphorylation at Ser496, it seems to also have an additional pronounced affect on releasing Kar9 from the SPB, and promoting its deployment to the microtubule +end (Maekawa and Schiebel, 2004; Moore and Miller, 2007). Bim1 phosphorylation may in turn, limit this specific phosphorylation event following the initial establishment of Kar9 asymmetry to the $SPB_{\mathbf{b}}$, possibly by temporally sequestering the regulatory machinery. By limiting this Kar9 phosphorylation event, associations between Bim1 and Kar9 and Kar9 and Stu2 would be stabilized at the $SPB_{\mathbf{b}}$.

Several lines of evidence led to the hypothesis that regulation of Bim1 influences phosphorylation of Kar9 at residue Ser197. First, the localization of Kar9 to the SPB_b is known to depend on Bim1 (Liakopoulos *et al.*, 2003). Additionally, constitutive phosphorylation of Kar9 at Ser197 (*kar9-197E*) appears to cause precocious release of Kar9 from the SPB_b and its enrichment at the +end (Maekawa and Schiebel, 2004; Moore and Miller, 2007). Notably, this is similar to the phenotype described for the *tub4-*Δ*dsyl* mutation (Cuschieri *et al.*, 2006). Finally, we have found that purified Kar9 protein extracts obtained from *tub4-*Δ*dsyl* cells treated with NZ have an enrichment of phosphorylated Kar9 relative to the wild-type, which would be expected if Bim1 phosphorylation is perturbed (see Figure A1 in appendix). As such, further investigation into whether Bim1 phosphorylation inhibits Kar9 phosphorylation at this residue will be an exciting area of study. We expect that phosphorylation of Bim1 would only reduce Kar9 phosphorylation for a limited time at the SPB, long enough to establish a complex. Following their assembly, it is likely that Kar9 is phosphorylated again, as this phosphorylation event appears to be required for localization and function on microtubule +ends (Moore and Miller, 2007). It will be interesting to test if constitutively inhibiting Kar9 phosphorylation (*kar9-197A*) rescues some of the defects in the *tub4-*Δ*dsyl* background, by enabling the formation of +TIP complexes at SPBs.

Presently we can only speculate regarding the functional significance of Bim1 phosphorylation as we currently do not know the phosphorylated residues. Further insight on this topic can be gained by mapping the amino acid residues that are phosphorylated using mass spectrometry and then conducting Quikchange mutagenesis (Stratagene) to create phospho-mimicking and phospho-inhibiting mutations that can be integrated into yeast and characterized for defects. Based on our hypothesis, we would expect that inhibition of Bim1 phosphorylation should phenocopy defects observed in *tub4-*Δ*dsyl* cells and potentially increase Kar9 phosphorylation. Unfortunately, these experiments have not yet been completed since we devoted a great deal of time on 2D SDS-PAGE analyses to obtain consistent Bim1 phosphorylation profiles. However,

we have created a functional Bim1-3XFLAG strain to purify Bim1 for mass spectrometry and we have also created a 2μ BIM1 over-expression vector that can be used to create and integrate the mutations into the genome.

4.2 Bim1 and Kar9 synergy on microtubule +ends

An interesting finding from our research is that the combined efforts of Bim1 and Kar9 are needed for proper early spindle placement. As was described in Chapter 2, merely localizing Kar9 to the +ends of targeted astral microtubules is not enough to confer efficient movement of the spindle. Bim1 and Kar9 appear to have a synergistic relationship with respect to promoting proper microtubule dynamics during spindle placement. If our hypothesis that Bim1 phosphorylation restricts Kar9 phosphorylation is correct, then it is possible that the synergy of these two +TIPs is based on their abilities to influence each other's affinity for the other and different sub-cellular structures like the SPB, microtubule and cortex. This would in turn promote microtubule dynamics. Bim1 is also known to synergistically promote microtubule dynamics with the +TIP Stu2 during early spindle placement and many other +TIP proteins have been shown to cooperate together as functional units in the regulation of microtubule dynamics (Wolyniak *et al.*, 2006; Niethammer *et al.*, 2007). It remains unclear how Kar9 localizes to a high degree on microtubule +ends with reduced Bim1 in *tub4-*Δ*dsyl* cells, though it may be stabilized on microtubule +ends by another +TIP such as Bik1 or Stu2 or through associations with the cortex.

Previously it was proposed that the sole function of Kar9 is to anchor microtubules to actin cables, based on a study that created a Bim1-Myo2 chimera protein and eliminated the requirement for Kar9 function (Hwang *et al.*, 2003). However, we believe that this is a simplistic view. While we do expect that defects arise in *tub4-*Δ*dsyl* cells primarily due to the loss of Bim1 function, our finding that non-functional Kar9 can have dramatic consequences on astral microtubule dynamics, is not consistent with this protein acting merely as a

linker protein. Furthermore, in that study it remains unclear how spindle asymmetry is established without Kar9 present. We aim to revisit these questions by introducing a Bim1-Myo2 chimera protein in a *tub4*-Δ*dsyl kar9*Δ background and assessing whether this can rescue some of the defects characteristic to the *tub4*-Δ*dsyl* mutant. Since we expect that Kar9 has additional functions at the cortex that are independent of its role in establishing SPB asymmetry and microtubule attachments to the cortex, then we would expect that the Bim1-Myo2 chimera would not restore the spindle positioning defects observed in the *tub4*-Δ*dsyl* mutant. Unlike the *kar9*Δ mutant, the defects in *tub4*-Δ*dsyl* cells arise from stabilized associations between microtubules and the cortex, which we attribute to a failed synergy between Bim1 and Kar9 on microtubule +ends. Thus, we expect that Kar9 is more than just a linker protein and that the *tub4*-Δ*dsyl* mutation has uncoupled some regulatory event at the SPB that is important for Kar9 mediated regulation of microtubule dynamics at the cortex. One interesting possibility is that the assembly of Bim1/Kar9 complexes at SPBs has functional relevance for microtubule capture and shrinkage at the cortex via the actin-interactor Bud6 (Amberg *et al.*, 1997; Segal *et al.*, 2002). It was previously shown that the role of Bud6 in regulating microtubule capture and shrinkage at the cortex is independent from the role of Kar9 in targeting microtubules into the bud (Huisman *et al.*, 2004). Thus, Bim1 may be important to release Kar9 from targeted microtubule +ends at cortical capture sites marked by Bud6, thereby enabling Bud6 to promote proper microtubule shrinkage and spindle placement. We observed that the *tub4*-Δ*dsyl* mutation appears to alter microtubule interactions with the bud cortex to a greater extent than microtubule interactions with the bud neck (unpublished observations). Though further microscopic quantification of these interactions using a microtubule +end marker and bud neck marker are warranted, this finding is consistent with the idea that proper Bim1-Kar9 stoichiometry is important for proper microtubule +end behaviour at the cortex, presumably via a Bud6 dependent mechanism.

4.3 Regulation of microtubule dynamics by Cdc28/cyclin complexes

Cdc28/cyclin complexes play a direct role during spindle placement by coordinating multiple aspects of Kar9 function and localization (Liakopoulos *et al.*, 2003; Maekawa *et al.*, 2003; Maekawa and Schiebel, 2004; Moore *et al.*, 2005; Moore and Miller, 2007). We hypothesize that Cdc28/cyclin complexes are also responsible for Bim1 phosphorylation. Support for this hypothesis comes from our result that Bim1 and Cdc28 co-purify (Figure 3.2.3). Consistently, these two proteins have also been shown to interact via yeast 2-hybrid analysis (Maekawa *et al.*, 2003). Additionally, we and other groups have shown that Cdc28 and Bim1 co-localize to SPBs and microtubule +ends. Finally, Bim1 phosphorylation is perturbed in the *cdc28-as1* mutant background. Unfortunately we have not yet confirmed that Cdc28 is the kinase responsible for phosphorylating Bim1 using an *in vitro* kinase assay, thus it is possible that a different kinase that is regulated by Cdc28 in responsible for Bim1 phosphorylation. Currently we are optimizing conditions to purify Bim1-3XFLAG from wild-type cells that is compatible with both mass spectrometry and an *in vitro* kinase assay.

Based on our current results, we predict that both Bim1 and Kar9 continuously cycle between phosphorylated and unphoshphorylated states at various cell cycle locations in a Cdc28/cyclin dependent manner. Such a system would efficiently coordinate the interactions and functions of these proteins at various locations by regulating their affinities for each other, microtubules, SPBs and the cortex (possibly via Myo2). As already mentioned, Cdc28/cyclin dependent Kar9 phosphorylation appears to promote its release from the $SPB_{\mathbf{b}}$ and localization to microtubule +ends (Moore and Miller, 2007). Additionally, Cdc28/Clb4 complexes appear to regulate the duration of time a microtubule dwells at the cortex (Maekawa and Schiebel, 2004). Thus, it is possible that the Cdc28/cyclin complexes differentially regulate Bim1-Kar9 complexes and other factors at the SPB and cortex to promote microtubule dynamics.

There is strong support that Cdc28/cyclin complexes function as the master controllers facilitating such microenvironments of regulation. The ability of cyclins to confer Cdc28 substrate specificity using a variety of different mechanisms (Loog and Morgan, 2005), provide Cdc28 with the required flexibility to coordinate regulation of many +TIPs at various cell cycle stages and locations. Additionally, based on our microscopy of Cdc28 in wild-type cells, it is apparent that Cdc28 localizes to a number of diverse localizations including SPBs, kinetochores, microtubule +ends, the bud neck and the bud cortex. How Cdc28 localizes to these various subcellular sites is still unclear and we have not ruled out the possibility that this is via microtubules. Our NZ experiments suggest that the maintained localization of Cdc28 to the bud neck and bud tip does not require microtubules. However, the initial localization of Cdc28 to these sites may be dependent on its initial assembly into +end complexes, which we have not yet tested.

We are intrigued why Cdc28 localization to the bud neck and bud tip is perturbed by the *tub4-*Δ*dsyl* mutation (Figure 3.2.4). If we are correct in postulating that Cdc28 localization to these sites is dependent on its assembly into +end complexes initially at SPBs, then the reduced localization of Cdc28 could result from the altered assembly of +TIP complexes at SPBs in this mutant. For instance, the localization or association of Cdc28 to the microtubule +end may depend on an interaction with Bim1. In this case, Cdc28 would fail to localize to the microtubule +end and ultimately the bud neck and bud tip in *tub4-*Δ*dsyl* cells, since Bim1 levels on microtubule +ends are reduced. This would provide an additional explanation why interactions between Cdc28 and Bim1 are perturbed in *tub4-*Δ*dsyl* cells and why *tub4-*Δ*dsyl* cells phenocopy *clb4*Δ cells in terms of microtubule dwelling, as both genetic backgrounds would perturb Cdc28/Clb4 complexes at the microtubule +end and cortex. Further investigation on whether the localization of Cdc28 to various cellular locations is dependent on events at SPBs via Tub4 may elucidate mechanisms that coordinate microtubule behaviour with +TIP function at various cellular locations.

4.4 Tub4 as a SPB scaffold for +TIP regulation by Cdc28/cyclin complexes

The major focus of our research has been to understand how Tub4 at SPBs can influence the formation of +TIP complexes on microtubule +ends. Our work reveals that +TIPs assemble into complexes at SPBs prior to their deployment to microtubule +ends in a Tub4 dependent manner. Understanding how this occurs mechanistically has proven to be a complicated task. We have been unsuccessful in purifying Tub4 with either Bim1 or Kar9, suggesting that Tub4 governs +TIP complex assembly via an alternate means. Though it is possible that these +TIPs interact with Tub4 transiently, we favour a model in which Tub4 modulates phosphorylation of Bim1 and Kar9 at SPBs by Cdc28/cyclin complexes, which is directly relevant for their complex assembly. Consistently, we have demonstrated that Bim1 phosphorylation is similarly perturbed in *tub4-*Δ*dsyl* cells and *cdc28-as1* cells (Figures 3.2.2 and 3.2.3). Furthermore, Kar9 phosphorylation, which decreases binding to Bim1 and stability at the SPB_b is enhanced by the *tub4-*Δ*dsyl* mutation, as seen following treatment with NZ (Figure A1 in Appendix).

Further evidence that Tub4 acts as a SPB scaffold for regulatory complexes is that Tub4 and Cdc28 co-purify (Figure 3.2.4). Surprisingly, in *tub4-*Δ*dsyl* cells this interaction remains intact. Therefore, it is unlikely that reduced Bim1 phosphorylation in *tub4-*Δ*dsyl* cells is due to decreased interactions between Cdc28 and Tub4. It is also unlikely that this is caused by a reduced localization of Cdc28 at SPBs. Rather we speculate that Tub4 acts as a SPB scaffold for cyclins involved in +TIP regulation, in particular Clb4 and Clb5. Δ*clb4* cells exhibit astral microtubule dwelling reminiscent of *tub4-*Δ*dsyl* cells, suggesting that a common regulatory event is disrupted in both mutant backgrounds. This could be an alteration of Bim1 phosphorylation or Kar9 phosphorylation, which affects their interactions with each other. Alternatively, a failure to scaffold Clb4 at SPBs in *tub4-*Δ*dsyl* cells may reduce the incorporation of Cdc28 into +TIP complexes, thereby affecting the localization of Cdc28 to the bud neck and tip. In this case, loss of Cdc28 at the bud tip in *tub4-*Δ*dsyl* cells, or

loss of Clb4 in *clb4*Δ cells would have the same affect on microtubule dwelling at the cortex.

Our preliminary data also suggests that Tub4 may scaffold Clb5 and that Cdc28/Clb5 complexes may phosphorylate Bim1. This hypothesis is largely based on the similar Bim1 phosphorylation profiles of *tub4-*Δ*dsyl* cells and *clb5*Δ cells. As already mentioned, Tub4 contains both a cyclin binding motif (RXL or *Cy*) and a Cdc28 phosphorylation consensus sequence (S/T)PX(K/R), which together act as bipartite substrate recognition motif for Cdc28/cyclin complexes (Adams *et al.*, 1996; Takeda *et al.*, 2001). Cdc28/Clb5 complexes are known to utilize these domains to confer regulation of substrates (Cross *et al.*, 1999; Loog and Morgan, 2005). The Cy domain within Tub4 may be important to scaffold cyclins, specifically Clb5, to the SPB. We speculate this association may be important for its own modification or to promote Bim1 phosphorylation. Currently the affect of mutating Serine 361 of the Tub4 Cdc28 consensus sequence is being characterized (personal communication J.Vogel and D. Chen).

The Tub4 carboxyl terminus comprising the DSYL residues is highly disordered and solvent accessible based on the crystal structure of human γ-tubulin (Aldaz *et al.*, 2005). It was previously shown that the tyrosine within the DSYL domain (Y445) is differentially phosphorylated during the cell cycle (Vogel *et al.*, 2001). Moreover, the DSYL domain is structurally positioned near the Cy domain, based on analysis of the γ-tubulin crstal structure. We predict that phosphorylation of Y445 may confer an alteration of the carboxyl terminus that influences the ability of the Cy domain to scaffold cyclins. Consistently, a mutation that inhibits phosphorylation of this residue (*tub4-Y445F*) has a genetic interaction profile similar to proteins involved in spindle positioning and the *tub4-*Δ*dsyl* mutation (personal communication J.Vogel and T. Nguyen). One candidate kinase that may phosphorylate Tub4 at Y445 is the dual-specificity kinase Swe1 (Booher *et al.*, 1993). Swe1 and Cdc28 have been shown to negatively regulate each other throughout the cell cycle (Harvey *et al.*, 2005) and therefore Tub4 may influence the phosphorylation of Bim1 and/or Kar9 by scaffolding (and consequently being regulated) by these two kinases at different

time-points. Thus, we are intrigued to further explore whether there is structure/function relationships between these two domains.

To investigate whether the Cy domain is important for Tub4 function in promoting +TIP complexes, we have created plasmid constructs that contain mutations within the Tub4 cyclin binding domain. These constructs completely abolish the RXL cyclin binding domain (*tub4-*Δ*cy*) or switch the XL to alanines (*tub4-cyAA*). We plan on integrating these mutations into the genome and characterizing the effects of these mutations on cyclin binding, +TIP complex assembly/regulation and spindle positioning. We expect that if these mutations are viable, they will phenocopy the *tub4-*Δ*dsyl* mutation and perturb Bim1 phosphorylation and +TIP complex assembly. Regardless of our results, we anticipate that understanding the structure/function relationship of the Cy domain will elucidate novel and exciting prospects of Tub4 mediated control of +TIP regulation at SPBs.

4.5 A role for Tub4 in the coordination of +TIP function with regulation at the SPB

Based on our current data, we have proposed a model explaining how Tub4 may coordinate multiple regulatory events at SPBs with +TIP function on microtubule +ends. During S phase, Cdc28/Clb5 complexes phosphorylate Kar9 in the cytoplasm at Ser496 to promote its asymmetric localization do the $SPB_{\mathbf{b}}$. Presumably, the affinity of phosphorylated Kar9 for the $SPB_{\mathbf{b}}$ is through some as of yet unknown inherent asymmetry between the two SPBs. Cdc28/Clb4 may also phosphorylate Kar9 at Ser197 but to a lesser extent. Kar9 and these regulatory complexes weakly localize to the $SPB_{\mathbf{b}}$ (Figure 4.5.1, i). At the $SPB_{\mathbf{b}}$, Tub4 scaffolds Clb5 and Clb4 via its Cy domain to promote its own phosphorylation and that of Bim1 (Figure 4.5.1, ii). Phosphorylation of Tub4 and Bim1 may sequester the phosphorylation machinery, which temporally decreases phosphorylation of Kar9 at Ser197 (Figure 4.5.1, ii). This enables Kar9 to form stable associations with the $SPB_{\mathbf{b}}$ by interacting with Bim1 and

Stu2. Furthermore, Bim1, Kar9, Cdc28 and Clb4 are all properly assembled into a complex (Figure 4.5.1, ii). As Clb5 levels begin to decrease and Clb4 levels increase, phosphorylation of both Tub4 and Bim1 decreases. This promotes an increase in phosphorylation of Kar9 at Ser197 and enables the release of Kar9 from Stu2 and its assembly with Bim1 to microtubule +ends (Figure 4.5.1, iii). Proper formation of this +TIP complex on microtubule +ends promotes the regulation of unknown factors at the cortex and appropriate dynamics between the +end and Myo2 and actin. It is likely that the phosphorylation states of Bim1, Kar9 and Tub4 cycle to promote microtubule dynamics.

Figure 4.5.1 A role for Tub4 in the coordination of +TIP function with regulation at the SPB

(i) During S phase, Cdc28/Clb5 complexes phosphorylate Kar9 (pink) in the cytoplasm at Ser496 to promote its asymmetric localization to the SPB_b (black). Cdc28/Clb4 (white and brown) may also phosphorylate Kar9 at Ser197 but to a lesser extent. Kar9 and these regulatory complexes localize to the to the SPB_b though their interactions are not stable. **(ii)** At the SPB_b, Tub4 (blue) scaffolds Clb5 (yellow) and Clb4 via its Cy domain to promote its own phosphorylation and that of Bim1 (orange). Phosphorylation of Tub4 and Bim1 may sequester the phosphorylation machinery, which locally decreases phosphorylation of Kar9 at Ser197. This enables Kar9 to form stable associations with the SPB_b by interacting with Bim1 and Stu2 (purple). Furthermore, Bim1, Kar9, Cdc28 and Clb4 are all properly assembled into a complex. **(iii)** As Clb5 levels begin to decrease and Clb4 levels increase, phosphorylation of both Tub4 and Bim1 decreases. This promotes an increase in phosphorylation of Kar9 at Ser197 and enables the release of Kar9 from Stu2 and its assembly with Bim1 to microtubule +ends. Proper formation of this +TIP complex on microtubule +ends promotes the regulation of unknown factors at the cortex and appropriate dynamics between the +end and Myo2 and actin. It is likely that the states of Bim1, Kar9 and Tub4 phosphorylation cycle (depicted by black arrows) continuously during S/G2 cell cycle stages.

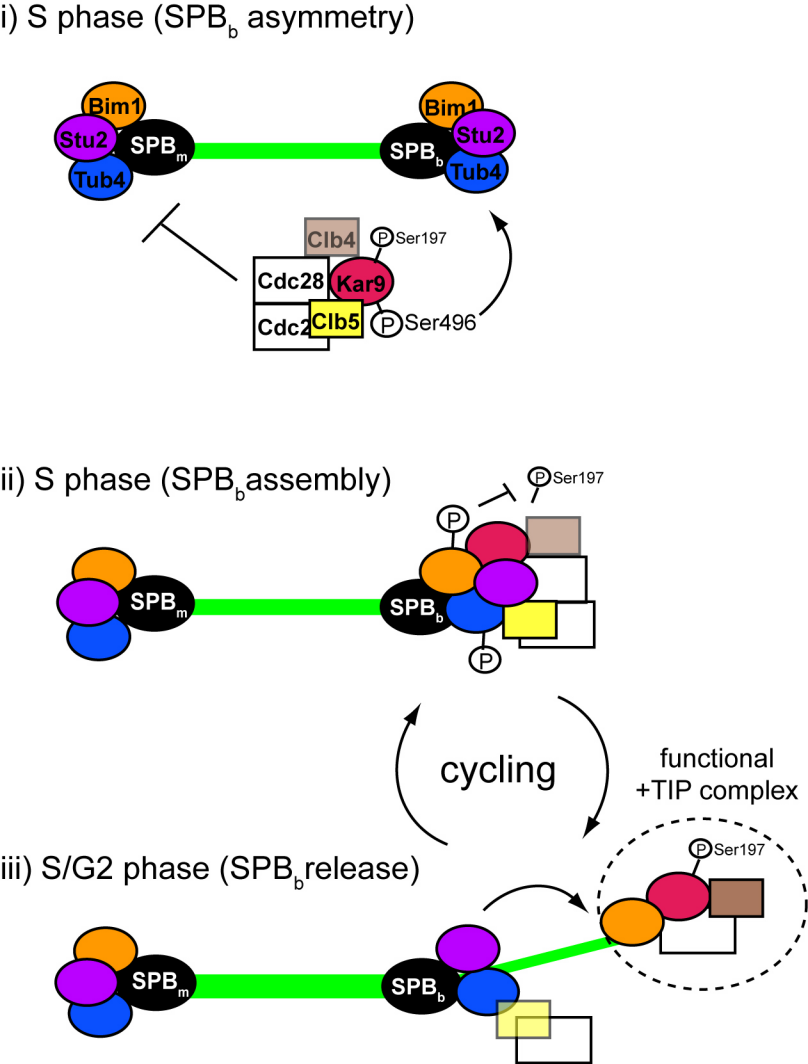
i) S phase (SPB$_b$ asymmetry)
Bim1
Stu2
SPB$_m$
Tub4
Bim1
Stu2
SPB$_b$
Tub4
Clb4
Ser197
Cdc28
Kar9
Cdc2
Clb5
Ser496
ii) S phase (SPB$_b$assembly)
Ser197
SPB$_m$
SPB$_b$
cycling
functional
+TIP complex
iii) S/G2 phase (SPB$_b$release)
Ser197
SPB$_m$
SPB$_b$

4.6 Conclusion

Understanding the processes that govern microtubule organization and dynamics is a large area of study. While many studies have revealed the contribution of +TIPs and motor proteins in this process, it is only recently that MTOC components such as γ-tubulin/Tub4 have also emerged as key regulators of microtubule organization and function. Finding the link between γ-tubulin/Tub4 function and microtubule +end behaviour has been a major challenge that has limited our understanding of this process.

The creation and characterization of the *tub4-Δdsyl* mutant, which does not perturb microtubule formation but rather microtubule organization, has provided us with a unique opportunity to study separate functional aspects of Tub4 in budding yeast. Using genetic, microscopic and biochemical techniques, we have elucidated a mechanism that links Tub4 function at SPBs with control at microtubule +ends. Our results suggest that Tub4 functions as a SPB scaffold for the proper regulation and assembly of +TIP complexes prior to their deployment to microtubule +ends. Mechanistically our data supports that Tub4 promotes phosphorylation of Bim1 and Kar9 by Cdc28/cyclin complexes via scaffolding cyclins to this site. Our study may reveal an evolutionarily conserved mechanism of control since many of the proteins involved are conserved across eukaryotes. Future work that focuses on understanding structure/function relationships of Tub4 will be beneficial to dissecting the diverse functions of Tub4 in yeast and γ-tubulin in higher eukaryotes during the cell cycle.

LIST OF REFERENCES

Aceto, D., Beers, M., and Kemphues, K.J. (2006). Interaction of PAR-6 with CDC-42 is required for maintenance but not establishment of PAR asymmetry in C. elegans. Dev Biol *299*, 386-397.

Adames, N.R., and Cooper, J.A. (2000). Microtubule interactions with the cell cortex causing nuclear movements in Saccharomyces cerevisiae. J Cell Biol *149*, 863-874.

Adams, A.E., Johnson, D.I., Longnecker, R.M., Sloat, B.F., and Pringle, J.R. (1990). CDC42 and CDC43, two additional genes involved in budding and the establishment of cell polarity in the yeast Saccharomyces cerevisiae. J Cell Biol *111*, 131-142.

Adams, A.E., and Pringle, J.R. (1984). Relationship of actin and tubulin distribution to bud growth in wild-type and morphogenetic-mutant Saccharomyces cerevisiae. J Cell Biol *98*, 934-945.

Adams, P.D., Sellers, W.R., Sharma, S.K., Wu, A.D., Nalin, C.M., and Kaelin, W.G., Jr. (1996). Identification of a cyclin-cdk2 recognition motif present in substrates and p21-like cyclin-dependent kinase inhibitors. Mol Cell Biol *16*, 6623-6633.

Aldaz, H., Rice, L.M., Stearns, T., and Agard, D.A. (2005). Insights into microtubule nucleation from the crystal structure of human gamma-tubulin. Nature *435*, 523-527.

Amaro, I.A., Costanzo, M., Boone, C., and Huffaker, T.C. (2008). The Saccharomyces cerevisiae homolog of p24 is essential for maintaining the association of p150Glued with the dynactin complex. Genetics *178*, 703-709.

Amberg, D.C., Zahner, J.E., Mulholland, J.W., Pringle, J.R., and Botstein, D. (1997). Aip3p/Bud6p, a yeast actin-interacting protein that is involved in morphogenesis and the selection of bipolar budding sites. Mol Biol Cell *8*, 729-753.

Atwood, S.X., Chabu, C., Penkert, R.R., Doe, C.Q., and Prehoda, K.E. (2007). Cdc42 acts downstream of Bazooka to regulate neuroblast polarity through Par-6 aPKC. J Cell Sci *120*, 3200-3206.

Beach, D.L., Thibodeaux, J., Maddox, P., Yeh, E., and Bloom, K. (2000). The role of the proteins Kar9 and Myo2 in orienting the mitotic spindle of budding yeast. Curr Biol *10*, 1497-1506.

Bender, A., and Pringle, J.R. (1989). Multicopy suppression of the cdc24 budding defect in yeast by CDC42 and three newly identified genes including the ras-related gene RSR1. Proc Natl Acad Sci U S A *86*, 9976-9980.

Berrueta, L., Kraeft, S.K., Tirnauer, J.S., Schuyler, S.C., Chen, L.B., Hill, D.E., Pellman, D., and Bierer, B.E. (1998). The adenomatous polyposis coli-binding protein EB1 is associated with cytoplasmic and spindle microtubules. Proc Natl Acad Sci U S A *95*, 10596-10601.

Berrueta, L., Tirnauer, J.S., Schuyler, S.C., Pellman, D., and Bierer, B.E. (1999). The APC-associated protein EB1 associates with components of the

dynactin complex and cytoplasmic dynein intermediate chain. Curr Biol *9*, 425-428.

Betschinger, J., and Knoblich, J.A. (2004). Dare to be different: asymmetric cell division in Drosophila, C. elegans and vertebrates. Curr Biol *14*, R674-685.

Binarova, P., Cenklova, V., Prochazkova, J., Doskocilova, A., Volc, J., Vrlik, M., and Bogre, L. (2006). Gamma-tubulin is essential for acentrosomal microtubule nucleation and coordination of late mitotic events in Arabidopsis. Plant Cell *18*, 1199-1212.

Bishop, A.C., Ubersax, J.A., Petsch, D.T., Matheos, D.P., Gray, N.S., Blethrow, J., Shimizu, E., Tsien, J.Z., Schultz, P.G., Rose, M.D., Wood, J.L., Morgan, D.O., and Shokat, K.M. (2000). A chemical switch for inhibitor-sensitive alleles of any protein kinase. Nature *407*, 395-401.

Booher, R.N., Deshaies, R.J., and Kirschner, M.W. (1993). Properties of Saccharomyces cerevisiae wee1 and its differential regulation of p34CDC28 in response to G1 and G2 cyclins. Embo J *12*, 3417-3426.

Bowman, S.K., Neumuller, R.A., Novatchkova, M., Du, Q., and Knoblich, J.A. (2006). The Drosophila NuMA Homolog Mud regulates spindle orientation in asymmetric cell division. Dev Cell *10*, 731-742.

Brachmann, C.B., Davies, A., Cost, G.J., Caputo, E., Li, J., Hieter, P., and Boeke, J.D. (1998). Designer deletion strains derived from Saccharomyces cerevisiae S288C: a useful set of strains and plasmids for PCR-mediated gene disruption and other applications. Yeast *14*, 115-132.

Browning, H., Hackney, D.D., and Nurse, P. (2003). Targeted movement of cell end factors in fission yeast. Nat Cell Biol *5*, 812-818.

Busch, K.E., and Brunner, D. (2004). The microtubule plus end-tracking proteins mal3p and tip1p cooperate for cell-end targeting of interphase microtubules. Curr Biol *14*, 548-559.

Busch, K.E., Hayles, J., Nurse, P., and Brunner, D. (2004). Tea2p kinesin is involved in spatial microtubule organization by transporting tip1p on microtubules. Dev Cell *6*, 831-843.

Byers, B., and Goetsch, L. (1974). Duplication of spindle plaques and integration of the yeast cell cycle. Cold Spring Harb Symp Quant Biol *38*, 123-131.

Byers, B., and Goetsch, L. (1975). Behavior of spindles and spindle plaques in the cell cycle and conjugation of Saccharomyces cerevisiae. J Bacteriol *124*, 511-523.

Carminati, J.L., and Stearns, T. (1997). Microtubules orient the mitotic spindle in yeast through dynein-dependent interactions with the cell cortex. J Cell Biol *138*, 629-641.

Carvalho, P., Gupta, M.L., Jr., Hoyt, M.A., and Pellman, D. (2004). Cell cycle control of kinesin-mediated transport of Bik1 (CLIP-170) regulates microtubule stability and dynein activation. Dev Cell *6*, 815-829.

Caudron, F., Andrieux, A., Job, D., and Boscheron, C. (2008). A new role for kinesin-directed transport of Bik1p (CLIP-170) in Saccharomyces cerevisiae. J Cell Sci.

Chang, F., and Peter, M. (2003). Yeasts make their mark. Nat Cell Biol *5*, 294-299.

Chant, J., Corrado, K., Pringle, J.R., and Herskowitz, I. (1991). Yeast BUD5, encoding a putative GDP-GTP exchange factor, is necessary for bud site selection and interacts with bud formation gene BEM1. Cell *65*, 1213-1224.

Chant, J., and Herskowitz, I. (1991). Genetic control of bud site selection in yeast by a set of gene products that constitute a morphogenetic pathway. Cell *65*, 1203-1212.

Chen, T., Hiroko, T., Chaudhuri, A., Inose, F., Lord, M., Tanaka, S., Chant, J., and Fujita, A. (2000). Multigenerational cortical inheritance of the Rax2 protein in orienting polarity and division in yeast. Science *290*, 1975-1978.

Chen, X.P., Yin, H., and Huffaker, T.C. (1998). The yeast spindle pole body component Spc72p interacts with Stu2p and is required for proper microtubule assembly. J Cell Biol *141*, 1169-1179.

Cheney, R.E., O'Shea, M.K., Heuser, J.E., Coelho, M.V., Wolenski, J.S., Espreafico, E.M., Forscher, P., Larson, R.E., and Mooseker, M.S. (1993). Brain myosin-V is a two-headed unconventional myosin with motor activity. Cell *75*, 13-23.

Chia, W., Somers, W.G., and Wang, H. (2008). Drosophila neuroblast asymmetric divisions: cell cycle regulators, asymmetric protein localization, and tumorigenesis. J Cell Biol *180*, 267-272.

Choi, J.H., Bertram, P.G., Drenan, R., Carvalho, J., Zhou, H.H., and Zheng, X.F. (2002). The FKBP12-rapamycin-associated protein (FRAP) is a CLIP-170 kinase. EMBO Rep *3*, 988-994.

Christianson, T.W., Sikorski, R.S., Dante, M., Shero, J.H., and Hieter, P. (1992). Multifunctional yeast high-copy-number shuttle vectors. Gene *110*, 119-122.

Colombo, K., Grill, S.W., Kimple, R.J., Willard, F.S., Siderovski, D.P., and Gonczy, P. (2003). Translation of polarity cues into asymmetric spindle positioning in Caenorhabditis elegans embryos. Science *300*, 1957-1961.

Cottingham, F.R., and Hoyt, M.A. (1997). Mitotic spindle positioning in Saccharomyces cerevisiae is accomplished by antagonistically acting microtubule motor proteins. J Cell Biol *138*, 1041-1053.

Cowan, C.R., and Hyman, A.A. (2004). Asymmetric cell division in C. elegans: cortical polarity and spindle positioning. Annu Rev Cell Dev Biol *20*, 427-453.

Cross, F.R., Yuste-Rojas, M., Gray, S., and Jacobson, M.D. (1999). Specialization and targeting of B-type cyclins. Mol Cell *4*, 11-19.

Cuschieri, L., Miller, R., and Vogel, J. (2006). {gamma}-Tubulin Is Required for Proper Recruitment and Assembly of Kar9-Bim1 Complexes in Budding Yeast. Mol Biol Cell *17*, 4420-4434.

Cuschieri, L., Nguyen, T., and Vogel, J. (2007). Control at the cell center: the role of spindle poles in cytoskeletal organization and cell cycle regulation. Cell Cycle *6*, 2788-2794.

DeMarini, D.J., Adams, A.E., Fares, H., De Virgilio, C., Valle, G., Chuang, J.S., and Pringle, J.R. (1997). A septin-based hierarchy of proteins required for

localized deposition of chitin in the Saccharomyces cerevisiae cell wall. J Cell Biol *139*, 75-93.

Desai, A., and Mitchison, T.J. (1997). Microtubule polymerization dynamics. Annu Rev Cell Dev Biol *13*, 83-117.

DeZwaan, T.M., Ellingson, E., Pellman, D., and Roof, D.M. (1997). Kinesin-related KIP3 of Saccharomyces cerevisiae is required for a distinct step in nuclear migration. J Cell Biol *138*, 1023-1040.

Dujardin, D., Wacker, U.I., Moreau, A., Schroer, T.A., Rickard, J.E., and De Mey, J.R. (1998). Evidence for a role of CLIP-170 in the establishment of metaphase chromosome alignment. J Cell Biol *141*, 849-862.

Endow, S.A., Kang, S.J., Satterwhite, L.L., Rose, M.D., Skeen, V.P., and Salmon, E.D. (1994). Yeast Kar3 is a minus-end microtubule motor protein that destabilizes microtubules preferentially at the minus ends. Embo J *13*, 2708-2713.

Eshel, D., Urrestarazu, L.A., Vissers, S., Jauniaux, J.C., van Vliet-Reedijk, J.C., Planta, R.J., and Gibbons, I.R. (1993). Cytoplasmic dynein is required for normal nuclear segregation in yeast. Proc Natl Acad Sci U S A *90*, 11172-11176.

Farkas, V., Kovarik, J., Kosinova, A., and Bauer, S. (1974). Autoradiographic study of mannan incorporation into the growing cell walls of Saccharomyces cerevisiae. J Bacteriol *117*, 265-269.

Farkasovsky, M., and Kuntzel, H. (2001). Cortical Num1p interacts with the dynein intermediate chain Pac11p and cytoplasmic microtubules in budding yeast. J Cell Biol *152*, 251-262.

Faulkner, N.E., Dujardin, D.L., Tai, C.Y., Vaughan, K.T., O'Connell, C.B., Wang, Y., and Vallee, R.B. (2000). A role for the lissencephaly gene LIS1 in mitosis and cytoplasmic dynein function. Nat Cell Biol *2*, 784-791.

Folker, E.S., Baker, B.M., and Goodson, H.V. (2005). Interactions between CLIP-170, tubulin, and microtubules: implications for the mechanism of Clip-170 plus-end tracking behavior. Mol Biol Cell *16*, 5373-5384.

Gardner, M.K., Haase, J., Mythreye, K., Molk, J.N., Anderson, M., Joglekar, A.P., O'Toole, E.T., Winey, M., Salmon, E.D., Odde, D.J., and Bloom, K. (2008). The microtubule-based motor Kar3 and plus end-binding protein Bim1 provide structural support for the anaphase spindle. J Cell Biol *180*, 91-100.

Gennerich, A., Carter, A.P., Reck-Peterson, S.L., and Vale, R.D. (2007). Force-induced bidirectional stepping of cytoplasmic dynein. Cell *131*, 952-965.

Goldstein, B., and Hird, S.N. (1996). Specification of the anteroposterior axis in Caenorhabditis elegans. Development *122*, 1467-1474.

Goodson, H.V., Skube, S.B., Stalder, R., Valetti, C., Kreis, T.E., Morrison, E.E., and Schroer, T.A. (2003). CLIP-170 interacts with dynactin complex and the APC-binding protein EB1 by different mechanisms. Cell Motil Cytoskeleton *55*, 156-173.

Grava, S., Schaerer, F., Faty, M., Philippsen, P., and Barral, Y. (2006). Asymmetric recruitment of dynein to spindle poles and microtubules promotes proper spindle orientation in yeast. Dev Cell *10*, 425-439.

Green, R.A., Wollman, R., and Kaplan, K.B. (2005). APC and EB1 function together in mitosis to regulate spindle dynamics and chromosome alignment. Mol Biol Cell *16*, 4609-4622.

Grill, S.W., Gonczy, P., Stelzer, E.H., and Hyman, A.A. (2001). Polarity controls forces governing asymmetric spindle positioning in the Caenorhabditis elegans embryo. Nature *409*, 630-633.

Grill, S.W., Howard, J., Schaffer, E., Stelzer, E.H., and Hyman, A.A. (2003). The distribution of active force generators controls mitotic spindle position. Science *301*, 518-521.

Groden, J., Thliveris, A., Samowitz, W., Carlson, M., Gelbert, L., Albertsen, H., Joslyn, G., Stevens, J., Spirio, L., Robertson, M., and et al. (1991). Identification and characterization of the familial adenomatous polyposis coli gene. Cell *66*, 589-600.

Gupta, M.L., Jr., Carvalho, P., Roof, D.M., and Pellman, D. (2006). Plus end-specific depolymerase activity of Kip3, a kinesin-8 protein, explains its role in positioning the yeast mitotic spindle. Nat Cell Biol *8*, 913-923.

Guthrie, C., and Fink, G.R. (ed.) (1991). Guide to Yeast Genetics and Molecular Biology Part B. Academic Press, Inc.: New York.

Haarer, B.K., Helfant, A.H., Nelson, S.A., Cooper, J.A., and Amberg, D.C. (2007). Stable preanaphase spindle positioning requires Bud6p and an apparent interaction between the spindle pole bodies and the neck. Eukaryot Cell *6*, 797-807.

Harvey, S.L., Charlet, A., Haas, W., Gygi, S.P., and Kellogg, D.R. (2005). Cdk1-dependent regulation of the mitotic inhibitor Wee1. Cell *122*, 407-420.

Heil-Chapdelaine, R.A., Oberle, J.R., and Cooper, J.A. (2000a). The cortical protein Num1p is essential for dynein-dependent interactions of microtubules with the cortex. J Cell Biol *151*, 1337-1344.

Heil-Chapdelaine, R.A., Tran, N.K., and Cooper, J.A. (2000b). Dynein-dependent movements of the mitotic spindle in Saccharomyces cerevisiae Do not require filamentous actin. Mol Biol Cell *11*, 863-872.

Hendrickson, T.W., Yao, J., Bhadury, S., Corbett, A.H., and Joshi, H.C. (2001). Conditional mutations in gamma-tubulin reveal its involvement in chromosome segregation and cytokinesis. Mol Biol Cell *12*, 2469-2481.

Hird, S.N., and White, J.G. (1993). Cortical and cytoplasmic flow polarity in early embryonic cells of Caenorhabditis elegans. J Cell Biol *121*, 1343-1355.

Honnappa, S., John, C.M., Kostrewa, D., Winkler, F.K., and Steinmetz, M.O. (2005). Structural insights into the EB1-APC interaction. Embo J *24*, 261-269.

Horio, T., Uzawa, S., Jung, M.K., Oakley, B.R., Tanaka, K., and Yanagida, M. (1991). The fission yeast gamma-tubulin is essential for mitosis and is localized at microtubule organizing centers. J Cell Sci *99 (Pt 4)*, 693-700.

Horvitz, H.R., and Herskowitz, I. (1992). Mechanisms of asymmetric cell division: two Bs or not two Bs, that is the question. Cell *68*, 237-255.

Howard, J., and Hyman, A.A. (2007). Microtubule polymerases and depolymerases. Curr Opin Cell Biol *19*, 31-35.

Huh, W.K., Falvo, J.V., Gerke, L.C., Carroll, A.S., Howson, R.W., Weissman, J.S., and O'Shea, E.K. (2003). Global analysis of protein localization in budding yeast. Nature *425*, 686-691.

Huisman, S.M., Bales, O.A., Bertrand, M., Smeets, M.F., Reed, S.I., and Segal, M. (2004). Differential contribution of Bud6p and Kar9p to microtubule capture and spindle orientation in S. cerevisiae. J Cell Biol *167*, 231-244.

Hwang, E., Kusch, J., Barral, Y., and Huffaker, T.C. (2003). Spindle orientation in Saccharomyces cerevisiae depends on the transport of microtubule ends along polarized actin cables. J Cell Biol *161*, 483-488.

Hyman, A.A. (1989). Centrosome movement in the early divisions of Caenorhabditis elegans: a cortical site determining centrosome position. J Cell Biol *109*, 1185-1193.

Izumi, Y., Hirose, T., Tamai, Y., Hirai, S., Nagashima, Y., Fujimoto, T., Tabuse, Y., Kemphues, K.J., and Ohno, S. (1998). An atypical PKC directly associates and colocalizes at the epithelial tight junction with ASIP, a mammalian homologue of Caenorhabditis elegans polarity protein PAR-3. J Cell Biol *143*, 95-106.

Izumi, Y., Ohta, N., Hisata, K., Raabe, T., and Matsuzaki, F. (2006). Drosophila Pins-binding protein Mud regulates spindle-polarity coupling and centrosome organization. Nat Cell Biol *8*, 586-593.

Joberty, G., Petersen, C., Gao, L., and Macara, I.G. (2000). The cell-polarity protein Par6 links Par3 and atypical protein kinase C to Cdc42. Nat Cell Biol *2*, 531-539.

Johnson, D.I., and Pringle, J.R. (1990). Molecular characterization of CDC42, a Saccharomyces cerevisiae gene involved in the development of cell polarity. J Cell Biol *111*, 143-152.

Johnston, G.C., Prendergast, J.A., and Singer, R.A. (1991). The Saccharomyces cerevisiae MYO2 gene encodes an essential myosin for vectorial transport of vesicles. J Cell Biol *113*, 539-551.

Kahana, J.A., Schlenstedt, G., Evanchuk, D.M., Geiser, J.R., Hoyt, M.A., and Silver, P.A. (1998). The yeast dynactin complex is involved in partitioning the mitotic spindle between mother and daughter cells during anaphase B. Mol Biol Cell *9*, 1741-1756.

Keating, T.J., and Borisy, G.G. (2000). Immunostructural evidence for the template mechanism of microtubule nucleation. Nat Cell Biol *2*, 352-357.

Kemphues, K. (2000). PARsing embryonic polarity. Cell *101*, 345-348.

Kemphues, K.J., Priess, J.R., Morton, D.G., and Cheng, N.S. (1988). Identification of genes required for cytoplasmic localization in early C. elegans embryos. Cell *52*, 311-320.

Kilmartin, J.V., and Adams, A.E. (1984). Structural rearrangements of tubulin and actin during the cell cycle of the yeast Saccharomyces. J Cell Biol *98*, 922-933.

Kimura, A., and Onami, S. (2007). Local cortical pulling-force repression switches centrosomal centration and posterior displacement in C. elegans. J Cell Biol *179*, 1347-1354.

King, S.J., and Schroer, T.A. (2000). Dynactin increases the processivity of the cytoplasmic dynein motor. Nat Cell Biol *2*, 20-24.

Knaus, M., Cameroni, E., Pedruzzi, I., Tatchell, K., De Virgilio, C., and Peter, M. (2005). The Bud14p-Glc7p complex functions as a cortical regulator of dynein in budding yeast. Embo J *24*, 3000-3011.

Knop, M., Pereira, G., Geissler, S., Grein, K., and Schiebel, E. (1997). The spindle pole body component Spc97p interacts with the gamma-tubulin of Saccharomyces cerevisiae and functions in microtubule organization and spindle pole body duplication. Embo J *16*, 1550-1564.

Knop, M., and Schiebel, E. (1997). Spc98p and Spc97p of the yeast gamma-tubulin complex mediate binding to the spindle pole body via their interaction with Spc110p. Embo J *16*, 6985-6995.

Knop, M., and Schiebel, E. (1998). Receptors determine the cellular localization of a gamma-tubulin complex and thereby the site of microtubule formation. Embo J *17*, 3952-3967.

Korinek, W.S., Copeland, M.J., Chaudhuri, A., and Chant, J. (2000). Molecular linkage underlying microtubule orientation toward cortical sites in yeast. Science *287*, 2257-2259.

Kosco, K.A., Pearson, C.G., Maddox, P.S., Wang, P.J., Adams, I.R., Salmon, E.D., Bloom, K., and Huffaker, T.C. (2001). Control of microtubule dynamics by Stu2p is essential for spindle orientation and metaphase chromosome alignment in yeast. Mol Biol Cell *12*, 2870-2880.

Kraut, R., Chia, W., Jan, L.Y., Jan, Y.N., and Knoblich, J.A. (1996). Role of inscuteable in orienting asymmetric cell divisions in Drosophila. Nature *383*, 50-55.

Kusch, J., Meyer, A., Snyder, M.P., and Barral, Y. (2002). Microtubule capture by the cleavage apparatus is required for proper spindle positioning in yeast. Genes Dev *16*, 1627-1639.

Labbe, J.C., Maddox, P.S., Salmon, E.D., and Goldstein, B. (2003). PAR proteins regulate microtubule dynamics at the cell cortex in C. elegans. Curr Biol *13*, 707-714.

Labbe, J.C., McCarthy, E.K., and Goldstein, B. (2004). The forces that position a mitotic spindle asymmetrically are tethered until after the time of spindle assembly. J Cell Biol *167*, 245-256.

Lee, L., Klee, S.K., Evangelista, M., Boone, C., and Pellman, D. (1999). Control of mitotic spindle position by the Saccharomyces cerevisiae formin Bni1p. J Cell Biol *144*, 947-961.

Lee, L., Tirnauer, J.S., Li, J., Schuyler, S.C., Liu, J.Y., and Pellman, D. (2000). Positioning of the mitotic spindle by a cortical-microtubule capture mechanism. Science *287*, 2260-2262.

Lee, M.J., Gergely, F., Jeffers, K., Peak-Chew, S.Y., and Raff, J.W. (2001). Msps/XMAP215 interacts with the centrosomal protein D-TACC to regulate microtubule behaviour. Nat Cell Biol *3*, 643-649.

Lee, W.L., Kaiser, M.A., and Cooper, J.A. (2005). The offloading model for dynein function: differential function of motor subunits. J Cell Biol *168*, 201-207.

Lee, W.L., Oberle, J.R., and Cooper, J.A. (2003). The role of the lissencephaly protein Pac1 during nuclear migration in budding yeast. J Cell Biol *160*, 355-364.

Legesse-Miller, A., Zhang, S., Santiago-Tirado, F.H., Van Pelt, C.K., and Bretscher, A. (2006). Regulated phosphorylation of budding yeast's essential myosin V heavy chain, Myo2p. Mol Biol Cell *17*, 1812-1821.

Lew, D.J., and Reed, S.I. (1993). Morphogenesis in the yeast cell cycle: regulation by Cdc28 and cyclins. J Cell Biol *120*, 1305-1320.

Li, J., Lee, W.L., and Cooper, J.A. (2005). NudEL targets dynein to microtubule ends through LIS1. Nat Cell Biol *7*, 686-690.

Li, Y.Y., Yeh, E., Hays, T., and Bloom, K. (1993). Disruption of mitotic spindle orientation in a yeast dynein mutant. Proc Natl Acad Sci U S A *90*, 10096-10100.

Liakopoulos, D., Kusch, J., Grava, S., Vogel, J., and Barral, Y. (2003). Asymmetric loading of Kar9 onto spindle poles and microtubules ensures proper spindle alignment. Cell *112*, 561-574.

Lin, D., Edwards, A.S., Fawcett, J.P., Mbamalu, G., Scott, J.D., and Pawson, T. (2000). A mammalian PAR-3-PAR-6 complex implicated in Cdc42/Rac1 and aPKC signalling and cell polarity. Nat Cell Biol *2*, 540-547.

Longtine, M.S., McKenzie, A., 3rd, Demarini, D.J., Shah, N.G., Wach, A., Brachat, A., Philippsen, P., and Pringle, J.R. (1998). Additional modules for versatile and economical PCR-based gene deletion and modification in Saccharomyces cerevisiae. Yeast *14*, 953-961.

Loog, M., and Morgan, D.O. (2005). Cyclin specificity in the phosphorylation of cyclin-dependent kinase substrates. Nature *434*, 104-108.

Louie, R.K., Bahmanyar, S., Siemers, K.A., Votin, V., Chang, P., Stearns, T., Nelson, W.J., and Barth, A.I. (2004). Adenomatous polyposis coli and EB1 localize in close proximity of the mother centriole and EB1 is a functional component of centrosomes. J Cell Sci *117*, 1117-1128.

Ma, L., McQueen, J., Cuschieri, L., Vogel, J., and Measday, V. (2007). Spc24 and Stu2 promote spindle integrity when DNA replication is stalled. Mol Biol Cell *18*, 2805-2816.

Maddox, P., Chin, E., Mallavarapu, A., Yeh, E., Salmon, E.D., and Bloom, K. (1999). Microtubule dynamics from mating through the first zygotic division in the budding yeast Saccharomyces cerevisiae. J Cell Biol *144*, 977-987.

Maddox, P.S., Bloom, K.S., and Salmon, E.D. (2000). The polarity and dynamics of microtubule assembly in the budding yeast Saccharomyces cerevisiae. Nat Cell Biol *2*, 36-41.

Maekawa, H., and Schiebel, E. (2004). Cdk1-Clb4 controls the interaction of astral microtubule plus ends with subdomains of the daughter cell cortex. Genes Dev *18*, 1709-1724.

Maekawa, H., Usui, T., Knop, M., and Schiebel, E. (2003). Yeast Cdk1 translocates to the plus end of cytoplasmic microtubules to regulate bud cortex interactions. Embo J *22*, 438-449.

Mandelkow, E., and Mandelkow, E.M. (1989). Microtubular structure and tubulin polymerization. Curr Opin Cell Biol *1*, 5-9.

Mandelkow, E., and Mandelkow, E.M. (1990). Microtubular structure and tubulin polymerization. Curr Opin Cell Biol *2*, 3-9.

Marschall, L.G., Jeng, R.L., Mulholland, J., and Stearns, T. (1996). Analysis of Tub4p, a yeast gamma-tubulin-like protein: implications for microtubule-organizing center function. J Cell Biol *134*, 443-454.

Masuda, H., and Shibata, T. (1996). Role of gamma-tubulin in mitosis-specific microtubule nucleation from the Schizosaccharomyces pombe spindle pole body. J Cell Sci *109 (Pt 1)*, 165-177.

Mata, J., and Nurse, P. (1998). Discovering the poles in yeast. Trends Cell Biol *8*, 163-167.

McMillan, J.N., and Tatchell, K. (1994). The JNM1 gene in the yeast Saccharomyces cerevisiae is required for nuclear migration and spindle orientation during the mitotic cell cycle. J Cell Biol *125*, 143-158.

Mehta, A.D., Rock, R.S., Rief, M., Spudich, J.A., Mooseker, M.S., and Cheney, R.E. (1999). Myosin-V is a processive actin-based motor. Nature *400*, 590-593.

Meluh, P.B., and Rose, M.D. (1990). KAR3, a kinesin-related gene required for yeast nuclear fusion. Cell *60*, 1029-1041.

Miller, R.K., Cheng, S.C., and Rose, M.D. (2000). Bim1p/Yeb1p mediates the Kar9p-dependent cortical attachment of cytoplasmic microtubules. Mol Biol Cell *11*, 2949-2959.

Miller, R.K., Heller, K.K., Frisen, L., Wallack, D.L., Loayza, D., Gammie, A.E., and Rose, M.D. (1998). The kinesin-related proteins, Kip2p and Kip3p, function differently in nuclear migration in yeast. Mol Biol Cell *9*, 2051-2068.

Miller, R.K., Matheos, D., and Rose, M.D. (1999). The cortical localization of the microtubule orientation protein, Kar9p, is dependent upon actin and proteins required for polarization. J Cell Biol *144*, 963-975.

Miller, R.K., and Rose, M.D. (1998). Kar9p is a novel cortical protein required for cytoplasmic microtubule orientation in yeast. J Cell Biol *140*, 377-390.

Mimori-Kiyosue, Y., Shiina, N., and Tsukita, S. (2000a). Adenomatous polyposis coli (APC) protein moves along microtubules and concentrates at their growing ends in epithelial cells. J Cell Biol *148*, 505-518.

Mimori-Kiyosue, Y., Shiina, N., and Tsukita, S. (2000b). The dynamic behavior of the APC-binding protein EB1 on the distal ends of microtubules. Curr Biol *10*, 865-868.

Mitchison, T., and Kirschner, M. (1984a). Dynamic instability of microtubule growth. Nature *312*, 237-242.

Mitchison, T., and Kirschner, M. (1984b). Microtubule assembly nucleated by isolated centrosomes. Nature *312*, 232-237.

Mitchison, T.J., and Salmon, E.D. (1992). Poleward kinetochore fiber movement occurs during both metaphase and anaphase-A in newt lung cell mitosis. J Cell Biol *119*, 569-582.

Moore, J.K., D'Silva, S., and Miller, R.K. (2005). The CLIP170 Homologue Bik1p Promotes the Phosphorylation and Asymmetric Localization of Kar9p. Mol Biol Cell.

Moore, J.K., Li, J., and Cooper, J.A. (2008). Dynactin function in mitotic spindle positioning. Traffic *9*, 510-527.

Moore, J.K., and Miller, R.K. (2007). The cyclin-dependent kinase Cdc28p regulates multiple aspects of Kar9p function in yeast. Mol Biol Cell *18*, 1187-1202.

Moritz, M., and Agard, D.A. (2001). Gamma-tubulin complexes and microtubule nucleation. Curr Opin Struct Biol *11*, 174-181.

Moritz, M., Zheng, Y., Alberts, B.M., and Oegema, K. (1998). Recruitment of the gamma-tubulin ring complex to Drosophila salt-stripped centrosome scaffolds. J Cell Biol *142*, 775-786.

Motegi, F., and Sugimoto, A. (2006). Sequential functioning of the ECT-2 RhoGEF, RHO-1 and CDC-42 establishes cell polarity in Caenorhabditis elegans embryos. Nat Cell Biol *8*, 978-985.

Muhua, L., Karpova, T.S., and Cooper, J.A. (1994). A yeast actin-related protein homologous to that in vertebrate dynactin complex is important for spindle orientation and nuclear migrationk. Cell *78*, 669-679.

Muller, H., Fogeron, M.L., Lehmann, V., Lehrach, H., and Lange, B.M. (2006). A centrosome-independent role for gamma-TuRC proteins in the spindle assembly checkpoint. Science *314*, 654-657.

Munro, E.M. (2006). PAR proteins and the cytoskeleton: a marriage of equals. Curr Opin Cell Biol *18*, 86-94.

Nakamura, M., Zhou, X.Z., and Lu, K.P. (2001). Critical role for the EB1 and APC interaction in the regulation of microtubule polymerization. Curr Biol *11*, 1062-1067.

Neuwald, A.F., Aravind, L., Spouge, J.L., and Koonin, E.V. (1999). AAA+: A class of chaperone-like ATPases associated with the assembly, operation, and disassembly of protein complexes. Genome Res *9*, 27-43.

Nguyen-Ngoc, T., Afshar, K., and Gonczy, P. (2007). Coupling of cortical dynein and G alpha proteins mediates spindle positioning in Caenorhabditis elegans. Nat Cell Biol *9*, 1294-1302.

Niederstrasser, H., Salehi-Had, H., Gan, E.C., Walczak, C., and Nogales, E. (2002). XKCM1 acts on a single protofilament and requires the C terminus of tubulin. J Mol Biol *316*, 817-828.

Niethammer, P., Kronja, I., Kandels-Lewis, S., Rybina, S., Bastiaens, P., and Karsenti, E. (2007). Discrete states of a protein interaction network govern interphase and mitotic microtubule dynamics. PLoS Biol *5*, e29.

Nipper, R.W., Siller, K.H., Smith, N.R., Doe, C.Q., and Prehoda, K.E. (2007). Galphai generates multiple Pins activation states to link cortical polarity and spindle orientation in Drosophila neuroblasts. Proc Natl Acad Sci U S A *104*, 14306-14311.

Nogales, E., Whittaker, M., Milligan, R.A., and Downing, K.H. (1999). High-resolution model of the microtubule. Cell *96*, 79-88.

Oakley, B.R., Oakley, C.E., Yoon, Y., and Jung, M.K. (1990). Gamma-tubulin is a component of the spindle pole body that is essential for microtubule function in Aspergillus nidulans. Cell *61*, 1289-1301.

Oakley, C.E., and Oakley, B.R. (1989). Identification of gamma-tubulin, a new member of the tubulin superfamily encoded by mipA gene of Aspergillus nidulans. Nature *338*, 662-664.

Oegema, K., Wiese, C., Martin, O.C., Milligan, R.A., Iwamatsu, A., Mitchison, T.J., and Zheng, Y. (1999). Characterization of two related Drosophila gamma-tubulin complexes that differ in their ability to nucleate microtubules. J Cell Biol *144*, 721-733.

Palmer, R.E., Sullivan, D.S., Huffaker, T., and Koshland, D.a. (1992). Role of astral microtubules and actin in spindle orientation and migration in the budding yeast, Saccharomyces cerevisiae. J Cell Biol *119*, 583-593.

Paluh, J.L., Nogales, E., Oakley, B.R., McDonald, K., Pidoux, A.L., and Cande, W.Z. (2000). A mutation in gamma-tubulin alters microtubule dynamics and organization and is synthetically lethal with the kinesin-like protein pkl1p. Mol Biol Cell *11*, 1225-1239.

Park, H.O., Sanson, A., and Herskowitz, I. (1999). Localization of bud2p, a GTPase-activating protein necessary for programming cell polarity in yeast to the presumptive bud site. Genes Dev *13*, 1912-1917.

Pearson, C.G., and Bloom, K. (2004). Dynamic microtubules lead the way for spindle positioning. Nat Rev Mol Cell Biol *5*, 481-492.

Pereira, G., Knop, M., and Schiebel, E. (1998). Spc98p directs the yeast gamma-tubulin complex into the nucleus and is subject to cell cycle-dependent phosphorylation on the nuclear side of the spindle pole body. Mol Biol Cell *9*, 775-793.

Pereira, G., Tanaka, T.U., Nasmyth, K., and Schiebel, E. (2001). Modes of spindle pole body inheritance and segregation of the Bfa1p-Bub2p checkpoint protein complex. Embo J *20*, 6359-6370.

Perez, F., Diamantopoulos, G.S., Stalder, R., and Kreis, T.E. (1999). CLIP-170 highlights growing microtubule ends in vivo. Cell *96*, 517-527.

Pierre, P., Scheel, J., Rickard, J.E., and Kreis, T.E. (1992). CLIP-170 links endocytic vesicles to microtubules. Cell *70*, 887-900.

Pot, I., Knockleby, J., Aneliunas, V., Nguyen, T., Ah-Kye, S., Liszt, G., Snyder, M., Hieter, P., and Vogel, J. (2005). Spindle Checkpoint Maintenance Requires Ame1 and Okp1. Cell Cycle *4*.

Prigozhina, N.L., Oakley, C.E., Lewis, A.M., Nayak, T., Osmani, S.A., and Oakley, B.R. (2004). gamma-tubulin plays an essential role in the coordination of mitotic events. Mol Biol Cell *15*, 1374-1386.

Puig, O., Caspary, F., Rigaut, G., Rutz, B., Bouveret, E., Bragado-Nilsson, E., Wilm, M., and Seraphin, B. (2001). The tandem affinity purification (TAP) method: a general procedure of protein complex purification. Methods *24*, 218-229.

Raynaud-Messina, B., and Merdes, A. (2007). Gamma-tubulin complexes and microtubule organization. Curr Opin Cell Biol *19*, 24-30.

Reck-Peterson, S.L., Tyska, M.J., Novick, P.J., and Mooseker, M.S. (2001). The yeast class V myosins, Myo2p and Myo4p, are nonprocessive actin-based motors. J Cell Biol *153*, 1121-1126.

Reck-Peterson, S.L., Yildiz, A., Carter, A.P., Gennerich, A., Zhang, N., and Vale, R.D. (2006). Single-molecule analysis of dynein processivity and stepping behavior. Cell *126*, 335-348.

Rickard, J.E., and Kreis, T.E. (1991). Binding of pp170 to microtubules is regulated by phosphorylation. J Biol Chem *266*, 17597-17605.

Rogers, S.L., Rogers, G.C., Sharp, D.J., and Vale, R.D. (2002). Drosophila EB1 is important for proper assembly, dynamics, and positioning of the mitotic spindle. J Cell Biol *158*, 873-884.

Sadler, P.L., and Shakes, D.C. (2000). Anucleate Caenorhabditis elegans sperm can crawl, fertilize oocytes and direct anterior-posterior polarization of the 1-cell embryo. Development *127*, 355-366.

Scadden, D.T. (2006). The stem-cell niche as an entity of action. Nature *441*, 1075-1079.

Schott, D., Ho, J., Pruyne, D., and Bretscher, A. (1999). The COOH-terminal domain of Myo2p, a yeast myosin V, has a direct role in secretory vesicle targeting. J Cell Biol *147*, 791-808.

Schroer, T.A. (2004). Dynactin. Annu Rev Cell Dev Biol *20*, 759-779.

Schroer, T.A., Steuer, E.R., and Sheetz, M.P. (1989). Cytoplasmic dynein is a minus end-directed motor for membranous organelles. Cell *56*, 937-946.

Schuyler, S.C., and Pellman, D. (2001). Microtubule "plus-end-tracking proteins": The end is just the beginning. Cell *105*, 421-424.

Schwartz, K., Richards, K., and Botstein, D. (1997). BIM1 encodes a microtubule-binding protein in yeast. Mol Biol Cell *8*, 2677-2691.

Segal, M., and Bloom, K. (2001). Control of spindle polarity and orientation in Saccharomyces cerevisiae. Trends Cell Biol *11*, 160-166.

Segal, M., Bloom, K., and Reed, S.I. (2002). Kar9p-independent microtubule capture at Bud6p cortical sites primes spindle polarity before bud emergence in Saccharomyces cerevisiae. Mol Biol Cell *13*, 4141-4155.

Segal, M., Clarke, D.J., Maddox, P., Salmon, E.D., Bloom, K., and Reed, S.I. (2000). Coordinated spindle assembly and orientation requires Clb5p-dependent kinase in budding yeast. J Cell Biol *148*, 441-452.

Sheeman, B., Carvalho, P., Sagot, I., Geiser, J., Kho, D., Hoyt, M.A., and Pellman, D. (2003). Determinants of S. cerevisiae dynein localization and activation: implications for the mechanism of spindle positioning. Curr Biol *13*, 364-372.

Sikorski, R.S., and Hieter, P. (1989). A system of shuttle vectors and yeast host strains designed for efficient manipulation of DNA in Saccharomyces cerevisiae. Genetics *122*, 19-27.

Siller, K.H., Cabernard, C., and Doe, C.Q. (2006). The NuMA-related Mud protein binds Pins and regulates spindle orientation in Drosophila neuroblasts. Nat Cell Biol *8*, 594-600.

Skowronek, K.J., Kocik, E., and Kasprzak, A.A. (2007). Subunits interactions in kinesin motors. Eur J Cell Biol *86*, 559-568.

Slep, K.C., and Vale, R.D. (2007). Structural basis of microtubule plus end tracking by XMAP215, CLIP-170, and EB1. Mol Cell *27*, 976-991.

Sloat, B.F., Adams, A., and Pringle, J.R. (1981). Roles of the CDC24 gene product in cellular morphogenesis during the Saccharomyces cerevisiae cell cycle. J Cell Biol *89*, 395-405.

Sobel, S.G., and Snyder, M. (1995). A highly divergent gamma-tubulin gene is essential for cell growth and proper microtubule organization in Saccharomyces cerevisiae. J Cell Biol *131*, 1775-1788.

Spang, A., Geissler, S., Grein, K., and Schiebel, E. (1996). gamma-Tubulin-like Tub4p of Saccharomyces cerevisiae is associated with the spindle pole body substructures that organize microtubules and is required for mitotic spindle formation. J Cell Biol *134*, 429-441.

Stearns, T., Evans, L., and Kirschner, M. (1991). Gamma-tubulin is a highly conserved component of the centrosome. Cell *65*, 825-836.

Stearns, T., and Kirschner, M. (1994). In vitro reconstitution of centrosome assembly and function: the central role of gamma-tubulin. Cell *76*, 623-637.

Stearns, T., and Winey, M. (1997). The cell center at 100. Cell *91*, 303-309.

Straight, A.F., Marshall, W.F., Sedat, J.W., and Murray, A.W. (1997). Mitosis in living budding yeast: anaphase A but no metaphase plate. Science *277*, 574-578.

Strome, S. (1986). Fluorescence visualization of the distribution of microfilaments in gonads and early embryos of the nematode Caenorhabditis elegans. J Cell Biol *103*, 2241-2252.

Su, L.K., Burrell, M., Hill, D.E., Gyuris, J., Brent, R., Wiltshire, R., Trent, J., Vogelstein, B., and Kinzler, K.W. (1995). APC binds to the novel protein EB1. Cancer Res *55*, 2972-2977.

Tabuse, Y., Izumi, Y., Piano, F., Kemphues, K.J., Miwa, J., and Ohno, S. (1998). Atypical protein kinase C cooperates with PAR-3 to establish embryonic polarity in Caenorhabditis elegans. Development *125*, 3607-3614.

Taheri, N., Kohler, T., Braus, G.H., and Mosch, H.U. (2000). Asymmetrically localized Bud8p and Bud9p proteins control yeast cell polarity and development. Embo J *19*, 6686-6696.

Takeda, D.Y., Wohlschlegel, J.A., and Dutta, A. (2001). A bipartite substrate recognition motif for cyclin-dependent kinases. J Biol Chem *276*, 1993-1997.

Theesfeld, C.L., Irazoqui, J.E., Bloom, K., and Lew, D.J. (1999). The role of actin in spindle orientation changes during the Saccharomyces cerevisiae cell cycle. J Cell Biol *146*, 1019-1032.

Tio, M., Udolph, G., Yang, X., and Chia, W. (2001). cdc2 links the Drosophila cell cycle and asymmetric division machineries. Nature *409*, 1063-1067.

Tirnauer, J.S., O'Toole, E., Berrueta, L., Bierer, B.E., and Pellman, D. (1999). Yeast Bim1p promotes the G1-specific dynamics of microtubules. J Cell Biol *145*, 993-1007.

Toba, S., Watanabe, T.M., Yamaguchi-Okimoto, L., Toyoshima, Y.Y., and Higuchi, H. (2006). Overlapping hand-over-hand mechanism of single molecular motility of cytoplasmic dynein. Proc Natl Acad Sci U S A *103*, 5741-5745.

Tolic-Norrelykke, I.M. (2008). Push-me-pull-you: how microtubules organize the cell interior. Eur Biophys J.

Tong, A.H., Evangelista, M., Parsons, A.B., Xu, H., Bader, G.D., Page, N., Robinson, M., Raghibizadeh, S., Hogue, C.W., Bussey, H., Andrews, B., Tyers, M., and Boone, C. (2001). Systematic genetic analysis with ordered arrays of yeast deletion mutants. Science *294*, 2364-2368.

Trzepacz, C., Lowy, A.M., Kordich, J.J., and Groden, J. (1997). Phosphorylation of the tumor suppressor adenomatous polyposis coli (APC) by the cyclin-dependent kinase p34. J Biol Chem *272*, 21681-21684.

Tsai, M.C., and Ahringer, J. (2007). Microtubules are involved in anterior-posterior axis formation in C. elegans embryos. J Cell Biol *179*, 397-402.

Usui, T., Maekawa, H., Pereira, G., and Schiebel, E. (2003). The XMAP215 homologue Stu2 at yeast spindle pole bodies regulates microtubule dynamics and anchorage. Embo J *22*, 4779-4793.

Usui, T., and Schiebel, E. (2001). Regulating microtubule properties by modifying their organizing minus ends. Mol Cell *8*, 931-932.

Vale, R.D., and Milligan, R.A. (2000). The way things move: looking under the hood of molecular motor proteins. Science *288*, 88-95.

Vallee, R.B., Tai, C., and Faulkner, N.E. (2001). LIS1: cellular function of a disease-causing gene. Trends Cell Biol *11*, 155-160.

Vallee, R.B., Williams, J.C., Varma, D., and Barnhart, L.E. (2004). Dynein: An ancient motor protein involved in multiple modes of transport. J Neurobiol *58*, 189-200.

van Breugel, M., Drechsel, D., and Hyman, A. (2003). Stu2p, the budding yeast member of the conserved Dis1/XMAP215 family of microtubule-associated proteins is a plus end-binding microtubule destabilizer. J Cell Biol *161*, 359-369.

Varga, V., Helenius, J., Tanaka, K., Hyman, A.A., Tanaka, T.U., and Howard, J. (2006). Yeast kinesin-8 depolymerizes microtubules in a length-dependent manner. Nat Cell Biol *8*, 957-962.

Vaughan, P.S., Miura, P., Henderson, M., Byrne, B., and Vaughan, K.T. (2002). A role for regulated binding of p150(Glued) to microtubule plus ends in organelle transport. J Cell Biol *158*, 305-319.

Verollet, C., Colombie, N., Daubon, T., Bourbon, H.M., Wright, M., and Raynaud-Messina, B. (2006). Drosophila melanogaster gamma-TuRC is dispensable for targeting gamma-tubulin to the centrosome and microtubule nucleation. J Cell Biol *172*, 517-528.

Vogel, J., Drapkin, B., Oomen, J., Beach, D., Bloom, K., and Snyder, M. (2001). Phosphorylation of gamma-tubulin regulates microtubule organization in budding yeast. Dev Cell *1*, 621-631.

Vogel, J., and Snyder, M. (2000). The carboxy terminus of Tub4p is required for gamma-tubulin function in budding yeast. J Cell Sci *113 Pt 21*, 3871-3882.

Vogel, J.M., Stearns, T., Rieder, C.L., and Palazzo, R.E. (1997). Centrosomes isolated from Spisula solidissima oocytes contain rings and an unusual stoichiometric ratio of alpha/beta tubulin. J Cell Biol *137*, 193-202.

Wang, P.J., and Huffaker, T.C. (1997). Stu2p: A microtubule-binding protein that is an essential component of the yeast spindle pole body. J Cell Biol *139*, 1271-1280.

Wiese, C., and Zheng, Y. (2000). A new function for the gamma-tubulin ring complex as a microtubule minus-end cap. Nat Cell Biol *2*, 358-364.

Wodarz, A., Ramrath, A., Kuchinke, U., and Knust, E. (1999). Bazooka provides an apical cue for Inscuteable localization in Drosophila neuroblasts. Nature *402*, 544-547.

Wolyniak, M.J., Blake-Hodek, K., Kosco, K., Hwang, E., You, L., and Huffaker, T.C. (2006). The regulation of microtubule dynamics in Saccharomyces cerevisiae by three interacting plus-end tracking proteins. Mol Biol Cell *17*, 2789-2798.

Wu, X., Xiang, X., and Hammer, J.A., 3rd. (2006). Motor proteins at the microtubule plus-end. Trends Cell Biol *16*, 135-143.

Xiang, X., Han, G., Winkelmann, D.A., Zuo, W., and Morris, N.R. (2000). Dynamics of cytoplasmic dynein in living cells and the effect of a mutation in the dynactin complex actin-related protein Arp1. Curr Biol *10*, 603-606.

Yeh, E., Skibbens, R.V., Cheng, J.W., Salmon, E.D., and Bloom, K. (1995). Spindle dynamics and cell cycle regulation of dynein in the budding yeast, Saccharomyces cerevisiae. J Cell Biol *130*, 687-700.

Yildiz, A., Forkey, J.N., McKinney, S.A., Ha, T., Goldman, Y.E., and Selvin, P.R. (2003). Myosin V walks hand-over-hand: single fluorophore imaging with 1.5-nm localization. Science *300*, 2061-2065.

Yildiz, A., Tomishige, M., Vale, R.D., and Selvin, P.R. (2004). Kinesin walks hand-over-hand. Science *303*, 676-678.

Yin, H., Pruyne, D., Huffaker, T.C., and Bretscher, A. (2000). Myosin V orientates the mitotic spindle in yeast. Nature *406*, 1013-1015.

Zahner, J.E., Harkins, H.A., and Pringle, J.R. (1996). Genetic analysis of the bipolar pattern of bud site selection in the yeast Saccharomyces cerevisiae. Mol Cell Biol *16*, 1857-1870.

Zheng, Y., Wong, M.L., Alberts, B., and Mitchison, T. (1995). Nucleation of microtubule assembly by a gamma-tubulin-containing ring complex. Nature *378*, 578-583.

Zheng, Y., Wong, M.L., Alberts, B., and Mitchison, T. (1998). Purification and assay of gamma tubulin ring complex. Methods Enzymol *298*, 218-228.

Zimmerman, S., and Chang, F. (2005). Effects of {gamma}-Tubulin Complex Proteins on Microtubule Nucleation and Catastrophe in Fission Yeast. Mol Biol Cell *16*, 2719-2733.

APPENDIX

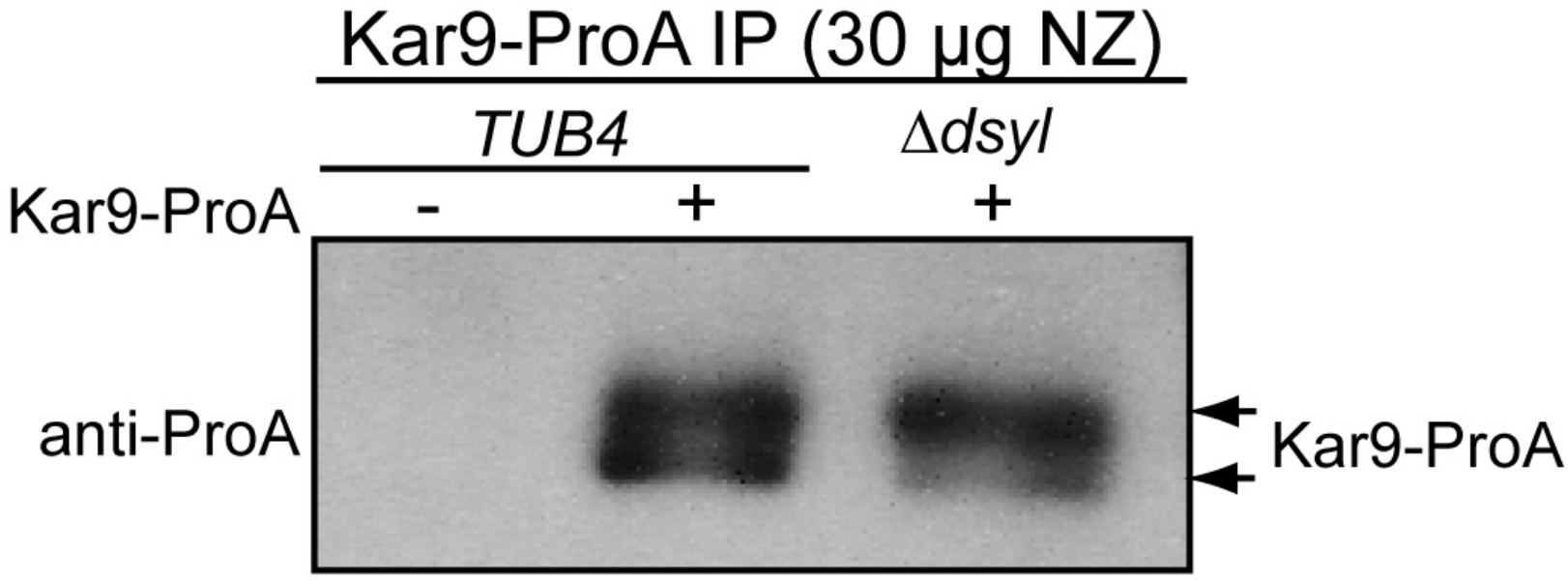

Figure A1: Kar9 is hyperphosphorylated in IP assays performed in *tub4-Δdsyl* extrats treated with 30 µg NZ relative to wild-type extracts.

McGill University

APPLICATION TO USE BIOHAZARDOUS MATERIALS

Projects involving potentially biohazardous materials should not be commenced without approval from Environmental Health & Safety. Submit applications before 1) starting new projects, 2) renewing existing projects, or 3) changing the nature of the biohazardous materials within existing projects.

1. PRINCIPAL INVESTIGATOR: Jackie Vogel PHONE: 514 398 5860
DEPARTMENT: Department of Biology FAX: 514-398-5069
ADDRESS: 1205 Dr. Penfield E-MAIL: jackie.vogel@mcgill.ca

PROJECT TITLE(S): analysis of cytoskeletal and chromosome dynamics in budding yeast

2. EMERGENCY: Person(s) designated to handle emergencies
Name: Jackie Vogel Phone No: work: _____ home: 514 298 9256
Name: _____ Phone No: work: _____ home: _____

3. FUNDING SOURCE OR AGENCY: list all sources when information in Sections 5-12 is identical:
Source CIHR Grant No. 205283 Start date 10/01/2006 End date 09/30/2011
Source NSERC Grant No. 204556 Start date 03/31/2008 End date 03/31/2013
Source _____ Grant No. _____ Start date _____ End date _____

4. Indicate if this is
☐ Renewal: procedures previously approved without alterations.
Approval End Date: _____
☐ New funding source: project previously reviewed and approved under an application to another agency.
Agency: _____ Approval End Date: _____
☑ New project: project not previously reviewed.
☐ Approved project: change in biohazardous materials or procedures.
☐ Work/project involving biohazardous materials in teaching/diagnostics.

CERTIFICATION STATEMENT: Environmental Health & Safety approves the experimental procedures proposed and certifies with the applicant that the experiment will be in accordance with the principles outlined in the Public Health Agency of Canada's "Laboratory Biosafety Guidelines" and in the "McGill Laboratoiy Biosafety Manual".

Containment Level (select one): ☑ 1 ☐ 2 ☐ 2 with additional precautions ☐ 3

Principal Investigator or course director: _____ (SIGNATURE) date: 23 (day) 05 (month) 2008 (year)

Approved by Environmental Health & Safety: _____ (SIGNATURE) date: 26 (day) 05 (month) 08 (year)

Expiry: 31 (day) 03 (month) 13 (year)

8047

5. RESEARCH PERSONNEL: (attach additional sheets if preferred)

Name	Department	Job Title/Classification	Trained in the safe use of biological safety cabinets within the last 3 years? If yes, indicate training date.
Daici Chen	Biology	graduate student	training fall 07
Thao Nguyen	Biology	graduate student	training fall 06
Lara Cuschieri	Biology	graduate student	training fall 06
James Knockleby	Biology	graduate student	training fall 06

6. Briefly describe:

i) the biohazardous material involved (e.g. bacteria, viruses, human tissues, toxins of biological origin) & designated biosafety risk group

saccharomyces cerevisiae, e coli (K12)

ii) the procedures involving biohazards

molecular genetics, genomics analysis of gene interactions, molecular biology (cloning), biochemistry

iii) the protocol for decontaminating spills

70% ethanol, 1% bleach

7. Does the protocol present conditions (e.g. handling of large volumes or high concentrations of pathogens) that could increase the hazards?

no

8. Do the specific procedures to be employed involving genetically engineered organisms have a history of safe use?

yes

9. What precautions will be taken to reduce production of infectious droplets and aerosols?

not applicable

10. Will the biohazardous materials in this project expose members of the research team to any risks that might require special training, vaccination or other protective measures? If yes, please explain.

no

11. Will this project produce combined hazardous waste – i.e. radioactive biohazardous waste, biohazardous animal carcasses contaminated with toxic chemicals, etc.? If yes, please explain how disposal will be handled.

no

12. List the biological safety cabinets to be used.

Building	Room No.	Manufacturer	Model No.	Serial No.	Date Certified
not applicable					